Mathematics

https://www.aimspress.com/journal/Math

AIMS Mathematics, 11(9): 28887–28949.
DOI:10.3934/math.20261150
Received: 30 April 2026
Revised: 24 August 2026
Accepted: 01 September 2026
Published: 09 September 2026

Research article

Two-parameter family of Unit distributions: theory, statistical inference, and reliability applications

Hebatalla H. Mohammad[1], Moustafa N. Mousa[2], Khalaf S. Sultan[3] and Mahmoud M. M. Mansour[4,*]

[1] Department of Mathematical Sciences, College of Science, Princess Nourah bint Abdulrahman University, Riyadh 11671, Saudi Arabia

[2] Department of Mathematics, Faculty of Science, Kafrelsheikh University, Kafrelsheikh 33516, Egypt

[3] Mathematics Department, Faculty of Science, Al-Azhar University, Nasr City, Cairo 11884, Egypt

[4] Department of Basic Science, Faculty of Engineering, The British University in Egypt, El Sherouk City, Cairo 11837, Egypt

* **Correspondence:** Email: mahmoud.mansour@bue.edu.eg.

Abstract: This paper develops a two-parameter family of unit distributions (TPFUD) by applying the standard unit transformation to a positive-support parent family to model data on the open unit interval $(0, 1)$, such as proportions, rates, percentages, and transformed lifetime observations. The proposed family admits tractable forms for the density, distribution, survival, hazard, cumulative hazard, reversed hazard, and odds functions, and it provides a unified framework for several Lindley-type unit models. Its main mathematical properties are derived, including its limiting behavior, quantile function, moments, incomplete moments, inequality measures, actuarial quantities, stress–strength reliability, order statistics, stochastic ordering, and entropy and extropy measures. A flexible one-parameter special case, called the unit Shanker distribution (UShD), is then examined in detail. For this model, maximum likelihood, the maximum product of spacings, and Bayesian estimation methods are developed for the unknown parameter and selected reliability functions. The existence and uniqueness of the maximum likelihood estimator are also established. A Monte Carlo simulation study shows that the estimators improve as the sample size increases, with informative Bayesian estimation giving the best finite-sample performance. Two real-data applications further demonstrate that the UShD provides competitive and flexible fits compared with existing unit distributions.

Keywords: family of unit distributions; unit shanker distribution; reliability analysis; maximum likelihood; maximum product spacing; Bayesian estimation; Monte Carlo simulation

Mathematics Subject Classification: 60G35, 62F10, 62F15, 62N01, 62N02, 62N05

1. Introduction

Accurate probability modeling for random variables supported on the unit interval $(0, 1)$ is of fundamental importance across many disciplines, including reliability, economics, finance, environmental science, medicine, and public health, where observations frequently arise in the form of proportions, rates, probabilities, percentages, and normalized indices. The intrinsic boundedness of such data often renders the direct use of classical unbounded distributions inappropriate, thereby motivating the development of flexible unit distributions.

Although the beta distribution remains the standard benchmark for bounded data due to its flexibility, its analytical structure can be cumbersome in applications requiring simple closed-form expressions, particularly for the cumulative distribution and quantile functions. This limitation has stimulated sustained interest in alternative bounded distributions that combine tractability with adequate flexibility. A major direction in this area consists of constructing unit models with explicit distributional and reliability characteristics and sufficient shape adaptability for practical data analysis. Representative recent contributions include the unit arcsine–exponential distribution [1], the unit arcsine–Rayleigh distribution [2], a flexible bounded model with a bathtub-shaped hazard rate [3], and the inverse unit new XLindley distribution [4].

Among the various models proposed for bounded data, analytically tractable unit distributions are especially attractive because of their interpretability and usefulness in statistical and reliability studies. In particular, the unit Lindley distribution [5] has received considerable attention due to its parsimonious structure and appealing theoretical properties, including explicit closed-form expressions, exponential family representation, bias-corrected maximum likelihood (ML) estimation, and mean-based regression modeling. These advantages motivate a common framework for studying related unit Lindley-type models and deriving their bounded data and reliability properties systematically.

Motivated by these considerations, this study applies the standard transformation $X = T/(1 + T)$, which maps $(0, \infty)$ onto $(0, 1)$, to the positive-support two-parameter family introduced in [6]. Rather than claiming novelty for this established unitizing transformation, the study develops a unified framework for the resulting unit family, deriving its distributional and reliability characteristics, quantiles, moments, actuarial measures, order statistics, entropy and extropy measures, and identifiability condition. It also provides a detailed classical and Bayesian inferential analysis of the UShD as a special case.

The remainder of this article is organized as follows. Section 2 develops the proposed two-parameter family of unit distributions (TPFUD) by presenting its basic formulation, reliability functions, relevant sub-models, and limiting behavior. Section 3 provides a comprehensive treatment of the main statistical properties of the proposed family. In Section 4, the UShD is examined as a distinguished special case within this framework. Classical and Bayesian inferential procedures are discussed in Sections 5 and 6, respectively. The finite-sample behavior of the estimators is assessed through a Monte Carlo simulation study in Section 7. Real-data applications are then presented in Section 8 to illustrate the flexibility and practical usefulness of the proposed model. Finally, Section 9 concludes the article by summarizing the main findings and outlining possible directions for future research.

2. Two-parameter family of unit distributions

Let T follow the two-parameter family of distributions introduced in [6], with a probability density function (PDF) given by

$$g(t;\alpha,\beta) = \frac{a_2^2}{a_0a_2 + a_1}(a_0 + a_1 t)\, e^{-a_2 t}, \qquad t > 0, \tag{2.1}$$

where $a_i = a_i(\alpha,\beta)$, $i = 0, 1, 2$, are real-valued coefficient functions of the parameters $\alpha > 0$ and $\beta > 0$. For any selected specification, define the admissible parameter domain by

$$\Theta = \left\{(\alpha,\beta) \in (0,\infty)^2 : a_0(\alpha,\beta) > 0,\ a_1(\alpha,\beta) > 0,\ a_2(\alpha,\beta) > 0\right\}.$$

Throughout the general TPFUD development, $(\alpha,\beta) \in \Theta$. To construct a bounded distribution on the unit interval, consider the monotone transformation $X = \frac{T}{1+T}$, whose inverse is $T = \frac{X}{1-X}$. By the change of variables formula, the PDF of X is

$$f(x;\alpha,\beta) = g\left(\frac{x}{1-x};\alpha,\beta\right)\frac{1}{(1-x)^2}, \qquad 0 < x < 1. \tag{2.2}$$

Substituting Eq (2.1) into Eq (2.2), we obtain

$$f(x;\alpha,\beta) = \frac{a_2^2\left(a_0 + a_1\frac{x}{1-x}\right)}{(a_0a_2 + a_1)(1-x)^2} e^{-a_2\frac{x}{1-x}}, \qquad 0 < x < 1. \tag{2.3}$$

A random variable having the PDF in Eq (2.3) is said to follow the TPFUD, denoted $X \sim$ TPFUD(α,β).

Theorem 2.1 (Validity of the PDF). *For $(\alpha,\beta) \in \Theta$, the function defined in Eq (2.3) is a valid PDF on* $(0, 1)$.

Proof. By the definition of Θ, we have $a_0 > 0$, $a_1 > 0$, and $a_2 > 0$. For $0 < x < 1$, it follows that

$$1 - x > 0, \qquad \frac{x}{1-x} > 0, \qquad (1-x)^2 > 0, \qquad e^{-a_2\frac{x}{1-x}} > 0,$$

and hence $f(x;\alpha,\beta) \geq 0$. Next, consider

$$\int_0^1 f(x;\alpha,\beta)\,dx = \frac{a_2^2}{a_0a_2 + a_1}\int_0^1 \left(a_0 + a_1\frac{x}{1-x}\right)\frac{e^{-a_2\frac{x}{1-x}}}{(1-x)^2}dx.$$

Using the transformation $t = \frac{x}{1-x}$, $dt = \frac{1}{(1-x)^2}dx$, we obtain

$$\int_0^1 f(x;\alpha,\beta)\,dx = \frac{a_2^2}{a_0a_2 + a_1}\int_0^\infty (a_0 + a_1 t)e^{-a_2 t}\,dt.$$

Using the standard identities $\int_0^\infty e^{-a_2 t}\,dt = \frac{1}{a_2}$ and $\int_0^\infty te^{-a_2 t}\,dt = \frac{1}{a_2^2}$, we obtain

$$\int_0^1 f(x;\alpha,\beta)\,dx = \frac{a_2^2}{a_0a_2 + a_1}\left(\frac{a_0}{a_2} + \frac{a_1}{a_2^2}\right) = 1.$$

Hence, $f(x;\alpha,\beta)$ is a valid PDF, which completes the proof. □

Remark 2.1 (Special cases of the TPFUD). *A key feature of the TPFUD is its ability to encompass several important submodels through suitable choices of the parameter functions* a_0*,* a_1*, and* a_2*. In particular, the unit-transformed counterparts of several classical and generalized lifetime distributions are recovered under the transformation* $X = T/(1+T)$*. These include the Lindley [7], Shanker [8], Komal [9], Garima [10], linear-exponential [11], Gemeay–Zeghdoudi [6], two-parameter Lindley [12], gamma-Lindley [13], quasi-Lindley [14], new quasi-Lindley [15], two-parameter Lindley II [16], pseudo-Lindley [17], and XLindley [18] distributions; see Table 1. Accordingly, the TPFUD constitutes a unified, flexible, and analytically tractable class of bounded distributions on* $(0,1)$*, providing a coherent framework that encompasses a wide range of existing Lindley-type models.*

Table 1. Special cases of the TPFUD corresponding to selected choices of a_0, a_1, and a_2.

Distribution	Abbrev.	Parameters	$\boldsymbol{a_0}$	$\boldsymbol{a_1}$	$\boldsymbol{a_2}$	Reference
Unit Lindley	ULD	$\alpha > 0$	1	1	α	[5]
Unit Shanker	UShD	$\alpha > 0$	α	1	α	This paper
Unit Komal	UKD	$\alpha > 0$	$1+\alpha$	1	α	$\cdots$
Unit Garima	UGD	$\alpha > 0$	$1+\alpha$	α	α	$\cdots$
Unit Linear-Exponential	ULED	$\alpha > 0$	α^2	1	α	$\cdots$
Unit Gemeay-Zeghdoudi	UGZD	$\alpha > 0,\ \beta > 0$	$\frac{\alpha}{\beta}$	β	$\frac{1}{\alpha}$	$\cdots$
Unit two-parameter Lindley I	UTPLD-I	$\alpha > 0,\ \beta > 0$	α	1	β	$\cdots$
Unit gamma-Lindley	UGLD	$\beta > 0,\ \alpha > \frac{\beta}{1+\beta}$	1	$\alpha+\alpha\beta-\beta$	β	$\cdots$
Unit quasi-Lindley	UQLD	$\alpha > 0,\ \beta > 0$	α	β	β	$\cdots$
Unit new quasi-Lindley	UNQLD	$\alpha > 0,\ \beta > 0$	β	α	β	$\cdots$
Unit two-parameter Lindley II	UTPLD-II	$\alpha > 0,\ \beta > 0$	1	α	β	$\cdots$
Unit pseudo-Lindley	UPLD	$\alpha > 1,\ \beta > 0$	$\alpha-1$	β	β	$\cdots$
Unit XLindley	UXLD	$\alpha > 0$	$2+\alpha$	1	α	$\cdots$

In Table 1, the symbol $(\cdots)$ represents further admissible parameter specifications that yield additional submodels of the proposed TPFUD. To the best of the authors' knowledge, these particular models have not previously been introduced or systematically investigated in the existing literature.

Theorem 2.2 (Identifiability of the TPFUD). *Let a TPFUD be defined on the admissible parameter space* Θ*, and define* $\eta(\alpha,\beta) = \left(a_2, \frac{a_1}{a_0}\right)$*. We then have the following for any* $(\alpha_1,\beta_1), (\alpha_2,\beta_2) \in \Theta$*:*

$$f(\,\cdot\,;\alpha_1,\beta_1) = f(\,\cdot\,;\alpha_2,\beta_2) \quad \Longleftrightarrow \quad \eta(\alpha_1,\beta_1) = \eta(\alpha_2,\beta_2).$$

Consequently, the TPFUD is identifiable on Θ if and only if η is one-to-one on Θ.

Proof. Let $q = \frac{a_1}{a_0} > 0$. Since $a_0 > 0$, the density in Eq (2.3) can be expressed as

$$(1-x)^2 f(x;\alpha,\beta) = \frac{a_2^2}{a_2+q}\left(1+q\frac{x}{1-x}\right)\exp\left(-a_2\frac{x}{1-x}\right), \qquad 0 < x < 1,$$

so the density depends on (α,β) only through the pair (a_2, q).

Suppose that two parameter pairs generate the same density. From the preceding representation, we have

$$\lim_{x\to 1^-} -\frac{1-x}{x}\log\left[(1-x)^2 f(x;\alpha,\beta)\right] = a_2.$$

Therefore, the corresponding values of a_2 must coincide. For this common value of a_2,

$$\lim_{x\to 0^+}(1-x)^2 f(x;\alpha,\beta) = \frac{a_2^2}{a_2+q}.$$

Define $\phi(q) = \frac{a_2^2}{a_2+q}$, $q>0$. For fixed $a_2>0$, $\phi'(q) = -\frac{a_2^2}{(a_2+q)^2} < 0$, so ϕ is strictly decreasing on $(0,\infty)$. Therefore, the corresponding values of $q = a_1/a_0$ must also coincide, and hence, $\eta(\alpha_1,\beta_1) = \eta(\alpha_2,\beta_2)$.

Conversely, equality of the two η-values implies equality of the corresponding a_2 and q, and the density representation above immediately yields $f(\cdot\,;\alpha_1,\beta_1) = f(\cdot\,;\alpha_2,\beta_2)$. Hence, the stated equivalence holds, and identifiability is equivalent to the injectivity of η, which completes the proof. □

Remark 2.2 (Identifiability of the submodels)**.** *By Theorem 2.2, the identifiability of each TPFUD submodel is determined by the corresponding mapping $\eta(\alpha,\beta) = (\eta_1(\alpha,\beta), \eta_2(\alpha,\beta)) = \left(a_2, \frac{a_1}{a_0}\right)$. For the submodels involving both parameters in Table 1, the corresponding components are summarized in Table 2.*

Table 2. Components of the identifiability mappings for the TPFUD submodels involving both parameters.

Model	UGZD	UTPLD-I	UGLD	UQLD	UNQLD	UTPLD-II	UPLD
$\boldsymbol{\eta_1}$	$\frac{1}{\alpha}$	β	β	β	β	β	β
$\boldsymbol{\eta_2}$	$\frac{\beta^2}{\alpha}$	$\frac{1}{\alpha}$	$\alpha(1+\beta)-\beta$	$\frac{\beta}{\alpha}$	$\frac{\alpha}{\beta}$	α	$\frac{\beta}{\alpha-1}$

Each mapping is one-to-one on its corresponding admissible parameter domain, since the equality of η_1 and η_2 uniquely determines α and β. Hence, all submodels involving both parameters in Table 1 are identifiable and exhibit no parameter redundancy. The one-parameter submodels are treated analogously on their corresponding one-dimensional parameter spaces.

It follows that the corresponding cumulative distribution function (CDF) is

$$F(x;\alpha,\beta) = 1 - \left[\frac{a_2\left(a_0 + a_1\frac{x}{1-x}\right) + a_1}{a_0a_2 + a_1}\right] e^{-a_2\frac{x}{1-x}}, \qquad 0<x<1. \tag{2.4}$$

Accordingly, the survival function (SF), or equivalently the reliability function (RF), is

$$R(x;\alpha,\beta) = 1 - F(x;\alpha,\beta) = \left[\frac{a_2\left(a_0 + a_1\frac{x}{1-x}\right) + a_1}{a_0a_2 + a_1}\right] e^{-a_2\frac{x}{1-x}}, \qquad 0<x<1, \tag{2.5}$$

whereas the hazard rate function (HF) is given by

$$h(x;\alpha,\beta) = \frac{f(x;\alpha,\beta)}{R(x;\alpha,\beta)} = \frac{a_2^2\left(a_0 + a_1\frac{x}{1-x}\right)}{(1-x)^2\left[a_2\left(a_0 + a_1\frac{x}{1-x}\right) + a_1\right]}, \qquad 0<x<1. \tag{2.6}$$

Remark 2.3 (Cumulative hazard, reversed hazard, and odds functions)**.** *For a random variable* $X \sim$ TPFUD(α,β) *with CDF* $F(x;\alpha,\beta)$ *and RF* $R(x;\alpha,\beta)$ *given in Eqs (2.4) and (2.5), the cumulative hazard rate function (CHF) is defined as*

$$H(x;\alpha,\beta) = \int_0^x h(u;\alpha,\beta)\,du = -\log R(x;\alpha,\beta).$$

Using Eq (2.5), we obtain the explicit form

$$H(x;\alpha,\beta) = a_2\frac{x}{1-x} - \log\left(\frac{a_2\left(a_0 + a_1\frac{x}{1-x}\right) + a_1}{a_0a_2 + a_1}\right), \quad 0 < x < 1. \tag{2.7}$$

The reversed hazard rate function (RHF) is given by

$$r(x;\alpha,\beta) = \frac{f(x;\alpha,\beta)}{F(x;\alpha,\beta)}, \quad 0 < x < 1,$$

and, upon substituting Eqs (2.3) and (2.4), it follows that

$$r(x;\alpha,\beta) = \frac{a_2^2\left(a_0 + a_1\frac{x}{1-x}\right)e^{-a_2\frac{x}{1-x}}}{(1-x)^2\left[a_0a_2 + a_1 - \left(a_2\left(a_0 + a_1\frac{x}{1-x}\right) + a_1\right)e^{-a_2\frac{x}{1-x}}\right]}, \quad 0 < x < 1. \tag{2.8}$$

Moreover, the odds function (OF) associated with the TPFUD is defined as

$$O(x;\alpha,\beta) = \frac{F(x;\alpha,\beta)}{R(x;\alpha,\beta)} = \frac{1}{R(x;\alpha,\beta)} - 1,$$

which, using Eq (2.5), reduces to

$$O(x;\alpha,\beta) = \frac{(a_0a_2 + a_1)\,e^{a_2\frac{x}{1-x}}}{a_2\left(a_0 + a_1\frac{x}{1-x}\right) + a_1} - 1, \quad 0 < x < 1. \tag{2.9}$$

These functions provide complementary perspectives on the failure behavior of the TPFUD, offering deeper insight into its reliability structure and facilitating further theoretical developments and practical applications.

2.1. Asymptotic behavior

The limiting behavior of the TPFUD functions at the boundaries $x \to 0^+$ and $x \to 1^-$ is summarized in Table 3. The PDF and HF approach finite positive limits at the lower endpoint, whereas the RHF diverges there. At the upper endpoint, the HF and CHF diverge, while the RHF converges to zero.

Table 3. Asymptotic behavior of the TPFUD functions.

Limit	PDF	CDF	RF	HF	CHF	RHF	OF
$x \to 0^+$	$\dfrac{a_2^2a_0}{a_0a_2 + a_1}$	0	1	$\dfrac{a_2^2a_0}{a_0a_2 + a_1}$	0	∞	0
$x \to 1^-$	0	1	0	∞	∞	0	∞

More precisely, the HF diverges at the following quadratic rate:

$$\lim_{x\to 1^-}(1-x)^2 h(x;\alpha,\beta) = a_2, \qquad h(x;\alpha,\beta) = \frac{a_2}{(1-x)^2}\{1+o(1)\}. \tag{2.10}$$

Indeed, multiplying Eq (2.6) by $(1-x)^2$ gives

$$(1-x)^2 h(x;\alpha,\beta) = \frac{a_2^2\left(a_0 + a_1\frac{x}{1-x}\right)}{a_2\left(a_0 + a_1\frac{x}{1-x}\right) + a_1}.$$

Since $a_0 + a_1\frac{x}{1-x} \to \infty$ as $x \to 1^-$, the preceding ratio converges to $\frac{a_2^2}{a_2} = a_2$. Thus, the conditional failure intensity increases without bound as the random variable approaches its upper endpoint.

The monotonicity of the HF can be established directly by differentiating Eq (2.6). Applying the quotient rule and simplifying yields

$$\frac{\mathrm{d}}{\mathrm{d}x}h(x;\alpha,\beta) = \frac{a_2^2\left\{a_1^2 + 2(1-x)\left(a_0 + a_1\frac{x}{1-x}\right)\left[a_2\left(a_0 + a_1\frac{x}{1-x}\right) + a_1\right]\right\}}{(1-x)^4\left[a_2\left(a_0 + a_1\frac{x}{1-x}\right) + a_1\right]^2}. \tag{2.11}$$

For every $x \in (0,1)$, the denominator in Eq (2.11) is strictly positive. Moreover,

$$a_1^2 > 0, \quad 1-x > 0, \quad a_0 + a_1\frac{x}{1-x} > 0, \quad \text{and} \quad a_2\left(a_0 + a_1\frac{x}{1-x}\right) + a_1 > 0.$$

Consequently,

$$\frac{\mathrm{d}}{\mathrm{d}x}h(x;\alpha,\beta) > 0, \qquad 0 < x < 1.$$

Therefore, the HF is strictly increasing throughout the unit interval, and the TPFUD belongs to the increasing failure rate (IFR) class. Since every IFR distribution belongs to the decreasing mean residual life (DMRL) class, that is, IFR $\Longrightarrow$ DMRL, the TPFUD also has the DMRL property. Accordingly, the TPFUD is well suited to bounded aging and wear-out phenomena characterized by a monotonically increasing failure intensity, rather than mechanisms requiring decreasing, nonmonotone, or asymptotically constant hazard patterns.

3. Statistical properties of the TPFUD

In this section, we derive the principal statistical and distributional properties of the TPFUD from its defining functions, including the mode, quantile function, moments and inequality measures, deviation and residual-life functions, actuarial quantities, stress–strength reliability, order statistics, stochastic orders, and entropy and extropy measures. Taken together, these results provide a comprehensive characterization of the model's shape, variability, uncertainty, and reliability behavior.

3.1. Mode

The mode describes the location at which the PDF of the TPFUD reaches its maximum and, therefore, provides a useful summary of the peak structure of the distribution. For the PDF given in Eq (2.3), the modal point is obtained from the stationary equation

$$\frac{\mathrm{d}}{\mathrm{d}x}\log f(x;\alpha,\beta) = 0.$$

Using Eq (2.3), the log-density can be written as

$$\log f(x;\alpha,\beta) = 2\log a_2 - \log(a_0a_2 + a_1) + \log\left(a_0 + a_1\frac{x}{1-x}\right) - 2\log(1-x) - a_2\frac{x}{1-x}.$$

Differentiation with respect to x gives

$$\frac{\mathrm{d}}{\mathrm{d}x}\log f(x;\alpha,\beta) = \frac{a_1}{(1-x)^2\left(a_0 + a_1\frac{x}{1-x}\right)} + \frac{2}{1-x} - \frac{a_2}{(1-x)^2}.$$

Setting this derivative equal to zero and introducing the transformation

$$z = \frac{x}{1-x}, \qquad x = \frac{z}{1+z}, \qquad z > 0,$$

the modal equation reduces to

$$a_1a_2z^2 + [a_2(a_0 + a_1) - 3a_1]\,z + (a_0a_2 - 2a_0 - a_1) = 0. \tag{3.1}$$

An interior mode exists precisely when $a_0a_2 < 2a_0 + a_1$. In this case, the leading coefficient of Eq (3.1) satisfies $a_1a_2 > 0$, whereas its constant term satisfies $a_0a_2 - 2a_0 - a_1 < 0$. Moreover, the discriminant is

$$\Delta = [a_2(a_0 + a_1) - 3a_1]^2 - 4a_1a_2(a_0a_2 - 2a_0 - a_1) > 0.$$

Thus, the quadratic has two real roots whose product is

$$z_1z_2 = \frac{a_0a_2 - 2a_0 - a_1}{a_1a_2} < 0.$$

Hence, the two roots have opposite signs, and Eq (3.1) has exactly one positive root in $z \in (0,\infty)$. Since $x = z/(1+z)$ maps $(0,\infty)$ bijectively onto $(0,1)$, this root determines a unique interior mode. The corresponding mode is

$$x^* = \frac{3a_1 - a_2(a_0 + a_1) + \sqrt{[a_2(a_0 + a_1) - 3a_1]^2 - 4a_1a_2(a_0a_2 - 2a_0 - a_1)}}{2a_1a_2 + 3a_1 - a_2(a_0 + a_1) + \sqrt{[a_2(a_0 + a_1) - 3a_1]^2 - 4a_1a_2(a_0a_2 - 2a_0 - a_1)}}. \tag{3.2}$$

If $a_0a_2 \geq 2a_0 + a_1$, then the density is decreasing over $(0,1)$. Consequently, the TPFUD has no interior mode, and its supremum is reached at the left boundary in the limiting sense:

$$\sup_{0<x<1} f(x;\alpha,\beta) = \lim_{x\to 0^+} f(x;\alpha,\beta) = \frac{a_2^2a_0}{a_0a_2 + a_1}.$$

Hence, the TPFUD is either unimodal with a unique interior mode given by Eq (3.2) or monotonically decreasing on $(0,1)$, according to whether $a_0a_2 < 2a_0 + a_1$ or $a_0a_2 \geq 2a_0 + a_1$.

3.2. Quantile function and random sample generation

This subsection derives the quantile function (QF) of the TPFUD, which plays a central role in statistical inference by specifying the threshold below which a given proportion of observations falls. Moreover, the QF enables random sample generation via the inverse transform method.

Theorem 3.1 (QF)**.** *Let $X \sim \mathrm{TPFUD}(\alpha,\beta)$ with CDF given in Eq (2.4). For $0 < u < 1$, the QF is given by*

$$Q_u = \frac{-a_1 W_{-1}\big(-c(1-u)e^{-c}\big) - b}{a_1 a_2 - a_1 W_{-1}\big(-c(1-u)e^{-c}\big) - b}, \tag{3.3}$$

where $b = a_0 a_2 + a_1$, $c = \frac{b}{a_1}$, and $W_{-1}(\cdot)$ denotes the lower real branch of the Lambert W function.

Proof. Let $F(x;\alpha,\beta) = u$. From Eq (2.4), $\left[\frac{a_2\left(a_0 + a_1\frac{x}{1-x}\right) + a_1}{b}\right] e^{-a_2\frac{x}{1-x}} = 1-u$. Setting $z = \frac{x}{1-x}$ yields

$$\left(1 + \frac{a_1 a_2}{b} z\right) e^{-a_2 z} = 1-u.$$

Substituting $t = 1 + \frac{a_1 a_2}{b} z$ gives $t\,e^{-\frac{b}{a_1}t} = (1-u)e^{-\frac{b}{a_1}}$. Multiplying by $-\frac{b}{a_1}$ and applying the Lambert W relation $W_k(\xi e^{\xi}) = \xi$ yields

$$-\frac{b}{a_1} t = W_k\!\left(-\frac{b}{a_1}(1-u)e^{-\frac{b}{a_1}}\right).$$

Since $c = \frac{b}{a_1} = 1 + \frac{a_0 a_2}{a_1} > 1$, and $0 < u < 1$, setting $\xi = -c(1-u)e^{-c}$ gives $-ce^{-c} < \xi < 0$. Moreover, because $c > 1$ implies $ce^{-c} < 1/e$, it follows that $\xi \in (-1/e, 0)$, on which both real branches W_0 and W_{-1} are defined.

For the principal branch, $-1 < W_0(\xi) < 0$, and hence $0 < -\frac{1}{c}W_0(\xi) < \frac{1}{c} < 1$. Thus $t < 1$, which gives $z = \frac{c}{a_2}(t-1) < 0$, so W_0 does not yield an admissible solution.

For the lower branch, W_{-1} is strictly decreasing on $(-1/e, 0)$ and $W_{-1}(-ce^{-c}) = -c$. Since $\xi > -ce^{-c}$, we obtain $W_{-1}(\xi) < -c$ and, therefore, $t = -\frac{1}{c}W_{-1}(\xi) > 1$. Hence, $z > 0$, which implies $x = z/(1+z) \in (0,1)$. Thus, W_{-1} is the unique admissible real branch.

Consequently, substituting $t = -\frac{1}{c}W_{-1}\big(-c(1-u)e^{-c}\big)$ into $z = \frac{c}{a_2}(t-1)$ and then into $x = \frac{z}{1+z}$ yields Eq (3.3), completing the proof. □

Remark 3.1 (Quartiles and shape characteristics)**.** *The first quartile ($Q_{0.25}$), second quartile ($Q_{0.5}$), and third quartile ($Q_{0.75}$) follow from Eq (3.3) with $u = 0.25, 0.5, 0.75$. Quantile-based descriptive measures include the following.*

- Bowley's skewness: $B_s = \dfrac{Q_{0.75} + Q_{0.25} - 2Q_{0.5}}{Q_{0.75} - Q_{0.25}}$;
- Moors' kurtosis: $M_k = \dfrac{Q_{0.875} - Q_{0.625} + Q_{0.375} - Q_{0.125}}{Q_{0.75} - Q_{0.25}}$;
- MacGillivray's skewness: $M_s(u) = \dfrac{Q_{1-u} + Q_u - 2Q_{0.5}}{Q_{1-u} - Q_u}$, $0 < u < 1$.

Remark 3.2 (Random sample generation)**.** *To generate a random sample of size n from* $\mathrm{TPFUD}(\alpha,\beta)$*, use the inverse transform method:*

Step 1. Generate $U_1, \ldots, U_n \overset{\text{i.i.d.}}{\sim}$ Uniform(0, 1);

Step 2. For each $i = 1, \ldots, n$, compute $X_i = \frac{-a_1 W_{-1}\left(-c(1-U_i)e^{-c}\right)-b}{a_1 a_2 - a_1 W_{-1}\left(-c(1-U_i)e^{-c}\right)-b}$, where $b = a_0 a_2 + a_1$ and $c = \frac{b}{a_1}$.

3.3. Moments and related statistical quantities

This subsection derives explicit expressions for the non-central moments, central moments, moment-generating function, characteristic function, cumulant-generating function, and incomplete moments of the TPFUD. In addition, key descriptive measures such as the mean, variance, skewness, kurtosis, and coefficient of variation are obtained and discussed.

Theorem 3.2 (Moments)**.** *Let $X \sim$ TPFUD(α,β) with the PDF given in Eq (2.3). Then for any real $r > -1$, the r^{th} non-central moment (N-CM) of X exists and is given by*

$$\mu'_r = \mathbb{E}[X^r] = \frac{a_2^2}{a_0 a_2 + a_1}\Big[a_0\,\Gamma(r+1)\,U(r+1, 2, a_2) + a_1\,\Gamma(r+2)\,U(r+2, 3, a_2)\Big], \tag{3.4}$$

where $U(\cdot,\cdot,\cdot)$ denotes Tricomi's confluent hypergeometric function.

Proof. By definition, we have

$$\mu'_r = \int_0^1 x^r f(x;\alpha,\beta)\,dx = \frac{a_2^2}{a_0 a_2 + a_1}\int_0^1 x^r\Big(a_0 + a_1\frac{x}{1-x}\Big)\frac{e^{-a_2\frac{x}{1-x}}}{(1-x)^2}\,dx.$$

Applying the transformation $t = \frac{x}{1-x}$, with $x = \frac{t}{1+t}$ and $\frac{dx}{(1-x)^2} = dt$, yields

$$\mu'_r = \frac{a_2^2}{a_0 a_2 + a_1}\int_0^\infty \Big(\frac{t}{1+t}\Big)^r (a_0 + a_1 t)e^{-a_2 t}\,dt.$$

Splitting the integral gives

$$\mu'_r = \frac{a_2^2}{a_0 a_2 + a_1}\Big[a_0\int_0^\infty t^r(1+t)^{-r}e^{-a_2 t}\,dt + a_1\int_0^\infty t^{r+1}(1+t)^{-r}e^{-a_2 t}\,dt\Big].$$

Using the integral representation of Tricomi's confluent hypergeometric function

$$U(a,b,z) = \frac{1}{\Gamma(a)}\int_0^\infty e^{-zt}t^{a-1}(1+t)^{b-a-1}\,dt, \qquad \Re(a) > 0,\ \Re(z) > 0. \tag{3.5}$$

By setting $a = r+1$, $b = 2$ for the first integral and $a = r+2$, $b = 3$ for the second, we obtain

$$\int_0^\infty t^r(1+t)^{-r}e^{-a_2 t}\,dt = \Gamma(r+1)\,U(r+1, 2, a_2),$$
$$\int_0^\infty t^{r+1}(1+t)^{-r}e^{-a_2 t}\,dt = \Gamma(r+2)\,U(r+2, 3, a_2).$$

Substituting these evaluations yields Eq (3.4). The condition $r > -1$ ensures convergence at $t = 0$, while $e^{-a_2 t}$ guarantees convergence as $t \to \infty$. □

Corollary 3.1 (Descriptive measures). *For $X \sim$ TPFUD(α,β), the descriptive measures are expressed in terms of the N-CMs from Theorem 3.2 as follows.*

- Mean (μ):

$$\mu = \mu_1' = \frac{a_2^2}{a_0a_2 + a_1}[a_0U(2,2,a_2) + 2a_1U(3,3,a_2)].$$

- Variance (σ^2):

$$\sigma^2 = \mu_2' - (\mu_1')^2,$$

where

$$\mu_2' = \frac{a_2^2}{a_0a_2 + a_1}[2a_0U(3,2,a_2) + 6a_1U(4,3,a_2)].$$

- Skewness (γ_1):

$$\gamma_1 = \frac{\mu_3' - 3\mu_1'\mu_2' + 2(\mu_1')^3}{\sigma^3},$$

where

$$\mu_3' = \frac{a_2^2}{a_0a_2 + a_1}[6a_0U(4,2,a_2) + 24a_1U(5,3,a_2)].$$

- Kurtosis (γ_2):

$$\gamma_2 = \frac{\mu_4' - 4\mu_1'\mu_3' + 6(\mu_1')^2\mu_2' - 3(\mu_1')^4}{\sigma^4} - 3,$$

where

$$\mu_4' = \frac{a_2^2}{a_0a_2 + a_1}[24a_0U(5,2,a_2) + 120a_1U(6,3,a_2)].$$

- Coefficient of variation ($\mathcal{CV}$):

$$\mathcal{CV} = \frac{\sqrt{\mu_2' - (\mu_1')^2}}{\mu_1'}.$$

- Coefficient of dispersion ($\mathcal{CD}$):

$$\mathcal{CD} = \frac{\mu_2' - (\mu_1')^2}{\mu_1'}.$$

Theorem 3.3 (Moment-generating function). *Let $X \sim$ TPFUD(α,β) with PDF given in Eq (2.3). Then the moment-generating function (MGF) of X exists for all $t \in \mathbb{R}$ and is given by*

$$M_X(t) = \mathbb{E}[e^{tX}] = \sum_{r=0}^{\infty} \frac{t^r}{r!} \frac{a_2^2}{a_0a_2 + a_1}[a_0\,\Gamma(r+1)\,U(r+1,2,a_2) + a_1\,\Gamma(r+2)\,U(r+2,3,a_2)], \tag{3.6}$$

where the series converges absolutely for all $t \in \mathbb{R}$.

Proof. By definition, we have

$$M_X(t) = \int_0^1 e^{tx} f(x;\alpha,\beta)\,dx.$$

Expanding $e^{tx} = \sum_{r=0}^{\infty} \frac{t^r x^r}{r!}$ and interchanging sum and integral (justified since $0 < X < 1$ ensures $\mathbb{E}(e^{tX}) < \infty$ for all $t \in \mathbb{R}$), we obtain

$$M_X(t) = \sum_{r=0}^{\infty} \frac{t^r}{r!} \int_0^1 x^r f(x;\alpha,\beta)\,dx = \sum_{r=0}^{\infty} \frac{t^r}{r!} \mu'_r.$$

Substituting Eq (3.4) yields Eq (3.6). □

Remark 3.3. *The r^{th} N-CM follows from Eq (3.6) as $\mu'_r = \frac{d^r}{dt^r} M_X(t)\big|_{t=0}$, $r = 1, 2, \ldots$.*

Definition 3.1 (Cumulant-generating function). *The cumulant-generating function (CGF) of a random variable X with MGF $M_X(t)$ is defined as*

$$K_X(t) = \log M_X(t), \tag{3.7}$$

for all t in an open neighborhood of the origin where $M_X(t)$ exists and is finite.

Remark 3.4. *For $X \sim$ TPFUD(α,β), the CGF exists for all $t \in \mathbb{R}$ and is given by*

$$K_X(t) = \log\left[\sum_{r=0}^{\infty} \frac{t^r}{r!} \frac{a_2^2}{a_0 a_2 + a_1}\left(a_0\,\Gamma(r+1)\,U(r+1,2,a_2) + a_1\,\Gamma(r+2)\,U(r+2,3,a_2)\right)\right]. \tag{3.8}$$

The r^{th} cumulant $\kappa_r = K_X^{(r)}(0) = \frac{d^r}{dt^r} K_X(t)\big|_{t=0}$, $r = 1, 2, \ldots$ yields the descriptive measures

$$\mu = \kappa_1, \qquad \sigma^2 = \kappa_2, \qquad \gamma_1 = \frac{\kappa_3}{\kappa_2^{3/2}}, \qquad \gamma_2 = \frac{\kappa_4}{\kappa_2^2} - 3.$$

Theorem 3.4 (Incomplete moments). *Let $X \sim$ TPFUD(α,β) with PDF given in Eq (2.3). Then for $0 < x < 1$ and any $r \in \mathbb{N}_0$, the r^{th} incomplete moment (IM)*

$$\psi_r(x) = \mathbb{E}[X^r \mathbf{1}_{\{X \le x\}}] = \int_0^x t^r f(t;\alpha,\beta)\,dt \tag{3.9}$$

admits the closed-form representation

$$\psi_r(x) = \frac{a_2^2}{a_0 a_2 + a_1}\left[a_0\,\mathcal{I}_r\!\left(\frac{x}{1-x}\right) + a_1\,\mathcal{J}_r\!\left(\frac{x}{1-x}\right)\right], \tag{3.10}$$

where, for $m \in \mathbb{N}_0$ and $y > 0$, we have

$$\mathcal{I}_m(y) = e^{a_2} \sum_{k=0}^{m} (-1)^k \binom{m}{k} a_2^{k-1}\left[\Gamma(1-k, a_2) - \Gamma(1-k, a_2(1+y))\right], \tag{3.11}$$

and

$$\mathcal{J}_m(y) = e^{a_2} \sum_{k=0}^{m+1} (-1)^k \binom{m+1}{k} a_2^{k-2}\left[\Gamma(2-k, a_2) - \Gamma(2-k, a_2(1+y))\right], \tag{3.12}$$

with $\Gamma(s,z) = \int_z^{\infty} t^{s-1} e^{-t}\,dt$ denoting the upper incomplete gamma function.

Proof. Substituting Eq (2.3) into Eq (3.9) and applying the transformation $u = \frac{t}{1-t}$, with $t = \frac{u}{1+u}$ and $\frac{dt}{(1-t)^2} = du$, yields

$$\psi_r(x) = \frac{a_2^2}{a_0a_2 + a_1}\left[a_0 \int_0^y u^r(1+u)^{-r}e^{-a_2u}\,du + a_1 \int_0^y u^{r+1}(1+u)^{-r}e^{-a_2u}\,du\right], \tag{3.13}$$

where $y = \frac{x}{1-x}$. Defining

$$\mathcal{I}_m(y) = \int_0^y u^m(1+u)^{-m}e^{-a_2u}\,du \quad \text{and} \quad \mathcal{J}_m(y) = \int_0^y u^{m+1}(1+u)^{-m}e^{-a_2u}\,du$$

establishes Eq (3.10).

To evaluate $\mathcal{I}_m(y)$, expand $(\frac{u}{1+u})^m = \sum_{k=0}^{m}(-1)^k\binom{m}{k}(1+u)^{-k}$ and substitute $v = 1+u$, $z = a_2v$ to obtain

$$\begin{aligned}\mathcal{I}_m(y) &= e^{a_2}\sum_{k=0}^{m}(-1)^k\binom{m}{k}\int_1^{1+y} v^{-k}e^{-a_2v}\,dv\\ &= e^{a_2}\sum_{k=0}^{m}(-1)^k\binom{m}{k}a_2^{k-1}\Big[\Gamma(1-k,a_2) - \Gamma(1-k,a_2(1+y))\Big],\end{aligned}$$

proving Eq (3.11). For $\mathcal{J}_m(y)$, use $u^{m+1}(1+u)^{-m} = \sum_{k=0}^{m+1}(-1)^k\binom{m+1}{k}(1+u)^{1-k}$ with the same substitutions to obtain

$$\begin{aligned}\mathcal{J}_m(y) &= e^{a_2}\sum_{k=0}^{m+1}(-1)^k\binom{m+1}{k}\int_1^{1+y} v^{1-k}e^{-a_2v}\,dv\\ &= e^{a_2}\sum_{k=0}^{m+1}(-1)^k\binom{m+1}{k}a_2^{k-2}\Big[\Gamma(2-k,a_2) - \Gamma(2-k,a_2(1+y))\Big],\end{aligned}$$

proving Eq (3.12). Substituting $\mathcal{I}_r(y)$ and $\mathcal{J}_r(y)$ into Eq (3.10) completes the proof. □

Remark 3.5. *In Eqs (3.11) and (3.12), the second argument of each upper incomplete gamma function satisfies $z \geq a_2 > 0$. For fixed $z > 0$, $\Gamma(s,z) = \int_z^\infty t^{s-1}e^{-t}\,\mathrm{d}t$ is an entire function of s. Hence, it is finite for every real s, including all nonpositive integers, and has no poles. This contrasts with the analytically continued complete gamma function $\Gamma(s)$, which has simple poles at $s = 0, -1, -2, \ldots$. The required values may be evaluated recursively using*

$$\Gamma(s+1,z) = s\,\Gamma(s,z) + z^s e^{-z}, \qquad \Gamma(0,z) = E_1(z) = -\,\mathrm{Ei}(-z), \tag{3.14}$$

with downward recursion when required. Hence, the finite differences in Eqs (3.11) and (3.12) are well defined and contain no mathematical singularities for all admissible parameter values.

This analytical regularity should, however, be distinguished from floating-point cancellation in the alternating finite sums. For large m, or when substantial cancellation occurs, the defining integral representations of $\mathcal{I}_m(y)$ and $\mathcal{J}_m(y)$ may be evaluated directly by adaptive quadrature, or the finite sums may be computed using increased precision.

Remark 3.6. *The r^{th} IM in Eq (3.10) is the truncated form of the r^{th} N-CM in Eq (3.4), with $\lim_{x\to 1^-} \psi_r(x) = \mu'_r$ for $r > -1$.*

Remark 3.7. *Two fundamental special cases arise from Theorem 3.4:*

(1) For $r = 0$, using $\Gamma(1, z) = e^{-z}$ and $\Gamma(2, z) = e^{-z}(1 + z)$ in Eqs (3.11) and (3.12) yields

$$\psi_0(x) = 1 - \frac{a_0a_2 + a_1 + a_1a_2\frac{x}{1-x}}{a_0a_2 + a_1}e^{-a_2\frac{x}{1-x}} = F(x; \alpha, \beta), \tag{3.15}$$

recovering Eq (2.4).

(2) For $r = 1$, using $\Gamma(0, z) = -\operatorname{Ei}(-z)$, $\Gamma(1, z) = e^{-z}$, and $\Gamma(2, z) = e^{-z}(1 + z)$ in Eqs (3.11) and (3.12) yields

$$\begin{aligned}\psi_1(x) = \frac{a_2^2}{a_0a_2 + a_1}\Bigg[&a_0\Bigg\{\frac{1 - e^{-a_2\frac{x}{1-x}}}{a_2} + e^{a_2}[\operatorname{Ei}(-a_2) - \operatorname{Ei}(-\frac{a_2}{1 - x})]\Bigg\}\\ &+ a_1\Bigg\{\frac{1 - a_2 + (a_2 - 1 - a_2\frac{x}{1-x})e^{-a_2\frac{x}{1-x}}}{a_2^2} + e^{a_2}[\operatorname{Ei}(-\frac{a_2}{1 - x}) - \operatorname{Ei}(-a_2)]\Bigg\}\Bigg],\end{aligned} \tag{3.16}$$

with $\lim_{x\to 1^-} \psi_1(x) = \mu$, connecting to the Lorenz and Bonferroni curves, mean and median deviations, and mean residual life function.

Theorem 3.5 (Probability-weighted moments)**.** *Let $X \sim$ TPFUD(α, β) with PDF, CDF, and RF given in Eqs (2.3)–(2.5). Then for any real $p > -1$ and the integers $r, s \in \mathbb{N}_0$, the probability-weighted moment*

$$M_{p,r,s} = \mathbb{E}[X^pF(X; \alpha, \beta)^rR(X; \alpha, \beta)^s] \tag{3.17}$$

exists and admits the finite-sum representation

$$\begin{aligned}M_{p,r,s} = \frac{a_2^2}{a_0a_2 + a_1}\sum_{j=0}^{r}(-1)^j\binom{r}{j}\sum_{i=0}^{j+s}\binom{j+s}{i}\left(\frac{a_1a_2}{a_0a_2 + a_1}\right)^i\Big[&a_0\,\Gamma(p + i + 1)\,U(p + i + 1, i + 2, (j + s + 1)a_2)\\ &+ a_1\,\Gamma(p + i + 2)\,U(p + i + 2, i + 3, (j + s + 1)a_2)\Big].\end{aligned} \tag{3.18}$$

Proof. By definition,

$$M_{p,r,s} = \int_0^1 x^pF(x; \alpha, \beta)^rR(x; \alpha, \beta)^sf(x; \alpha, \beta)\,dx. \tag{3.19}$$

Since $0 \le F(x; \alpha, \beta) \le 1$ and $0 \le R(x; \alpha, \beta) \le 1$ for $0 < x < 1$, we have

$$0 \le x^pF(x)^rR(x)^sf(x) \le x^pf(x).$$

Hence, $M_{p,r,s}$ is well defined for all $p > -1$. Substituting Eqs (2.3)–(2.5) into Eq (3.19) with $b = a_0a_2 + a_1$ yields

$$M_{p,r,s} = \frac{a_2^2}{b^{s+1}} \int_0^1 x^p \Big[1 - \frac{a_2(a_0 + a_1 \frac{x}{1-x}) + a_1}{b} e^{-a_2 \frac{x}{1-x}}\Big]^r \big[a_2(a_0 + a_1 \frac{x}{1-x}) + a_1\big]^s (a_0 + a_1 \frac{x}{1-x})$$
$$\times \frac{e^{-(s+1)a_2 \frac{x}{1-x}}}{(1-x)^2}\, dx. \tag{3.20}$$

Applying the transformation $t = \frac{x}{1-x}$, with $x = \frac{t}{1+t}$ and $\frac{dx}{(1-x)^2} = dt$, Eq (3.20) becomes

$$M_{p,r,s} = \frac{a_2^2}{b^{s+1}} \int_0^\infty \Big(\frac{t}{1+t}\Big)^p \Big[1 - \frac{b + a_1 a_2 t}{b} e^{-a_2 t}\Big]^r (b + a_1 a_2 t)^s (a_0 + a_1 t) e^{-(s+1)a_2 t}\, dt. \tag{3.21}$$

Since $r \in \mathbb{N}_0$, the binomial theorem gives

$$\Big[1 - \frac{b + a_1 a_2 t}{b} e^{-a_2 t}\Big]^r = \sum_{j=0}^{r} (-1)^j \binom{r}{j} \Big(\frac{b + a_1 a_2 t}{b}\Big)^j e^{-j a_2 t}. \tag{3.22}$$

Substituting Eq (3.22) into Eq (3.21) yields

$$M_{p,r,s} = \frac{a_2^2}{b^{s+1}} \sum_{j=0}^{r} (-1)^j \binom{r}{j} \frac{1}{b^j} \int_0^\infty \Big(\frac{t}{1+t}\Big)^p (b + a_1 a_2 t)^{j+s} (a_0 + a_1 t) e^{-(j+s+1)a_2 t}\, dt. \tag{3.23}$$

Since $j + s \in \mathbb{N}_0$, another application of the binomial theorem gives

$$(b + a_1 a_2 t)^{j+s} = \sum_{i=0}^{j+s} \binom{j+s}{i} b^{j+s-i} (a_1 a_2)^i t^i. \tag{3.24}$$

Substituting Eq (3.24) into Eq (3.23) yields

$$M_{p,r,s} = \frac{a_2^2}{b} \sum_{j=0}^{r} (-1)^j \binom{r}{j} \sum_{i=0}^{j+s} \binom{j+s}{i} \Big(\frac{a_1 a_2}{b}\Big)^i \int_0^\infty t^{p+i} (1+t)^{-p} (a_0 + a_1 t) e^{-(j+s+1)a_2 t}\, dt. \tag{3.25}$$

Splitting the integral in Eq (3.25) and using the Tricomi representation

$$U(a, b, z) = \frac{1}{\Gamma(a)} \int_0^\infty e^{-zt} t^{a-1} (1+t)^{b-a-1} dt$$

with $z = (j + s + 1)a_2$ gives

$$\int_0^\infty t^{p+i} (1+t)^{-p} e^{-(j+s+1)a_2 t}\, dt = \Gamma(p + i + 1)\, U\big(p + i + 1, i + 2, (j + s + 1)a_2\big),$$
$$\int_0^\infty t^{p+i+1} (1+t)^{-p} e^{-(j+s+1)a_2 t}\, dt = \Gamma(p + i + 2)\, U\big(p + i + 2, i + 3, (j + s + 1)a_2\big).$$

Substituting these evaluations into Eq (3.25) and replacing $b = a_0 a_2 + a_1$ yields Eq (3.18). □

Remark 3.8 (Special case $r = s = 0$)**.** *Setting $r = s = 0$ in Eq (3.18) gives $M_{p,0,0} = \mu'_p$, confirming that the PWM family extends the conventional moment structure.*

3.4. Lorenz and bonferroni curves

The Lorenz ($\mathcal{L}_O$) and Bonferroni ($\mathcal{B}_O$) curves are important tools in economics, insurance, medicine, demography, reliability analysis, and related fields, providing informative measures of concentration, inequality, and heterogeneity for bounded data. For $X \sim$ TPFUD(α,β), these curves are defined, respectively, by

$$\mathcal{L}_O(u) = \frac{1}{\mu}\int_0^{Q_u} x f(x;\alpha,\beta)\,dx, \quad \mathcal{B}_O(u) = \frac{1}{u\mu}\int_0^{Q_u} x f(x;\alpha,\beta)\,dx, \quad 0 < u < 1, \tag{3.26}$$

where $\mu = \mathbb{E}(X)$ is given in Corollary 3.1 and Q_u denotes the QF from Eq (3.3).

Expressing Eq (3.26) in terms of the first IM yields the compact representations

$$\mathcal{L}_O(u) = \frac{\psi_1(Q_u)}{\mu}, \quad \mathcal{B}_O(u) = \frac{\psi_1(Q_u)}{u\mu} = \frac{\mathcal{L}_O(u)}{u}, \quad 0 < u < 1. \tag{3.27}$$

Substituting the expression for μ from Corollary 3.1, together with Eq (3.16), into Eq (3.27) yields

$$\begin{aligned}\mathcal{L}_O(u) = \frac{1}{a_0 U(2,2,a_2) + 2a_1 U(3,3,a_2)}\Bigg[a_0\Bigg\{\frac{1 - e^{-a_2\frac{Q_u}{1-Q_u}}}{a_2} + e^{a_2}[\mathrm{Ei}(-a_2) - \mathrm{Ei}(-\frac{a_2}{1-Q_u})]\Bigg\}\\ + a_1\Bigg\{\frac{1 - a_2 + (a_2 - 1 - a_2\frac{Q_u}{1-Q_u})e^{-a_2\frac{Q_u}{1-Q_u}}}{a_2^2} + e^{a_2}[\mathrm{Ei}(-\frac{a_2}{1-Q_u}) - \mathrm{Ei}(-a_2)]\Bigg\}\Bigg], \quad 0 < u < 1,\end{aligned} \tag{3.28}$$

and

$$\begin{aligned}\mathcal{B}_O(u) = \frac{1}{u[a_0 U(2,2,a_2) + 2a_1 U(3,3,a_2)]}\Bigg[a_0\Bigg\{\frac{1 - e^{-a_2\frac{Q_u}{1-Q_u}}}{a_2} + e^{a_2}[\mathrm{Ei}(-a_2) - \mathrm{Ei}(-\frac{a_2}{1-Q_u})]\Bigg\}\\ + a_1\Bigg\{\frac{1 - a_2 + (a_2 - 1 - a_2\frac{Q_u}{1-Q_u})e^{-a_2\frac{Q_u}{1-Q_u}}}{a_2^2} + e^{a_2}[\mathrm{Ei}(-\frac{a_2}{1-Q_u}) - \mathrm{Ei}(-a_2)]\Bigg\}\Bigg], \quad 0 < u < 1.\end{aligned} \tag{3.29}$$

3.5. Mean and median deviations

Measures of absolute dispersion about the mean and the median provide useful summaries of the variability of a bounded distribution. For $X \sim$ TPFUD(α,β), the mean deviation (MD) about the mean $\mu = \mathbb{E}(X)$ and the MD about the median $M = Q_{0.5}$ are defined, respectively, by

$$\delta_\mu = \mathbb{E}[|X - \mu|] = \int_0^1 |x - \mu| f(x;\alpha,\beta)\,dx, \tag{3.30}$$

and

$$\delta_M = \mathbb{E}[|X - M|] = \int_0^1 |x - M| f(x;\alpha,\beta)\,dx. \tag{3.31}$$

By splitting the integrals in Eqs (3.30) and (3.31) at $x = \mu$ and $x = M$, respectively, and using $F(M; \alpha, \beta) = \frac{1}{2}$, we obtain the compact representations

$$\delta_\mu = 2\mu F(\mu; \alpha, \beta) - 2\psi_1(\mu), \tag{3.32}$$

and

$$\delta_M = \mu - 2\psi_1(M). \tag{3.33}$$

Substituting Eqs (2.4) and (3.16) into Eq (3.32) yields

$$\begin{aligned}\delta_\mu = 2\mu\Big\{1 - \Big[\frac{a_2(a_0 + a_1\frac{\mu}{1-\mu}) + a_1}{a_0a_2 + a_1}\Big]e^{-a_2\frac{\mu}{1-\mu}}\Big\} - \frac{2a_2^2}{a_0a_2 + a_1}\Big[a_0\Big\{\frac{1 - e^{-a_2\frac{\mu}{1-\mu}}}{a_2} + e^{a_2}[\mathrm{Ei}(-a_2) - \mathrm{Ei}(-\frac{a_2}{1-\mu})]\Big\}\\ + a_1\Big\{\frac{1 - a_2 + (a_2 - 1 - a_2\frac{\mu}{1-\mu})e^{-a_2\frac{\mu}{1-\mu}}}{a_2^2} + e^{a_2}[\mathrm{Ei}(-\frac{a_2}{1-\mu}) - \mathrm{Ei}(-a_2)]\Big\}\Big].\end{aligned} \tag{3.34}$$

Similarly, substituting Eq (3.16) into Eq (3.33) yields

$$\begin{aligned}\delta_M = \mu - \frac{2a_2^2}{a_0a_2 + a_1}\Big[a_0\Big\{\frac{1 - e^{-a_2\frac{M}{1-M}}}{a_2} + e^{a_2}[\mathrm{Ei}(-a_2) - \mathrm{Ei}(-\frac{a_2}{1-M})]\Big\}\\ + a_1\Big\{\frac{1 - a_2 + (a_2 - 1 - a_2\frac{M}{1-M})e^{-a_2\frac{M}{1-M}}}{a_2^2} + e^{a_2}[\mathrm{Ei}(-\frac{a_2}{1-M}) - \mathrm{Ei}(-a_2)]\Big\}\Big],\end{aligned} \tag{3.35}$$

where $M = Q_{0.5}$ is obtained from Eq (3.3) by setting $u = \frac{1}{2}$.

3.6. Mean residual life and mean inactivity time

The mean residual life (MRL) and mean inactivity time (MIT) functions characterize the conditional behavior of a lifetime variable beyond and before a fixed time point, respectively. For $X \sim$ TPFUD(α, β), the MRL at $x \in (0, 1)$ is defined by

$$m_r(x; \alpha, \beta) = \mathbb{E}[X - x \mid X > x] = \frac{1}{R(x; \alpha, \beta)} \int_x^1 (t - x) f(t; \alpha, \beta)\, dt. \tag{3.36}$$

Expanding the integrand in Eq (3.36) and using $\int_x^1 f(t; \alpha, \beta)\, dt = R(x; \alpha, \beta)$ yields

$$m_r(x; \alpha, \beta) = \frac{1}{R(x; \alpha, \beta)} \int_x^1 t f(t; \alpha, \beta)\, dt - x.$$

Since $\int_x^1 t f(t; \alpha, \beta)\, dt = \mu - \psi_1(x)$, where ψ_1 denotes the first IM, the MRL admits the compact representation

$$m_r(x; \alpha, \beta) = \frac{\mu - \psi_1(x)}{R(x; \alpha, \beta)} - x, \quad 0 < x < 1. \tag{3.37}$$

Substituting the expression for μ given in Corollary 3.1, together with Eqs (2.5) and (3.16), into Eq (3.37) yields

$$m_r(x;\alpha,\beta) = \frac{a_2^2 e^{a_2 \frac{x}{1-x}}}{a_2(a_0 + a_1 \frac{x}{1-x}) + a_1}\Bigg[a_0 U(2,2,a_2) + 2a_1 U(3,3,a_2) - a_0\Big\{\frac{1 - e^{-a_2 \frac{x}{1-x}}}{a_2} + e^{a_2}[\mathrm{Ei}(-a_2) - \mathrm{Ei}(-\frac{a_2}{1-x})]\Big\} - a_1\Big\{\frac{1 - a_2 + (a_2 - 1 - a_2 \frac{x}{1-x})e^{-a_2 \frac{x}{1-x}}}{a_2^2} + e^{a_2}[\mathrm{Ei}(-\frac{a_2}{1-x}) - \mathrm{Ei}(-a_2)]\Big\}\Bigg] - x. \tag{3.38}$$

Similarly, the MIT at $x \in (0,1)$ is defined by

$$m_i(x;\alpha,\beta) = \mathbb{E}[x - X \mid X \le x] = \frac{1}{F(x;\alpha,\beta)} \int_0^x (x-t) f(t;\alpha,\beta)\,dt. \tag{3.39}$$

Expanding and simplifying Eq (3.39) yields the compact representation

$$m_i(x;\alpha,\beta) = x - \frac{\psi_1(x)}{F(x;\alpha,\beta)}, \quad 0 < x < 1. \tag{3.40}$$

Substituting Eqs (2.4) and (3.16) into Eq (3.40) gives

$$m_i(x;\alpha,\beta) = x - \Big\{a_0 a_2(1 - e^{-a_2 \frac{x}{1-x}}) + a_1[1 - a_2 + (a_2 - 1 - a_2 \frac{x}{1-x})e^{-a_2 \frac{x}{1-x}}] + (a_0 - a_1)a_2^2 e^{a_2}[\mathrm{Ei}(-a_2) - \mathrm{Ei}(-\frac{a_2}{1-x})]\Big\}\Big\{a_0 a_2 + a_1 - (a_0 a_2 + a_1 + a_1 a_2 \frac{x}{1-x})e^{-a_2 \frac{x}{1-x}}\Big\}^{-1}. \tag{3.41}$$

In particular, the MRL and MIT exhibit the boundary behaviors

$$\lim_{x\to 0^+} m_r(x;\alpha,\beta) = \mu, \quad \lim_{x\to 1^-} m_r(x;\alpha,\beta) = 0,$$

$$\lim_{x\to 0^+} m_i(x;\alpha,\beta) = 0, \quad \lim_{x\to 1^-} m_i(x;\alpha,\beta) = 1 - \mu,$$

providing complementary descriptions of upper-tail and lower-tail lifetime behavior.

3.7. Actuarial measures

In this section, actuarial measures of the TPFUD are presented, with a particular emphasis on tail-based risk summaries that are useful in insurance mathematics and risk management. Let $X \sim \mathrm{TPFUD}(\alpha,\beta)$ with PDF, CDF, RF, and QF given in Eqs (2.3)–(2.5) and (3.3), respectively.

3.7.1. Mean excess function

In actuarial science, the mean excess (ME) function, also called the ME loss function, is defined as the expected excess over a threshold x, given that the loss exceeds x:

$$e(x;\alpha,\beta) = \mathbb{E}(X - x \mid X > x), \quad 0 < x < 1.$$

This quantity is identical to the MRL function $m_r(x;\alpha,\beta)$ derived in Eqs (3.36) and (3.38), where the relationship $e(x;\alpha,\beta) = m_r(x;\alpha,\beta)$ holds for all $x \in (0,1)$.

3.7.2. Tail value at risk

The tail value at risk (TVaR), also known as the conditional tail expectation, is the conditional mean of the loss, given that it exceeds the corresponding quantile. For the TPFUD, it is defined by

$$\mathrm{TVaR}(u) = \mathbb{E}(X \mid X > Q_u) = \frac{1}{1-u}\int_{Q_u}^{1} t\, f(t;\alpha,\beta)\, dt = \frac{\mu - \psi_1(Q_u)}{1-u}, \quad 0 < u < 1. \tag{3.42}$$

Substituting the explicit expressions of μ and $\psi_1(Q_u)$ into Eq (3.42), we obtain

$$\begin{aligned}\mathrm{TVaR}(u) = \frac{1}{1-u}\Bigg[&\frac{a_2^2}{a_0a_2+a_1}\Big(a_0U(2,2,a_2)+2a_1U(3,3,a_2)\Big)\\ &-\frac{a_2^2}{a_0a_2+a_1}\Bigg(a_0\Bigg\{\frac{1-e^{-a_2\frac{Q_u}{1-Q_u}}}{a_2}+e^{a_2}\Big[\mathrm{Ei}(-a_2)-\mathrm{Ei}\Big(-\frac{a_2}{1-Q_u}\Big)\Big]\Bigg\}\\ &+a_1\Bigg\{\frac{1-a_2+\Big(a_2-1-a_2\frac{Q_u}{1-Q_u}\Big)e^{-a_2\frac{Q_u}{1-Q_u}}}{a_2^2}+e^{a_2}\Big[\mathrm{Ei}\Big(-\frac{a_2}{1-Q_u}\Big)-\mathrm{Ei}(-a_2)\Big]\Bigg\}\Bigg)\Bigg], \quad 0<u<1.\end{aligned} \tag{3.43}$$

3.7.3. Tail variance

The tail variance (TV) measures the conditional variability of losses beyond the corresponding value at risk, providing a second-order assessment of tail risk. It is defined as

$$\begin{aligned}\mathrm{TV}(u) &= \mathrm{Var}(X \mid X > Q_u)\\ &= \mathbb{E}\Big(X^2 \mid X > Q_u\Big) - \Big[\mathbb{E}(X \mid X > Q_u)\Big]^2\\ &= \frac{1}{1-u}\int_{Q_u}^{1} t^2 f(t;\alpha,\beta)\, dt - [\mathrm{TVaR}(u)]^2\\ &= \frac{\mu_2' - \psi_2(Q_u)}{1-u} - [\mathrm{TVaR}(u)]^2, \quad 0<u<1,\end{aligned} \tag{3.44}$$

where $\mu_2' = \mathbb{E}(X^2)$ is the second N-CM and $\psi_2(\cdot)$ is the second IM. Using Corollary 3.1 and Eq (3.10), we have

$$\psi_2(x) = \frac{a_2^2}{a_0a_2+a_1}\left[a_0\,\mathcal{I}_2\Big(\frac{x}{1-x}\Big) + a_1\,\mathcal{J}_2\Big(\frac{x}{1-x}\Big)\right],$$

where

$$\mathcal{I}_2(y) = e^{a_2}\sum_{k=0}^{2}(-1)^k\binom{2}{k}a_2^{k-1}\Big[\Gamma(1-k,a_2)-\Gamma(1-k,a_2(1+y))\Big],$$

and

$$\mathcal{J}_2(y) = e^{a_2}\sum_{k=0}^{3}(-1)^k\binom{3}{k}a_2^{k-2}\Big[\Gamma(2-k,a_2)-\Gamma(2-k,a_2(1+y))\Big].$$

Therefore, the TV of the TPFUD is given by

$$\mathrm{TV}(u)=\frac{1}{1-u}\left\{\frac{a_2^2}{a_0a_2+a_1}\left[2a_0U(3,2,a_2)+6a_1U(4,3,a_2)-a_0\,\mathcal{I}_2\!\left(\frac{Q_u}{1-Q_u}\right)-a_1\,\mathcal{J}_2\!\left(\frac{Q_u}{1-Q_u}\right)\right]\right\}$$
$$-\left[\mathrm{TVaR}(u)\right]^2, \tag{3.45}$$

for $0<u<1$.

The measures above provide informative summaries of tail risk for the TPFUD and may be useful in applications involving excess-loss pricing, reinsurance analysis, and risk-based decision-making for bounded losses.

3.8. Stress–strength reliability

Stress–strength reliability (SSR) is defined as the probability that the system's strength exceeds the applied stress. Let X_1 and X_2 denote the strength and stress variables, respectively, with

$$X_1 \sim \mathrm{TPFUD}(\alpha_1,\beta_1), \quad X_2 \sim \mathrm{TPFUD}(\alpha_2,\beta_2),$$

where X_1 and X_2 are independent. For $k=1,2$, write

$$a_{0k}=a_0(\alpha_k,\beta_k), \quad a_{1k}=a_1(\alpha_k,\beta_k), \quad a_{2k}=a_2(\alpha_k,\beta_k),$$

and define $b_k=a_{0k}a_{2k}+a_{1k}$, where $\alpha_k,\beta_k>0$. The SSR is given by

$$\mathcal{R}_{ss}=\mathbb{P}(X_1>X_2)=\int_0^1 f_{X_1}(x;\alpha_1,\beta_1)\,F_{X_2}(x;\alpha_2,\beta_2)\,dx. \tag{3.46}$$

Substituting Eqs (2.3) and (2.4) into Eq (3.46) yields

$$\mathcal{R}_{ss}=\int_0^1 \frac{a_{21}^2\left(a_{01}+a_{11}\frac{x}{1-x}\right)}{b_1(1-x)^2}e^{-a_{21}\frac{x}{1-x}}\left\{1-\frac{a_{22}\left(a_{02}+a_{12}\frac{x}{1-x}\right)+a_{12}}{b_2}e^{-a_{22}\frac{x}{1-x}}\right\}dx. \tag{3.47}$$

If we apply the transformation $t=\frac{x}{1-x}$, with $x=\frac{t}{1+t}$ and $\frac{dx}{(1-x)^2}=dt$, Eq (3.47) becomes

$$\mathcal{R}_{ss}=\frac{a_{21}^2}{b_1}\int_0^\infty(a_{01}+a_{11}t)e^{-a_{21}t}\,dt-\frac{a_{21}^2}{b_1b_2}\int_0^\infty(a_{01}+a_{11}t)(b_2+a_{12}a_{22}t)e^{-(a_{21}+a_{22})t}\,dt. \tag{3.48}$$

Since $\frac{a_{21}^2}{b_1}\int_0^\infty(a_{01}+a_{11}t)e^{-a_{21}t}\,dt=1$, expanding the integrand in the second term of Eq (3.48) with $\lambda=a_{21}+a_{22}$ gives

$$\mathcal{R}_{ss}=1-\frac{a_{21}^2}{b_1b_2}\int_0^\infty\left[a_{01}b_2+(a_{01}a_{12}a_{22}+a_{11}b_2)t+a_{11}a_{12}a_{22}t^2\right]e^{-\lambda t}\,dt. \tag{3.49}$$

Evaluating Eq (3.49) using $\int_0^\infty t^ne^{-\lambda t}dt=\frac{n!}{\lambda^{n+1}}$ for $n=0,1,2$ yields the closed-form expression

$$\mathcal{R}_{ss}=1-\frac{a_{21}^2a_{01}}{b_1\lambda}-\frac{a_{21}^2(a_{01}a_{12}a_{22}+a_{11}b_2)}{b_1b_2\lambda^2}-\frac{2a_{21}^2a_{11}a_{12}a_{22}}{b_1b_2\lambda^3}, \quad \lambda=a_{21}+a_{22}. \tag{3.50}$$

Equivalently, substituting $\lambda = a_{21} + a_{22}$ gives

$$\mathcal{R}_{ss} = 1 - \frac{a_{21}^2 a_{01}}{b_1(a_{21}+a_{22})} - \frac{a_{21}^2(a_{01}a_{12}a_{22} + a_{11}b_2)}{b_1 b_2 (a_{21}+a_{22})^2} - \frac{2a_{21}^2 a_{11}a_{12}a_{22}}{b_1 b_2(a_{21}+a_{22})^3}. \tag{3.51}$$

When $(\alpha_1,\beta_1) = (\alpha_2,\beta_2)$, symmetry requires $\mathcal{R}_{ss} = \frac{1}{2}$. Setting $a_{0k} = a_0$, $a_{1k} = a_1$, $a_{2k} = a_2$, and $b_k = b = a_0a_2 + a_1$ in Eq (3.51), the last three terms sum to

$$\frac{a_0a_2}{2b} + \frac{2a_0a_1a_2 + 2a_1^2}{4b^2} = \frac{a_0a_2}{2b} + \frac{a_1(a_0a_2+a_1)}{2b^2} = \frac{a_0a_2+a_1}{2b} = \frac{1}{2},$$

whence $\mathcal{R}_{ss} = \frac{1}{2}$ as expected.

3.9. Order statistics

Order statistics are fundamental in the analysis of extremes, tail behavior, and sample dispersion, particularly in reliability theory and life-testing studies. This subsection derives the distributional properties of the order statistics for the TPFUD, with special emphasis on the sample extrema and the sample range.

Let $X_{1:n} \le X_{2:n} \le \cdots \le X_{n:n}$ denote the order statistics of a random sample of size n from $X \sim$ TPFUD(α,β). For $r = 1, 2, \ldots, n$, the PDF of the r^{th} order statistic is

$$f_{X_{r:n}}(x;\alpha,\beta) = \frac{n!}{(r-1)!(n-r)!}[F(x;\alpha,\beta)]^{r-1}[1 - F(x;\alpha,\beta)]^{n-r} f(x;\alpha,\beta), \qquad 0 < x < 1, \tag{3.52}$$

and the corresponding CDF is given by

$$F_{X_{r:n}}(x;\alpha,\beta) = \sum_{k=r}^{n}\sum_{m=0}^{n-k}\binom{n}{k}\binom{n-k}{m}(-1)^m [F(x;\alpha,\beta)]^{m+k}, \qquad 0 < x < 1. \tag{3.53}$$

Substituting the PDF and CDF of the TPFUD from Eqs (2.3) and (2.4) into Eqs (3.52) and (3.53), we obtain

$$\begin{aligned} f_{X_{r:n}}(x;\alpha,\beta) = {} & \frac{n!}{(r-1)!(n-r)!}\left[1 - \left(\frac{a_2\left(a_0 + a_1\frac{x}{1-x}\right) + a_1}{a_0a_2 + a_1}\right)e^{-a_2\frac{x}{1-x}}\right]^{r-1}\left[\left(\frac{a_2\left(a_0 + a_1\frac{x}{1-x}\right) + a_1}{a_0a_2 + a_1}\right)e^{-a_2\frac{x}{1-x}}\right]^{n-r} \\ & \times \frac{a_2^2\left(a_0 + a_1\frac{x}{1-x}\right)}{(a_0a_2 + a_1)(1-x)^2}e^{-a_2\frac{x}{1-x}}, \qquad 0 < x < 1, \end{aligned} \tag{3.54}$$

and

$$F_{X_{r:n}}(x;\alpha,\beta) = \sum_{k=r}^{n}\sum_{m=0}^{n-k}\binom{n}{k}\binom{n-k}{m}(-1)^m\left[1 - \left(\frac{a_2\left(a_0 + a_1\frac{x}{1-x}\right) + a_1}{a_0a_2 + a_1}\right)e^{-a_2\frac{x}{1-x}}\right]^{m+k}, \qquad 0 < x < 1. \tag{3.55}$$

Of particular interest are the extreme order statistics, namely, the sample minimum $X_{1:n}$ and the sample maximum $X_{n:n}$. These follow directly from Eq (3.54). For $r = 1$, the PDF of the sample minimum is

$$f_{X_{1:n}}(x;\alpha,\beta) = n\left[\left(\frac{a_2\left(a_0 + a_1\frac{x}{1-x}\right) + a_1}{a_0a_2 + a_1}\right)e^{-a_2\frac{x}{1-x}}\right]^{n-1}\frac{a_2^2\left(a_0 + a_1\frac{x}{1-x}\right)}{(a_0a_2 + a_1)(1-x)^2}e^{-a_2\frac{x}{1-x}}, \qquad 0 < x < 1,$$

whereas for $r = n$, the PDF of the sample maximum is

$$f_{X_{n:n}}(x;\alpha,\beta) = n\left[1 - \left(\frac{a_2\left(a_0 + a_1\frac{x}{1-x}\right) + a_1}{a_0a_2 + a_1}\right)e^{-a_2\frac{x}{1-x}}\right]^{n-1}\frac{a_2^2\left(a_0 + a_1\frac{x}{1-x}\right)}{(a_0a_2 + a_1)(1-x)^2}e^{-a_2\frac{x}{1-x}}, \qquad 0 < x < 1.$$

In addition to the sample extrema, an important measure of sample dispersion is the range. Let $\mathcal{R} = X_{n:n} - X_{1:n}$ denote the sample range, which measures the spread between the largest and smallest observations in the sample. Since the TPFUD is supported on $(0, 1)$, the CDF of the range is given by

$$F_{\mathcal{R}}(r) = n\int_0^{1-r}\left[F(x + r;\alpha,\beta) - F(x;\alpha,\beta)\right]^{n-1} f(x;\alpha,\beta)\,dx + \left[R(1 - r;\alpha,\beta)\right]^n, \qquad 0 < r < 1, \quad (3.56)$$

where the second term accounts for the event $X_{1:n} > 1 - r$, for which the sample range is necessarily less than r. Here, we have

$$F(x + r;\alpha,\beta) - F(x;\alpha,\beta) = \left(\frac{a_2\left(a_0 + a_1\frac{x}{1-x}\right) + a_1}{a_0a_2 + a_1}\right)e^{-a_2\frac{x}{1-x}} - \left(\frac{a_2\left(a_0 + a_1\frac{x+r}{1-x-r}\right) + a_1}{a_0a_2 + a_1}\right)e^{-a_2\frac{x+r}{1-x-r}}.$$

For fixed $n \geq 2$, the endpoint behavior of the range satisfies

$$F_{\mathcal{R}}(r) \sim nr^{n-1}\int_0^1 [f(x;\alpha,\beta)]^n\,dx, \qquad r \to 0^+,$$

whereas

$$1 - F_{\mathcal{R}}(r) \sim \frac{n(n-1)a_0a_1a_2^2e^{a_2}}{(a_0a_2 + a_1)^2}(1 - r)\exp\left(-\frac{a_2}{1 - r}\right), \qquad r \to 1^-.$$

Thus, $F_{\mathcal{R}}(r) \to 0$ as $r \to 0^+$ and $F_{\mathcal{R}}(r) \to 1$ as $r \to 1^-$. Moreover, as $n \to \infty$,

$$nX_{1:n} \xrightarrow{d} \mathrm{Exp}\left(\frac{a_0a_2^2}{a_0a_2 + a_1}\right), \qquad (\log n)(1 - X_{n:n}) \xrightarrow{p} a_2,$$

where $\mathrm{Exp}(\lambda)$ denotes the exponential distribution with the rate parameter λ. Since $1 - \mathcal{R} = X_{1:n} + (1 - X_{n:n})$ and $(\log n)X_{1:n} \xrightarrow{p} 0$, it follows that $(\log n)(1 - \mathcal{R}) \xrightarrow{p} a_2$. Hence, $\mathcal{R} \xrightarrow{p} 1$ as $n \to \infty$.

Theorem 3.6 (Moments of the order statistics of the TPFUD). *Let $X_{r:n}$ denote the r^{th} order statistic from a random sample of size n drawn from $X \sim$ TPFUD(α,β). Then for any real $q > -1$, the q^{th} N-CM of $X_{r:n}$ is given by*

$$\mu_{r:n}^{(q)} = \frac{n!}{(r-1)!(n-r)!}\frac{a_2^2}{a_0a_2+a_1}\sum_{j=0}^{r-1}(-1)^j\binom{r-1}{j}\sum_{i=0}^{j+n-r}\binom{j+n-r}{i}\left(\frac{a_1a_2}{a_0a_2+a_1}\right)^i\Big[a_0\,\Gamma(q+i+1)$$
$$\times U(q+i+1,\ i+2,\ (j+n-r+1)a_2) + a_1\,\Gamma(q+i+2)\,U(q+i+2,\ i+3,\ (j+n-r+1)a_2)\Big]. \tag{3.57}$$

Proof. By definition, the q^{th} N-CM of the r^{th} order statistic is

$$\mu_{r:n}^{(q)} = \mathbb{E}[X_{r:n}^q] = \int_0^1 x^q f_{X_{r:n}}(x;\alpha,\beta)\,dx.$$

Substituting the PDF of the r^{th} order statistic from Eq (3.52) into the integral above yields

$$\mu_{r:n}^{(q)} = \frac{n!}{(r-1)!(n-r)!}\int_0^1 x^q[F(x;\alpha,\beta)]^{r-1}[R(x;\alpha,\beta)]^{n-r}f(x;\alpha,\beta)\,dx.$$

By the definition of the PWMs of the TPFUD given in Eq (3.17), we obtain

$$M_{q,r-1,n-r} = \mathbb{E}\Big[X^qF(X;\alpha,\beta)^{r-1}R(X;\alpha,\beta)^{n-r}\Big].$$

It follows that

$$\mu_{r:n}^{(q)} = \frac{n!}{(r-1)!(n-r)!}\,M_{q,r-1,n-r}.$$

Finally, applying the closed-form expression in Eq (3.18) with $p = q$, r replaced by $r-1$, and s replaced by $n-r$, we obtain Eq (3.57). □

Remark 3.9. *The validity of Eq (3.57) can be checked through the standard identities for order statistics. In particular, for $q = 1$, $\sum_{r=1}^{n}\mu_{r:n}^{(1)} = n\,\mathbb{E}[X] = n\mu$, which provides a useful consistency check [19].*

Some important special cases are as follows.

(1) If $n = r = 1$, then Eq (3.57) reduces to

$$\mu_{1:1}^{(q)} = \frac{a_2^2}{a_0a_2+a_1}\Big[a_0\,\Gamma(q+1)\,U(q+1,2,a_2) + a_1\,\Gamma(q+2)\,U(q+2,3,a_2)\Big] = \mu_q',$$

which coincides with the q^{th} N-CM of the TPFUD given in Eq (3.4).

(2) If $r = 1$, then Eq (3.57) reduces to the q^{th} moment of the sample minimum

$$\mu_{1:n}^{(q)} = n\,\frac{a_2^2}{a_0a_2+a_1}\sum_{i=0}^{n-1}\binom{n-1}{i}\left(\frac{a_1a_2}{a_0a_2+a_1}\right)^i\Big[a_0\,\Gamma(q+i+1)\,U(q+i+1,i+2,na_2)$$
$$+ a_1\,\Gamma(q+i+2)\,U(q+i+2,i+3,na_2)\Big].$$

(3) If $r = n$, then Eq (3.57) reduces to the q^{th} moment of the sample maximum

$$\mu_{n:n}^{(q)} = n\,\frac{a_2^2}{a_0a_2+a_1}\sum_{j=0}^{n-1}(-1)^j\binom{n-1}{j}\sum_{i=0}^{j}\binom{j}{i}\left(\frac{a_1a_2}{a_0a_2+a_1}\right)^i\Big[a_0\,\Gamma(q+i+1)$$
$$\times\,U(q+i+1,i+2,(j+1)a_2)+a_1\,\Gamma(q+i+2)\,U(q+i+2,i+3,(j+1)a_2)\Big].$$

Corollary 3.2 (L-moments of the TPFUD)**.** *Let $X_1,\ldots,X_r$ be a random sample from the TPFUD, and let $X_{1:r}\le\cdots\le X_{r:r}$ denote the corresponding order statistics. Then the r^{th} L-moment of X is given by*

$$\lambda_r = \frac{1}{r}\sum_{k=0}^{r-1}(-1)^k\binom{r-1}{k}\mathbb{E}[X_{r-k:r}]\,,\qquad r\ge 1. \tag{3.58}$$

By setting $q = 1$, $n = r$, and $r \to r-k$ in Eq (3.57) and substituting into Eq (3.58), we obtain

$$\lambda_r = \frac{1}{r}\sum_{k=0}^{r-1}(-1)^k\binom{r-1}{k}\frac{r!}{(r-k-1)!k!}\frac{a_2^2}{a_0a_2+a_1}\sum_{j=0}^{r-k-1}(-1)^j\binom{r-k-1}{j}\sum_{i=0}^{j+k}\binom{j+k}{i}\left(\frac{a_1a_2}{a_0a_2+a_1}\right)^i$$
$$\times\Bigg[a_0\,\Gamma(i+2)\,U(i+2,\;i+2,\;(j+k+1)a_2)+a_1\,\Gamma(i+3)\,U(i+3,\;i+3,\;(j+k+1)a_2)\Bigg]. \tag{3.59}$$

Remark 3.10 (First four population L-moments of the TPFUD)**.** *The first four population L-moments of the* TPFUD *are obtained directly from Eq (3.59) by setting $r = 1,2,3,$ and 4. The resulting expressions can be written in closed form in terms of Tricomi's confluent hypergeometric function as follows.*

(1) The first L-moment (L-location), defined as $\lambda_1 = \mu_{1:1}^{(1)}$, is given by

$$\lambda_1 = \frac{a_2^2}{a_0a_2+a_1}\Big[a_0\,U(2,2,a_2)+2a_1\,U(3,3,a_2)\Big] = \mathbb{E}[X]. \tag{3.60}$$

(2) The second L-moment (L-scale), defined as $\lambda_2 = \frac{1}{2}\left(\mu_{2:2}^{(1)}-\mu_{1:2}^{(1)}\right)$, is given by

$$\lambda_2 = \frac{1}{2}\Bigg[2\,\frac{a_2^2}{a_0a_2+a_1}\sum_{j=0}^{1}(-1)^j\binom{1}{j}\sum_{i=0}^{j}\binom{j}{i}\left(\frac{a_1a_2}{a_0a_2+a_1}\right)^i\Big(a_0\,\Gamma(i+2)\,U(i+2,i+2,(j+1)a_2)$$
$$+\,a_1\,\Gamma(i+3)\,U(i+3,i+3,(j+1)a_2)\Big)-2\,\frac{a_2^2}{a_0a_2+a_1}\sum_{i=0}^{1}\binom{1}{i}\left(\frac{a_1a_2}{a_0a_2+a_1}\right)^i$$
$$\times\Big(a_0\,\Gamma(i+2)\,U(i+2,i+2,2a_2)+a_1\,\Gamma(i+3)\,U(i+3,i+3,2a_2)\Big)\Bigg]. \tag{3.61}$$

(3) The third L-moment, defined as $\lambda_3 = \frac{1}{3}\left(\mu_{3:3}^{(1)}-2\mu_{2:3}^{(1)}+\mu_{1:3}^{(1)}\right)$, is given by

$$\lambda_3 = \frac{1}{3}\Bigg[3\,\frac{a_2^2}{a_0a_2+a_1}\sum_{j=0}^{2}(-1)^j\binom{2}{j}\sum_{i=0}^{j}\binom{j}{i}\left(\frac{a_1a_2}{a_0a_2+a_1}\right)^i\Big(a_0\,\Gamma(i+2)\,U(i+2,i+2,(j+1)a_2)$$
$$+\,a_1\,\Gamma(i+3)\,U(i+3,i+3,(j+1)a_2)\Big)-12\,\frac{a_2^2}{a_0a_2+a_1}\sum_{j=0}^{1}(-1)^j\binom{1}{j}\sum_{i=0}^{j+1}\binom{j+1}{i}\left(\frac{a_1a_2}{a_0a_2+a_1}\right)^i$$
$$\times\Big(a_0\,\Gamma(i+2)\,U(i+2,i+2,(j+2)a_2)+a_1\,\Gamma(i+3)\,U(i+3,i+3,(j+2)a_2)\Big)+3\,\frac{a_2^2}{a_0a_2+a_1}$$
$$\times\sum_{i=0}^{2}\binom{2}{i}\left(\frac{a_1a_2}{a_0a_2+a_1}\right)^i\Big(a_0\,\Gamma(i+2)\,U(i+2,i+2,3a_2)+a_1\,\Gamma(i+3)\,U(i+3,i+3,3a_2)\Big)\Bigg]. \tag{3.62}$$

(4) The fourth L-moment, defined as $\lambda_4 = \frac{1}{4}\left(\mu^{(1)}_{4:4} - 3\mu^{(1)}_{3:4} + 3\mu^{(1)}_{2:4} - \mu^{(1)}_{1:4}\right)$, is given by

$$\lambda_4 = \frac{1}{4}\Bigg[4\,\frac{a_2^2}{a_0a_2+a_1}\sum_{j=0}^{3}(-1)^j\binom{3}{j}\sum_{i=0}^{j}\binom{j}{i}\left(\frac{a_1a_2}{a_0a_2+a_1}\right)^i\Big(a_0\,\Gamma(i+2)\,U(i+2,i+2,(j+1)a_2)$$
$$+\,a_1\,\Gamma(i+3)\,U(i+3,i+3,(j+1)a_2)\Big)-36\,\frac{a_2^2}{a_0a_2+a_1}\sum_{j=0}^{2}(-1)^j\binom{2}{j}\sum_{i=0}^{j+1}\binom{j+1}{i}\left(\frac{a_1a_2}{a_0a_2+a_1}\right)^i$$
$$\times\Big(a_0\,\Gamma(i+2)\,U(i+2,i+2,(j+2)a_2)+a_1\,\Gamma(i+3)\,U(i+3,i+3,(j+2)a_2)\Big)+36\,\frac{a_2^2}{a_0a_2+a_1}$$
$$\times\sum_{j=0}^{1}(-1)^j\binom{1}{j}\sum_{i=0}^{j+2}\binom{j+2}{i}\left(\frac{a_1a_2}{a_0a_2+a_1}\right)^i\Big(a_0\,\Gamma(i+2)\,U(i+2,i+2,(j+3)a_2)+a_1\,\Gamma(i+3)$$
$$\times\,U(i+3,i+3,(j+3)a_2)\Big)-4\,\frac{a_2^2}{a_0a_2+a_1}\sum_{i=0}^{3}\binom{3}{i}\left(\frac{a_1a_2}{a_0a_2+a_1}\right)^i\Big(a_0\,\Gamma(i+2)$$
$$\times\,U(i+2,i+2,4a_2)+a_1\,\Gamma(i+3)\,U(i+3,i+3,4a_2)\Big)\Bigg]. \tag{3.63}$$

Corollary 3.3 (L-moment ratios of the TPFUD)**.** *Let $X \sim$ TPFUD(α,β) and let λ_r, $r \geq 1$, denote its L-moments. The principal L-moment ratios, which characterize variability and shape, are given as follows.*

(1) The L-coefficient of variation (L-CV) is given by

$$\tau = \frac{\lambda_2}{\lambda_1}, \qquad \lambda_1 \neq 0,$$

where λ_1 and λ_2 are defined in Eqs (3.60) and (3.61).

(2) The L-skewness is defined as

$$\tau_3 = \frac{\lambda_3}{\lambda_2}, \qquad \lambda_2 \neq 0,$$

where λ_2 and λ_3 are given in Eqs (3.61) and (3.62).

(3) The L-kurtosis is given by
$$\tau_4 = \frac{\lambda_4}{\lambda_2}, \qquad \lambda_2 \neq 0,$$
where λ_2 and λ_4 are defined in Eqs (3.61) and (3.63).

The L-moment ratios τ, τ_3, and τ_4 provide interpretable measures of the relative dispersion, asymmetry, and tail behavior, respectively. Since they are constructed from linear combinations of the order statistics, they are generally less sensitive to extreme observations than conventional moment-based measures.

3.10. Stochastic orders

Stochastic orders provide a rigorous framework for comparing probability distributions in terms of magnitude, aging behavior, and reliability characteristics. They are widely used in probability theory, reliability analysis, actuarial science, and survival studies to determine when one random variable may be regarded as smaller or larger than another in a probabilistic sense.

Let X and Y be any two random variables with the PDFs f_X and f_Y, the CDFs F_X and F_Y, the RFs R_X and R_Y, and the HFs h_X and h_Y, respectively. Then X is said to be smaller than Y in the following senses:

- *Likelihood ratio order*, denoted by $X \leq_{lr} Y$, if $\frac{f_X(x)}{f_Y(x)}$ is decreasing in $x \in (0,1)$;
- *Hazard rate order*, denoted by $X \leq_{hr} Y$, if $h_X(x) \geq h_Y(x)$ for all $x \in (0,1)$;
- *Stochastic order*, denoted by $X \leq_{st} Y$, if $F_X(x) \geq F_Y(x)$ for all $x \in (0,1)$, or equivalently $R_X(x) \leq R_Y(x)$ for all $x \in (0,1)$.

As established in [20], these stochastic orders are related through the standard chain of implications
$$X \leq_{lr} Y \quad \Longrightarrow \quad X \leq_{hr} Y \quad \Longrightarrow \quad X \leq_{st} Y.$$

The following theorem establishes sufficient conditions under which these orderings hold for the TPFUD.

Theorem 3.7 (Stochastic ordering for the TPFUD)**.** *Let $X \sim$ TPFUD(α_1,β_1) and $Y \sim$ TPFUD(α_2,β_2). Define $a_{0j} = a_0(\alpha_j,\beta_j)$, $a_{1j} = a_1(\alpha_j,\beta_j)$, and $a_{2j} = a_2(\alpha_j,\beta_j)$ for $j = 1,2$. Let $b_j = a_{0j}a_{2j} + a_{1j}$ for $j = 1,2$. If $a_{11}a_{02} \leq a_{12}a_{01}$ and $a_{21} \geq a_{22}$, then $X \leq_{lr} Y$. Consequently, $X \leq_{hr} Y$ and $X \leq_{st} Y$.*

Proof. From Eq (2.3), the likelihood ratio of X and Y is given by
$$\frac{f_X(x)}{f_Y(x)} = \frac{a_{21}^2 b_2}{a_{22}^2 b_1} \cdot \frac{a_{01} + a_{11}\dfrac{x}{1-x}}{a_{02} + a_{12}\dfrac{x}{1-x}} \cdot e^{-(a_{21}-a_{22})\frac{x}{1-x}}, \quad 0 < x < 1. \tag{3.64}$$

To investigate the monotonicity of $\frac{f_X(x)}{f_Y(x)}$, let $z = \frac{x}{1-x}$, so that $z > 0$ for $0 < x < 1$, and $\frac{dz}{dx} = \frac{1}{(1-x)^2} > 0$. Taking logarithms in Eq (3.64), we obtain
$$\log\left(\frac{f_X(x)}{f_Y(x)}\right) = \log\left(\frac{a_{21}^2 b_2}{a_{22}^2 b_1}\right) + \log(a_{01} + a_{11}z) - \log(a_{02} + a_{12}z) - (a_{21} - a_{22})z.$$

Differentiating with respect to x yields

$$\begin{aligned}\frac{d}{dx}\log\left(\frac{f_X(x)}{f_Y(x)}\right) &= \frac{1}{(1-x)^2}\left[\frac{a_{11}}{a_{01}+a_{11}z} - \frac{a_{12}}{a_{02}+a_{12}z} - (a_{21}-a_{22})\right]\\ &= \frac{1}{(1-x)^2}\left[\frac{a_{11}a_{02}-a_{12}a_{01}}{(a_{01}+a_{11}z)(a_{02}+a_{12}z)} - (a_{21}-a_{22})\right].\end{aligned} \tag{3.65}$$

Since $0 < x < 1$, we have $(1-x)^2 > 0$. Moreover, by the positivity assumptions of the model, $a_{0j} > 0$ and $a_{1j} > 0$ for $j = 1, 2$, and hence $a_{01} + a_{11}z > 0$ and $a_{02} + a_{12}z > 0$ for all $z > 0$. Therefore, if $a_{11}a_{02} \le a_{12}a_{01}$ and $a_{21} \ge a_{22}$, then the right-hand side of Eq (3.65) is non-positive for all $x \in (0, 1)$. Consequently,

$$\frac{d}{dx}\log\left(\frac{f_X(x)}{f_Y(x)}\right) \le 0, \qquad 0 < x < 1,$$

which shows that $\frac{f_X(x)}{f_Y(x)}$ is decreasing in x. Hence, $X \le_{lr} Y$. The remaining assertions follow immediately from the standard implication chain

$$X \le_{lr} Y \quad \Longrightarrow \quad X \le_{hr} Y \quad \Longrightarrow \quad X \le_{st} Y.$$

Thus, $X \le_{lr} Y$, $X \le_{hr} Y$, and $X \le_{st} Y$. This completes the proof. □

3.11. Entropy measures

Entropy measures quantify the uncertainty associated with a probability distribution and are widely used in information theory, reliability analysis, and statistical inference. For the TPFUD, the entropy measures considered below are based on the generalized entropy integral

$$\mathcal{I}_\delta(\alpha,\beta) = \int_0^1 [f(x;\alpha,\beta)]^\delta \, \mathrm{d}x, \qquad \delta > 0, \quad \delta \ne 1. \tag{3.66}$$

Substituting the PDF in Eq (2.3) into Eq (3.66) gives

$$\mathcal{I}_\delta(\alpha,\beta) = \left(\frac{a_2^2}{a_0a_2+a_1}\right)^\delta \int_0^1 \left(a_0 + a_1\frac{x}{1-x}\right)^\delta (1-x)^{-2\delta} e^{-\delta a_2 \frac{x}{1-x}}\, dx.$$

Applying the transformation $t = \frac{x}{1-x}$, where $x = \frac{t}{1+t}$ and $\frac{dx}{(1-x)^2} = dt$, we obtain

$$\mathcal{I}_\delta(\alpha,\beta) = \left(\frac{a_2^2}{a_0a_2+a_1}\right)^\delta \int_0^\infty (a_0+a_1t)^\delta (1+t)^{2\delta-2} e^{-\delta a_2 t}\, \mathrm{d}t. \tag{3.67}$$

Globally convergent series representations can be obtained by factoring the larger of a_0 and a_1 before applying the generalized binomial theorem. Two cases are considered.

(1) Suppose that $a_0 \ge a_1$ and define $q_0 = 1 - \frac{a_1}{a_0}$, $0 \le q_0 < 1$. Then $a_0 + a_1t = a_0(1+t)\left(1 - q_0\frac{t}{1+t}\right)$, where

$$0 \le q_0\frac{t}{1+t} < q_0 < 1, \qquad t \ge 0.$$

Applying the generalized binomial expansion and integrating term by term, using the Tricomi confluent hypergeometric representation in Eq (3.5), yields

$$\mathcal{I}_\delta(\alpha,\beta) = \left(\frac{a_2^2}{a_0a_2+a_1}\right)^\delta a_0^\delta \sum_{k=0}^\infty \binom{\delta}{k}(-q_0)^k \Gamma(k+1) U(k+1, 3\delta, \delta a_2)\,. \tag{3.68}$$

(2) Suppose that $a_1 > a_0$ and define $q_1 = 1 - \frac{a_0}{a_1},\ 0 < q_1 < 1$. In this case, $a_0 + a_1 t = a_1(1+t)\left(1 - \frac{q_1}{1+t}\right)$, where

$$0 < \frac{q_1}{1+t} \leq q_1 < 1, \qquad t \geq 0.$$

It follows that

$$\mathcal{I}_\delta(\alpha,\beta) = \left(\frac{a_2^2}{a_0 a_2 + a_1}\right)^\delta a_1^\delta \sum_{k=0}^{\infty} \binom{\delta}{k} (-q_1)^k U(1, 3\delta - k, \delta a_2)\,. \tag{3.69}$$

Both series converge absolutely and uniformly for every $\delta > 0$, since the corresponding binomial arguments are bounded in magnitude by constants strictly smaller than one. When $a_0 = a_1$, $q_0 = 0$, and the first series reduces to its $k = 0$ term. If δ is a positive integer, the relevant series also terminates after finitely many terms. When q_0 or q_1 is close to one, however, the convergence of the corresponding infinite series may become slow. In such cases, $\mathcal{I}_\delta(\alpha,\beta)$ may be evaluated directly from Eq (3.67) using adaptive numerical quadrature with a prescribed tolerance, thereby avoiding truncation and cancellation errors. The corresponding entropy measures are given below.

(1) The Rényi entropy of order δ, denoted by $\mathcal{R}_\delta$ [21], is defined as

$$\mathcal{R}_\delta(\alpha,\beta) = \frac{1}{1-\delta} \log[\mathcal{I}_\delta(\alpha,\beta)]\,, \qquad \delta > 0, \quad \delta \neq 1.$$

(2) The Arimoto entropy of order δ, denoted by $\mathcal{A}_\delta$ [22], is defined as

$$\mathcal{A}_\delta(\alpha,\beta) = \frac{\delta}{1-\delta}\left[\mathcal{I}_\delta(\alpha,\beta)^{1/\delta} - 1\right], \qquad \delta > 0, \quad \delta \neq 1.$$

(3) The Tsallis entropy of order δ, denoted by $\mathcal{T}_\delta$ [23], is defined as

$$\mathcal{T}_\delta(\alpha,\beta) = \frac{1 - \mathcal{I}_\delta(\alpha,\beta)}{\delta - 1}, \qquad \delta > 0, \quad \delta \neq 1.$$

(4) The Havrda–Charvát entropy of order δ, denoted by $\mathcal{HC}_\delta$ [24], is defined as

$$\mathcal{HC}_\delta(\alpha,\beta) = \frac{\mathcal{I}_\delta(\alpha,\beta) - 1}{2^{1-\delta} - 1}, \qquad \delta > 0, \quad \delta \neq 1.$$

5) The Mathai–Haubold entropy of order δ, denoted by $\mathcal{MH}_\delta$ [25], is defined as

$$\mathcal{MH}_\delta(\alpha,\beta) = \frac{\mathcal{I}_{2-\delta}(\alpha,\beta) - 1}{\delta - 1}, \qquad 0 < \delta < 2, \quad \delta \neq 1.$$

For $\mathcal{R}_\delta$, $\mathcal{A}_\delta$, $\mathcal{T}_\delta$, and $\mathcal{HC}_\delta$, $\mathcal{I}_\delta(\alpha,\beta)$ may be evaluated using the applicable series representation in Eqs (3.68) and (3.69) or by direct numerical integration of Eq (3.67) while for $\mathcal{MH}_\delta$, the same representations apply after replacing δ by $2 - \delta$.

3.11.1. Shannon entropy

The Shannon entropy, denoted $\mathcal{S}_h$, is another classical measure of uncertainty in information theory [26]. For $X \sim \text{TPFUD}(\alpha, \beta)$, it is defined by

$$\mathcal{S}_h(\alpha, \beta) = -\mathbb{E}[\log f(X; \alpha, \beta)] = -\int_0^1 f(x; \alpha, \beta) \log f(x; \alpha, \beta)\, dx.$$

Using Eq (2.3), the log-density is given by

$$\log f(x; \alpha, \beta) = \log\left(\frac{a_2^2}{a_0 a_2 + a_1}\right) + \log\left(a_0 + a_1 \frac{x}{1-x}\right) - 2\log(1-x) - a_2 \frac{x}{1-x}. \tag{3.70}$$

Substituting Eq (3.70) into the definition of $\mathcal{S}_h$ gives

$$\begin{aligned}\mathcal{S}_h(\alpha, \beta) = &-\log\left(\frac{a_2^2}{a_0 a_2 + a_1}\right) \int_0^1 f(x; \alpha, \beta)\, dx - \int_0^1 \log\left(a_0 + a_1 \frac{x}{1-x}\right) f(x; \alpha, \beta)\, dx \\ &+ 2\int_0^1 \log(1-x) f(x; \alpha, \beta)\, dx + \int_0^1 a_2 \frac{x}{1-x} f(x; \alpha, \beta)\, dx. \end{aligned} \tag{3.71}$$

The first integral in Eq (3.71) equals unity by the normalization of the PDF. For the remaining terms, apply the transformation $t = \frac{x}{1-x}$, with $x = \frac{t}{1+t}$ and $\frac{dx}{(1-x)^2} = dt$, to obtain

$$\mathcal{S}_h(\alpha, \beta) = -\log\left(\frac{a_2^2}{a_0 a_2 + a_1}\right) - \frac{a_2^2}{a_0 a_2 + a_1}\mathcal{I}_1 - \frac{2a_2^2}{a_0 a_2 + a_1}\mathcal{I}_2 + \frac{a_2^3}{a_0 a_2 + a_1}\mathcal{I}_3, \tag{3.72}$$

where

$$\begin{aligned}\mathcal{I}_1 &= \int_0^\infty \log(a_0 + a_1 t)(a_0 + a_1 t) e^{-a_2 t}\, dt \\ &= \frac{1}{a_2^2}\left[-a_1 e^{\frac{a_0 a_2}{a_1}} \operatorname{Ei}\left(-\frac{a_0 a_2}{a_1}\right) + (a_0 a_2 + a_1)\log(a_0) + a_1\right],\end{aligned}$$

$$\mathcal{I}_2 = \int_0^\infty \log(1+t)(a_0 + a_1 t) e^{-a_2 t}\, dt = \frac{1}{a_2^2}\left\{a_1 + [a_1(a_2 - 1) - a_0 a_2]\, e^{a_2} \operatorname{Ei}(-a_2)\right\},$$

and

$$\mathcal{I}_3 = \int_0^\infty t(a_0 + a_1 t) e^{-a_2 t}\, dt = \frac{a_0}{a_2^2} + \frac{2a_1}{a_2^3}.$$

Combining these evaluations, the $\mathcal{S}_h$ of the TPFUD is obtained in closed form as

$$\begin{aligned}\mathcal{S}_h(\alpha, \beta) = &-\log\left(\frac{a_0 a_2^2}{a_0 a_2 + a_1}\right) + \frac{1}{a_0 a_2 + a_1}\Big\{a_0 a_2 - a_1 - 2[a_1(a_2 - 1) - a_0 a_2] e^{a_2} \\ &\times \operatorname{Ei}(-a_2) + a_1 e^{\frac{a_0 a_2}{a_1}} \operatorname{Ei}\left(-\frac{a_0 a_2}{a_1}\right)\Big\}.\end{aligned} \tag{3.73}$$

3.12. Extropy measures

As a complementary duality of entropy, extropy provides an alternative measure of uncertainty and information. Owing to its distinct interpretation, it offers additional insight into the distributional structure of random variables beyond that conveyed by entropy alone.

3.12.1. Extropy

The extropy ($\mathcal{J}$) of a continuous random variable X characterized by a PDF $f(x;\alpha,\beta)$, as described in [27], is given by

$$\mathcal{J}(\alpha,\beta) = -\frac{1}{2}\int_0^1 [f(x;\alpha,\beta)]^2\,dx. \tag{3.74}$$

For $X \sim \text{TPFUD}(\alpha,\beta)$, substituting the PDF from Eq (2.3), we obtain

$$\mathcal{J}(\alpha,\beta) = -\frac{1}{2}\left(\frac{a_2^2}{a_0a_2 + a_1}\right)^2 \int_0^1 \left(a_0 + a_1\frac{x}{1-x}\right)^2 (1-x)^{-4} e^{-2a_2\frac{x}{1-x}}\,dx.$$

Applying the transformation $t = \frac{x}{1-x}$, where $x = \frac{t}{1+t}$ and $dx = (1+t)^{-2}\,dt$, we obtain

$$\mathcal{J}(\alpha,\beta) = -\frac{1}{2}\left(\frac{a_2^2}{a_0a_2 + a_1}\right)^2 \int_0^\infty (a_0 + a_1t)^2(1+t)^2 e^{-2a_2t}\,dt.$$

Expanding the integrand and applying the gamma integral identity

$$\int_0^\infty t^k e^{-\lambda t}\,dt = \frac{k!}{\lambda^{k+1}}, \quad \lambda > 0, \tag{3.75}$$

with $\lambda = 2a_2$, we obtain

$$\mathcal{J}(\alpha,\beta) = -\frac{a_0^2a_2^2(2a_2^2 + 2a_2 + 1) + a_0a_1a_2(2a_2^2 + 4a_2 + 3) + a_1^2(a_2^2 + 3a_2 + 3)}{8a_2\,(a_0a_2 + a_1)^2}. \tag{3.76}$$

3.12.2. Cumulative residual extropy

The cumulative residual extropy ($\mathcal{J}_{\mathcal{CR}}$) of a continuous random variable X with RF $R(x;\alpha,\beta)$, as introduced in [28, 29], is defined by

$$\mathcal{J}_{\mathcal{CR}}(\alpha,\beta) = -\frac{1}{2}\int_0^1 [R(x;\alpha,\beta)]^2\,dx. \tag{3.77}$$

For $X \sim \text{TPFUD}(\alpha,\beta)$, substituting the RF from Eq (2.5), we obtain

$$\mathcal{J}_{\mathcal{CR}}(\alpha,\beta) = -\frac{1}{2(a_0a_2 + a_1)^2}\int_0^1 \left[a_2\left(a_0 + a_1\frac{x}{1-x}\right) + a_1\right]^2 e^{-2a_2\frac{x}{1-x}}\,dx.$$

Applying the transformation $t = \frac{x}{1-x}$, where $x = \frac{t}{1+t}$ and $dx = (1+t)^{-2}\,dt$, we obtain

$$\mathcal{J}_{\mathcal{CR}}(\alpha,\beta) = -\frac{1}{2(a_0a_2 + a_1)^2}\int_0^\infty [a_2(a_0 + a_1t) + a_1]^2\,\frac{e^{-2a_2t}}{(1+t)^2}\,dt.$$

Expanding the integrand and applying the exponential-integral identity

$$\int_0^\infty (1+t)^{-k} e^{-\lambda t}\, dt = e^{\lambda} E_k(\lambda), \quad \lambda > 0, \tag{3.78}$$

together with the relation $E_1(x) = -\operatorname{Ei}(-x)$ and the recurrence formula $E_2(x) = e^{-x} - xE_1(x)$, we obtain

$$\begin{aligned}\mathcal{J}_{C\mathcal{R}}(\alpha,\beta) = -\frac{1}{2(a_0a_2+a_1)^2}\Big[& a_1^2 + \frac{1}{2}a_1a_2(4a_0-3a_1) + a_2^2(a_0-a_1)^2 \\ & + 2a_2^2 e^{2a_2}(a_0-a_1)(a_0a_2-a_1a_2+a_1)\operatorname{Ei}(-2a_2)\Big].\end{aligned} \tag{3.79}$$

For a fixed $a_0, a_1 > 0$, the apparent logarithmic singularity in Eq (3.79) is removable. Indeed, as $a_2 \to 0^+$, $\operatorname{Ei}(-2a_2) = \gamma + \log(2a_2) - 2a_2 + O(a_2^2)$, where γ denotes the Euler–Mascheroni constant. Consequently, $a_2^2 \operatorname{Ei}(-2a_2) \to 0$ and $\mathcal{J}_{C\mathcal{R}}(\alpha,\beta) = -\frac{1}{2} + \frac{3}{4}a_2 + O\Big(a_2^2|\log a_2|\Big)$, $a_2 \to 0^+$. Therefore, we have

$$\lim_{a_2\to 0^+} \mathcal{J}_{C\mathcal{R}}(\alpha,\beta) = -\frac{1}{2},$$

showing that the closed-form expression admits a finite limiting value despite the logarithmic behavior of $\operatorname{Ei}(-2a_2)$. For very small a_2, the preceding asymptotic expansion may also be used for stable numerical evaluation.

3.12.3. Negative cumulative extropy

The negative cumulative extropy ($\mathcal{J}_{\mathcal{N}C}$) of a continuous random variable X with CDF $F(x;\alpha,\beta)$, as proposed in [30], is defined by

$$\mathcal{J}_{\mathcal{N}C}(\alpha,\beta) = \frac{1}{2}\int_0^1 \Big(1 - [F(x;\alpha,\beta)]^2\Big)\, dx. \tag{3.80}$$

For $X \sim \text{TPFUD}(\alpha,\beta)$, substituting the CDF from Eq (2.4), we obtain

$$\begin{aligned}\mathcal{J}_{\mathcal{N}C}(\alpha,\beta) &= \frac{1}{2}\int_0^1 \Big[1 - (1 - R(x;\alpha,\beta))^2\Big]\, dx \\ &= \frac{1}{2}\int_0^1 \Big[2R(x;\alpha,\beta) - R(x;\alpha,\beta)^2\Big]\, dx \\ &= \int_0^1 R(x;\alpha,\beta)\, dx - \frac{1}{2}\int_0^1 [R(x;\alpha,\beta)]^2\, dx.\end{aligned}$$

Since, for any non-negative random variable supported on $(0,1)$, the mean admits the tail-integral representation

$$\mu = \mathbb{E}(X) = \int_0^1 R(x;\alpha,\beta)\, dx,$$

it follows immediately from Eq (3.77) that

$$\mathcal{J}_{\mathcal{N}C}(\alpha,\beta) = \mu + \mathcal{J}_{C\mathcal{R}}(\alpha,\beta). \tag{3.81}$$

Substituting μ and $\mathcal{J}_{\mathcal{CR}}(\alpha,\beta)$ from Corollary 3.1 and Eq (3.79) into Eq (3.81), we obtain

$$\mathcal{J}_{\mathcal{NC}}(\alpha,\beta) = \frac{a_2^2}{a_0a_2 + a_1}[a_0U(2,2,a_2) + 2a_1U(3,3,a_2)] - \frac{1}{2(a_0a_2 + a_1)^2}\Big\{a_1^2 + \frac{1}{2}a_1a_2(4a_0 - 3a_1) + a_2^2(a_0 - a_1)^2 + 2a_2^2e^{2a_2}(a_0 - a_1)(a_0a_2 - a_1a_2 + a_1)\,\mathrm{Ei}(-2a_2)\Big\}. \tag{3.82}$$

3.12.4. Weighted extropy

The weighted extropy ($\mathcal{J}_{\mathcal{W}}$) of a continuous random variable X with PDF $f(x;\alpha,\beta)$, as proposed in [31], is defined by

$$\mathcal{J}_{\mathcal{W}}(\alpha,\beta) = -\frac{1}{2}\int_0^1 x[f(x;\alpha,\beta)]^2\,dx. \tag{3.83}$$

For $X \sim$ TPFUD(α,β), substituting the PDF from Eq (2.3), we obtain

$$\mathcal{J}_{\mathcal{W}}(\alpha,\beta) = -\frac{1}{2}\left(\frac{a_2^2}{a_0a_2 + a_1}\right)^2\int_0^1 x\left(a_0 + a_1\frac{x}{1-x}\right)^2(1-x)^{-4}e^{-2a_2\frac{x}{1-x}}\,dx.$$

Applying the transformation $t = \frac{x}{1-x}$, where $x = \frac{t}{1+t}$ and $dx = (1+t)^{-2}\,dt$, we obtain

$$\mathcal{J}_{\mathcal{W}}(\alpha,\beta) = -\frac{1}{2}\left(\frac{a_2^2}{a_0a_2 + a_1}\right)^2\int_0^\infty t(a_0 + a_1t)^2(1+t)\,e^{-2a_2t}\,dt.$$

Expanding the integrand and applying the gamma-integral identity in Eq (3.75) with $\lambda = 2a_2$ and simplifying, we obtain

$$\mathcal{J}_{\mathcal{W}}(\alpha,\beta) = -\frac{2a_0^2a_2^2(a_2+1) + 2a_0a_1a_2(2a_2+3) + 3a_1^2(a_2+2)}{16a_2(a_0a_2 + a_1)^2}. \tag{3.84}$$

3.12.5. Weighted cumulative residual extropy

The weighted cumulative residual extropy ($\mathcal{J}_{\mathcal{WCR}}$) of a continuous random variable X with RF $R(x;\alpha,\beta)$, as proposed in [32], is defined by

$$\mathcal{J}_{\mathcal{WCR}}(\alpha,\beta) = -\frac{1}{2}\int_0^1 x[R(x;\alpha,\beta)]^2\,dx. \tag{3.85}$$

For $X \sim$ TPFUD(α,β), substituting the RF from Eq (2.5), we obtain

$$\mathcal{J}_{\mathcal{WCR}}(\alpha,\beta) = -\frac{1}{2(a_0a_2 + a_1)^2}\int_0^1 x\left[a_2\left(a_0 + a_1\frac{x}{1-x}\right) + a_1\right]^2 e^{-2a_2\frac{x}{1-x}}\,dx.$$

Applying the transformation $t = \frac{x}{1-x}$, where $x = \frac{t}{1+t}$ and $dx = (1+t)^{-2}\,dt$, we obtain

$$\mathcal{J}_{\mathcal{WCR}}(\alpha,\beta) = -\frac{1}{2(a_0a_2 + a_1)^2}\int_0^\infty t\,[a_2(a_0 + a_1t) + a_1]^2\,\frac{e^{-2a_2t}}{(1+t)^3}\,dt.$$

Expanding the integrand and applying the exponential-integral identity in Eq (3.78) with $\lambda = 2a_2$ and simplifying, we obtain

$$\begin{aligned}\mathcal{J}_{WCR}(\alpha,\beta) = -\frac{1}{4(a_0a_2+a_1)^2}\Big\{&a_1^2a_2 + (2a_2+1)(a_0a_2 - a_1a_2 + a_1)^2 - 4a_1a_2(a_0a_2\\&- a_1a_2 + a_1) + 2\Big[a_1^2a_2^2 - 2(2a_2+1)a_1a_2(a_0a_2 - a_1a_2 + a_1) + 2a_2(a_2+1)\\&\times (a_0a_2 - a_1a_2 + a_1)^2\Big]e^{2a_2}\,\mathrm{Ei}(-2a_2)\Big\}.\end{aligned} \tag{3.86}$$

The representations established in Eqs (3.76), (3.79), (3.82), (3.84), and (3.86) provide comprehensive analytical tools for evaluating information-theoretic uncertainty within the TPFUD framework, complementing the entropy measures derived in the preceding section.

4. A special case of the TPFUD: The UShD

The effective parameterization of the TPFUD depends on the particular specification of $a_i(\alpha,\beta)$, $i = 0, 1, 2$. In this section, we consider the UShD , a simple special case with closed-form distributional and reliability functions. It is obtained by specifying

$$a_0(\alpha,\beta) = \alpha, \qquad a_1(\alpha,\beta) = 1, \qquad a_2(\alpha,\beta) = \alpha, \qquad \alpha > 0,$$

as indicated in Table 1. Under this specification, the functions a_0, a_1, and a_2 do not depend on β, so the general TPFUD reduces to a one-parameter submodel. Thus, the absence of β from the UShD analysis is a direct consequence of this particular parameter specification and does not affect the general two-parameter construction of the TPFUD. Substitution into Eqs (2.3)–(2.6) gives the PDF, CDF, RF, and HF of the UShD, respectively.

$$f(x;\alpha) = \frac{\alpha^2[\alpha - (\alpha-1)x]}{(\alpha^2+1)(1-x)^3}\, e^{-\frac{\alpha x}{1-x}}, \qquad 0 < x < 1, \tag{4.1}$$

$$F(x;\alpha) = 1 - \frac{(\alpha^2+1)(1-x) + \alpha x}{(\alpha^2+1)(1-x)}\, e^{-\frac{\alpha x}{1-x}}, \qquad 0 < x < 1, \tag{4.2}$$

$$R(x;\alpha) = \frac{(\alpha^2+1)(1-x) + \alpha x}{(\alpha^2+1)(1-x)}\, e^{-\frac{\alpha x}{1-x}}, \qquad 0 < x < 1, \tag{4.3}$$

and

$$h(x;\alpha) = \frac{\alpha^2[\alpha - (\alpha-1)x]}{(1-x)^2[(\alpha^2+1)(1-x) + \alpha x]}, \qquad 0 < x < 1. \tag{4.4}$$

As illustrated in Figure 1, variation in α produces increasing, decreasing, and unimodal density shapes, together with convex, concave, and sigmoidal distribution functions. The HF remains increasing, while its magnitude and curvature vary with α. Accordingly, the UShD provides a simple model for bounded aging and wear-out phenomena. However, as a one-parameter submodel, it does not offer independent control over the distributional shape and scale and is not intended to represent decreasing, constant, bathtub-shaped, or other nonmonotone hazard patterns.

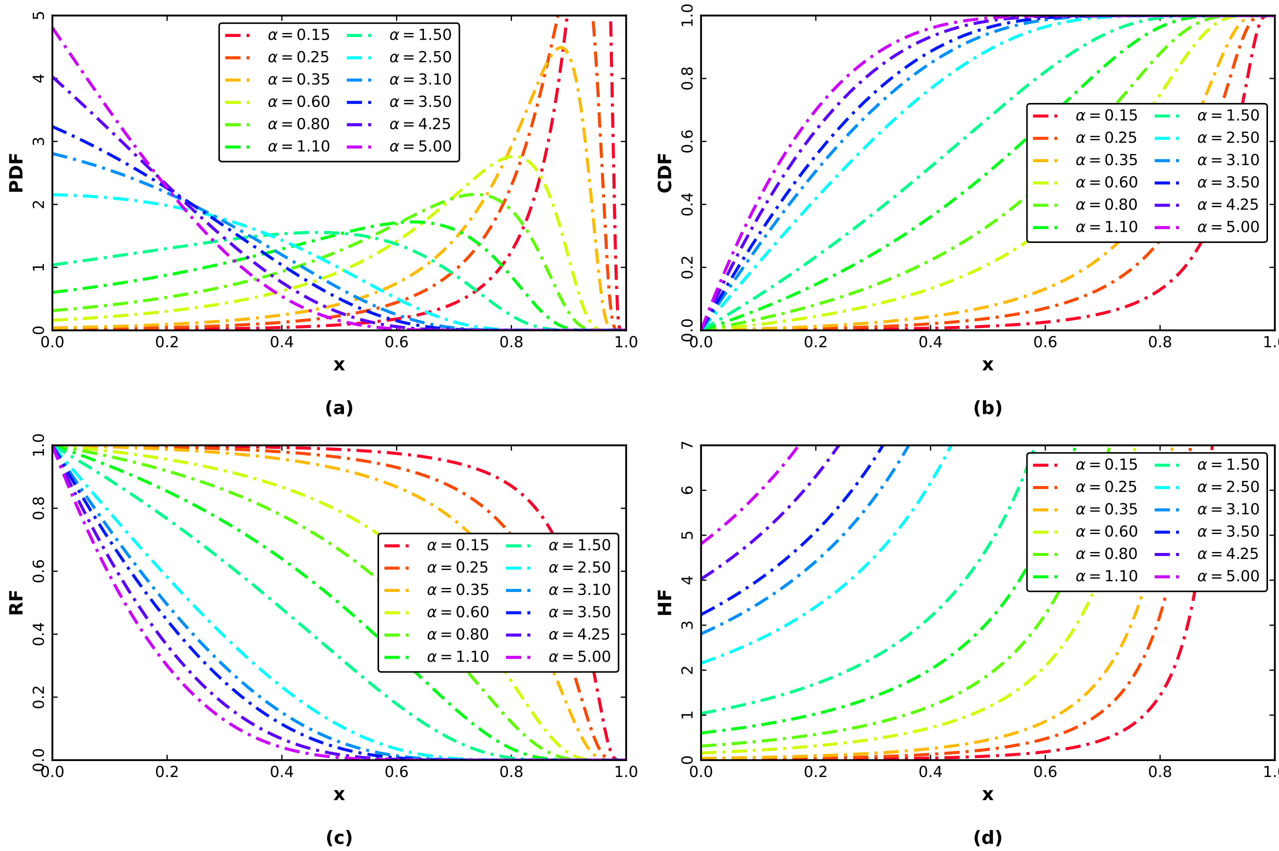

Figure 1. Graphical illustrations of the PDF (a), CDF (b), RF (c), and HF (d) of the UShD for selected values of the parameter α.

5. Non-Bayesian estimation of the UShD

This section focuses on estimating the parameter α for the UShD, along with its associated RF $R(x;\alpha)$ and HF $h(x;\alpha)$, using classical (frequentist) inferential methodologies. The estimation procedures are systematically categorized into two main frameworks: Likelihood-based techniques and spacing-based approaches. Additionally, the derivation of asymptotic confidence intervals (ACIs) for the model parameter and its corresponding functions is discussed.

5.1. Maximum likelihood estimation

Suppose that $x_1, x_2, \ldots, x_n$ constitute a random sample of size n generated from the UShD with parameter $\alpha > 0$ and PDF presented in Eq (4.1). The corresponding likelihood function can then be expressed as

$$\mathcal{L}(\alpha) = \prod_{i=1}^{n} f(x_i;\alpha) = \prod_{i=1}^{n} \left[\frac{\alpha^2[\alpha - (\alpha - 1)x_i]}{(\alpha^2 + 1)(1 - x_i)^3} e^{-\frac{\alpha x_i}{1 - x_i}} \right], \qquad 0 < x_i < 1. \tag{5.1}$$

Taking the natural logarithm of $\mathcal{L}(\alpha)$, the log-likelihood function can be written as

$$\ell_{\mathrm{ML}}(\alpha)=2n\log\alpha-n\log(\alpha^2+1)-3\sum_{i=1}^{n}\log(1-x_i)+\sum_{i=1}^{n}\log[\alpha-(\alpha-1)x_i]-\alpha\sum_{i=1}^{n}\frac{x_i}{1-x_i}. \quad (5.2)$$

The ML estimator of α, denoted $\widehat{\alpha}_{\mathrm{ML}}$, is derived through the maximization of $\ell_{\mathrm{ML}}(\alpha)$ defined in Eq (5.2), namely $\widehat{\alpha}_{\mathrm{ML}}=\arg\max_{\alpha>0}\ \ell_{\mathrm{ML}}(\alpha)$. Differentiation of $\ell_{\mathrm{ML}}(\alpha)$ with respect to α, followed by equating the resultant expression to zero, yields the estimating equation

$$\frac{\partial\ell_{\mathrm{ML}}(\alpha)}{\partial\alpha}=\frac{2n}{\alpha}-\frac{2n\alpha}{\alpha^2+1}+\sum_{i=1}^{n}\frac{1-x_i}{\alpha-(\alpha-1)x_i}-\sum_{i=1}^{n}\frac{x_i}{1-x_i}=0. \quad (5.3)$$

5.2. Maximum product of spacings estimation

The maximum product of spacings (MPS) methodology provides a viable alternative to ML estimation. This approach is based on maximizing the geometric mean of uniform spacings, which is equivalent to maximizing the logarithmic sum of these spacings [33].

Suppose that $x_{1:n}<x_{2:n}<\cdots<x_{n:n}$ constitute an ordered random sample of size n generated from the UShD with the parameter $\alpha>0$ and the CDF presented in Eq (4.2). The corresponding function of the product of spacings can then be expressed as

$$\mathcal{P}(\alpha)=\left\{\prod_{i=1}^{n+1}\mathcal{D}_i(\alpha)\right\}^{\frac{1}{n+1}},\qquad \mathcal{D}_i(\alpha)=\begin{cases}F(x_{1:n};\alpha), & i=1,\\ F(x_{i:n};\alpha)-F(x_{(i-1):n};\alpha), & i=2,\dots,n,\\ 1-F(x_{n:n};\alpha), & i=n+1,\end{cases} \quad (5.4)$$

where $\mathcal{D}_i(\alpha)$, $i=1,2,\dots,n+1$, constitute the uniform spacings and satisfy the constraint $\sum_{i=1}^{n+1}\mathcal{D}_i(\alpha)=1$. By substituting from Eq (4.2), the product of spacings admits the following explicit representation:

$$\begin{aligned}\mathcal{P}(\alpha)=\Bigg\{&\left[1-\frac{(\alpha^2+1)(1-x_{1:n})+\alpha x_{1:n}}{(\alpha^2+1)(1-x_{1:n})}\,e^{-\frac{\alpha x_{1:n}}{1-x_{1:n}}}\right]\times\left[\frac{(\alpha^2+1)(1-x_{n:n})+\alpha x_{n:n}}{(\alpha^2+1)(1-x_{n:n})}\,e^{-\frac{\alpha x_{n:n}}{1-x_{n:n}}}\right]\\&\times\prod_{i=2}^{n}\left[\frac{(\alpha^2+1)(1-x_{(i-1):n})+\alpha x_{(i-1):n}}{(\alpha^2+1)(1-x_{(i-1):n})}\,e^{-\frac{\alpha x_{(i-1):n}}{1-x_{(i-1):n}}}-\frac{(\alpha^2+1)(1-x_{i:n})+\alpha x_{i:n}}{(\alpha^2+1)(1-x_{i:n})}\,e^{-\frac{\alpha x_{i:n}}{1-x_{i:n}}}\right]\Bigg\}^{\frac{1}{n+1}}.\end{aligned} \quad (5.5)$$

Taking the natural logarithm of $\mathcal{P}(\alpha)$ yields the log product of the spacings function, which can be written as

$$\begin{aligned}\ell_{\mathrm{MPS}}(\alpha)=\frac{1}{n+1}\Bigg\{&\log\left[1-\frac{(\alpha^2+1)(1-x_{1:n})+\alpha x_{1:n}}{(\alpha^2+1)(1-x_{1:n})}\,e^{-\frac{\alpha x_{1:n}}{1-x_{1:n}}}\right]+\log\left[\frac{(\alpha^2+1)(1-x_{n:n})+\alpha x_{n:n}}{(\alpha^2+1)(1-x_{n:n})}\,e^{-\frac{\alpha x_{n:n}}{1-x_{n:n}}}\right]\\&+\sum_{i=2}^{n}\log\left[\frac{(\alpha^2+1)(1-x_{(i-1):n})+\alpha x_{(i-1):n}}{(\alpha^2+1)(1-x_{(i-1):n})}\,e^{-\frac{\alpha x_{(i-1):n}}{1-x_{(i-1):n}}}-\frac{(\alpha^2+1)(1-x_{i:n})+\alpha x_{i:n}}{(\alpha^2+1)(1-x_{i:n})}\,e^{-\frac{\alpha x_{i:n}}{1-x_{i:n}}}\right]\Bigg\}.\end{aligned} \quad (5.6)$$

The MPS estimator of α, denoted $\widehat{\alpha}_{\mathrm{MPS}}$, is derived through the maximization of $\ell_{\mathrm{MPS}}(\alpha)$ defined in Eq (5.6), namely $\widehat{\alpha}_{\mathrm{MPS}} = \arg\max_{\alpha>0} \ell_{\mathrm{MPS}}(\alpha)$. Differentiation of $\ell_{\mathrm{MPS}}(\alpha)$ with respect to α, followed by equating the resultant expression to zero, yields the estimating equation

$$\frac{\partial \ell_{\mathrm{MPS}}(\alpha)}{\partial \alpha} = \frac{1}{n+1}\left\{ \frac{\frac{\alpha x_{1:n}\left[\alpha(\alpha^2+3)(1-x_{1:n})+(\alpha^2+1)x_{1:n}\right]}{(\alpha^2+1)^2(1-x_{1:n})^2} e^{-\frac{\alpha x_{1:n}}{1-x_{1:n}}}}{1-\frac{(\alpha^2+1)(1-x_{1:n})+\alpha x_{1:n}}{(\alpha^2+1)(1-x_{1:n})} e^{-\frac{\alpha x_{1:n}}{1-x_{1:n}}}} - \frac{\frac{\alpha x_{n:n}\left[\alpha(\alpha^2+3)(1-x_{n:n})+(\alpha^2+1)x_{n:n}\right]}{(\alpha^2+1)^2(1-x_{n:n})^2} e^{-\frac{\alpha x_{n:n}}{1-x_{n:n}}}}{\frac{(\alpha^2+1)(1-x_{n:n})+\alpha x_{n:n}}{(\alpha^2+1)(1-x_{n:n})} e^{-\frac{\alpha x_{n:n}}{1-x_{n:n}}}} \right.$$
$$\left. + \sum_{i=2}^{n} \frac{\frac{\alpha x_{i:n}\left[\alpha(\alpha^2+3)(1-x_{i:n})+(\alpha^2+1)x_{i:n}\right]}{(\alpha^2+1)^2(1-x_{i:n})^2} e^{-\frac{\alpha x_{i:n}}{1-x_{i:n}}} - \frac{\alpha x_{(i-1):n}\left[\alpha(\alpha^2+3)(1-x_{(i-1):n})+(\alpha^2+1)x_{(i-1):n}\right]}{(\alpha^2+1)^2(1-x_{(i-1):n})^2} e^{-\frac{\alpha x_{(i-1):n}}{1-x_{(i-1):n}}}}{\frac{(\alpha^2+1)(1-x_{(i-1):n})+\alpha x_{(i-1):n}}{(\alpha^2+1)(1-x_{(i-1):n})} e^{-\frac{\alpha x_{(i-1):n}}{1-x_{(i-1):n}}} - \frac{(\alpha^2+1)(1-x_{i:n})+\alpha x_{i:n}}{(\alpha^2+1)(1-x_{i:n})} e^{-\frac{\alpha x_{i:n}}{1-x_{i:n}}}} \right\} = 0. \tag{5.7}$$

Owing to the nonlinearity in Eqs (5.3) and (5.7), the analytical derivation of $\widehat{\alpha}_{\mathrm{ML}}$ and $\widehat{\alpha}_{\mathrm{MPS}}$ is not feasible. Consequently, both estimators are obtained via numerical maximization of the corresponding objective functions. The existence and uniqueness of the ML estimator $\widehat{\alpha}_{\mathrm{ML}}$ are formally established in Theorem 5.1; corresponding results for the MPS estimator $\widehat{\alpha}_{\mathrm{MPS}}$ follow by parallel reasoning, though the proof is omitted here for brevity. In this study, the limited-memory Broyden–Fletcher–Goldfarb–Shanno algorithm with bound constraints (L-BFGS-B) [34], implemented in SciPy within Python 3.10 on the Google Colab platform, is used to maximize $\ell_{\mathrm{ML}}(\alpha)$ and $\ell_{\mathrm{MPS}}(\alpha)$. Since the UShD is supported on the open interval $(0, 1)$, all observations used in the numerical experiments and applications satisfy $0 < x_i < 1$. As $x_i \to 0^+$, the terms in Eq (5.2) remain finite, whereas numerical sensitivity may arise as $x_i \to 1^-$ because $x_i/(1 - x_i)$ becomes large. No exact boundary observations occur in the analyses considered in this study. Although the real data are reported to five decimal places, this rounding does not generate boundary observations, and the observed values remain sufficiently separated from the upper endpoint for the numerical optimization considered here. As illustrated in Figure 2, the objective functions exhibit smooth unimodal behavior over the admissible domain $\alpha > 0$, supporting stable numerical optimization for a wide range of initial values.

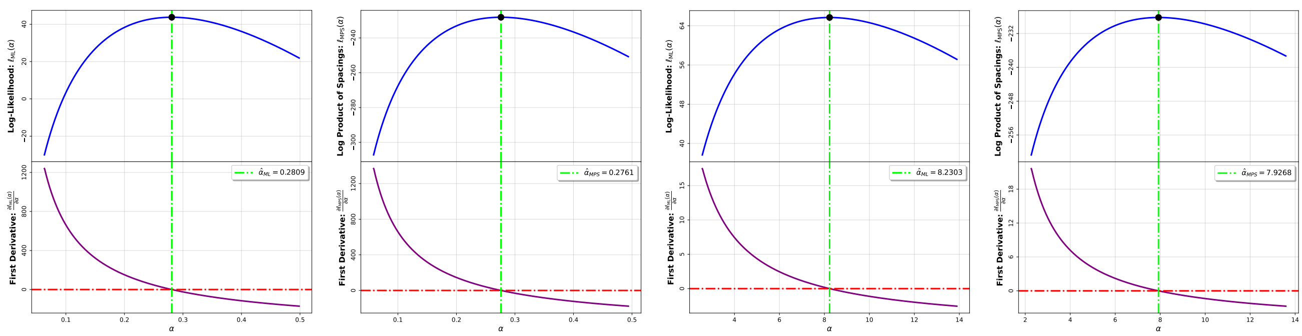

(a) $\alpha = 0.25$ **(b)** $\alpha = 7.0$

Figure 2. Profiles of the log-likelihood and log-product of spacings functions, together with their corresponding first-order derivatives. The black markers indicate the ML and MPS estimates obtained for the true values of the parameter α.

In accordance with the invariance principle related to the ML and MPS methods [35, 36], the RF and HF are estimated by evaluating them at their respective parameter estimates. Specifically, the plug-in estimators for the RF are given by $R(x;\widehat{\alpha}_{\mathrm{ML}})$ and $R(x;\widehat{\alpha}_{\mathrm{MPS}})$, while the estimators for the HF are represented by $h(x;\widehat{\alpha}_{\mathrm{ML}})$ and $h(x;\widehat{\alpha}_{\mathrm{MPS}})$.

Theorem 5.1 (Existence and uniqueness of the ML estimator)**.** *Let $x_1, x_2, \ldots, x_n$ be an independent random sample from the UShD with the parameter $\alpha > 0$ and PDF given in Eq (4.1). Let $\ell_{\mathrm{ML}}(\alpha)$ denote the log-likelihood function introduced in Eq (5.2), and define the associated score function by*

$$\wp(\alpha) = \frac{\partial \ell_{\mathrm{ML}}(\alpha)}{\partial \alpha} = \frac{2n}{\alpha} - \frac{2n\alpha}{\alpha^2+1} + \sum_{i=1}^{n} \frac{1-x_i}{\alpha-(\alpha-1)x_i} - \sum_{i=1}^{n} \frac{x_i}{1-x_i}, \qquad \alpha > 0, \tag{5.8}$$

where $0 < x_i < 1$ for all $i = 1, \ldots, n$. Then the likelihood equation $\wp(\alpha) = 0$ has exactly one solution in $(0, \infty)$. Consequently, the ML estimator $\widehat{\alpha}_{\mathrm{ML}}$ exists uniquely and is the only global maximizer of $\ell_{\mathrm{ML}}(\alpha)$ over the admissible parameter space.

Proof. The argument proceeds in two stages: First, we show that the score function admits at least one zero in $(0, \infty)$; second, we prove that such a zero cannot occur more than once.

Step 1. Existence of a solution. Since $0 < x_i < 1$ for all $i = 1, \ldots, n$, we have

$$\alpha - (\alpha-1)x_i = \alpha(1-x_i) + x_i > 0 \quad \text{for all} \quad \alpha > 0.$$

Therefore, every term appearing in Eq (5.8) is well defined and continuous on $(0, \infty)$, which implies that $\wp(\alpha)$ is continuous throughout the parameter space.

We now examine the limiting behavior of $\wp(\alpha)$ at the boundaries. As $\alpha \to 0$,

$$\frac{2n}{\alpha} \to +\infty, \qquad \frac{2n\alpha}{\alpha^2+1} \to 0, \qquad \frac{1-x_i}{\alpha-(\alpha-1)x_i} \to \frac{1-x_i}{x_i},$$

while the last summation in Eq (5.8) is constant with respect to α. Hence,

$$\lim_{\alpha \to 0} \wp(\alpha) = +\infty. \tag{5.9}$$

Next, let $\alpha \to \infty$. Then

$$\frac{2n}{\alpha} \to 0, \qquad \frac{2n\alpha}{\alpha^2+1} \to 0, \qquad \frac{1-x_i}{\alpha-(\alpha-1)x_i} = \frac{1-x_i}{\alpha(1-x_i)+x_i} \to 0.$$

Accordingly

$$\lim_{\alpha \to \infty} \wp(\alpha) = -\sum_{i=1}^{n} \frac{x_i}{1-x_i} < 0, \tag{5.10}$$

because each $\frac{x_i}{1-x_i}$ is strictly positive for $0 < x_i < 1$.

By the continuity of $\wp(\alpha)$ and the conditions in Eqs (5.9) and (5.10), we can apply the intermediate value theorem. Consequently, at least one point $\widehat{\alpha}_{\mathrm{ML}} \in (0, \infty)$ exists such that $\wp(\widehat{\alpha}_{\mathrm{ML}}) = 0$.

Step 2. Uniqueness of the solution. To establish uniqueness, it is sufficient to show that the score function is strictly decreasing on $(0, \infty)$. Differentiating Eq (5.8) with respect to α yields

$$\wp'(\alpha) = -\frac{2n}{\alpha^2} - \frac{2n(1-\alpha^2)}{(\alpha^2+1)^2} - \sum_{i=1}^{n} \frac{(1-x_i)^2}{\left[\alpha - (\alpha-1)x_i\right]^2}. \tag{5.11}$$

We begin with the first two terms on the right-hand side of Eq (5.11). Combining them over a common denominator gives

$$-\frac{2n}{\alpha^2} - \frac{2n(1-\alpha^2)}{(\alpha^2+1)^2} = -\frac{2n(3\alpha^2+1)}{\alpha^2(\alpha^2+1)^2}. \tag{5.12}$$

Because $n > 0$ and $\alpha > 0$, both the numerator $2n(3\alpha^2 + 1)$ and the denominator $\alpha^2(\alpha^2 + 1)^2$ are strictly positive. Hence, the expression in Eq (5.12) is negative for all $\alpha > 0$.

Regarding the third term in Eq (5.11), we have

$$-\sum_{i=1}^{n} \frac{(1-x_i)^2}{\left[\alpha - (\alpha-1)x_i\right]^2} < 0 \qquad \text{for all } \alpha > 0. \tag{5.13}$$

Combining Eqs (5.12) and (5.13), we obtain $\wp'(\alpha) < 0$ for every $\alpha \in (0, \infty)$.

Thus, $\wp(\alpha)$ is strictly decreasing on the whole parameter space. A continuous strictly decreasing function can vanish at most once; since the existence of a zero has already been established, that zero must be unique.

Finally, because the unique root of the score equation corresponds to the only stationary point of $\ell_{\mathrm{ML}}(\alpha)$ and the derivative of the score is strictly negative at that point, the log-likelihood is locally concave there. In view of the global monotonic behavior of $\wp(\alpha)$, no competing stationary values can arise, and the corresponding estimator $\widehat{\alpha}_{\mathrm{ML}}$ is therefore the unique global maximizer of $\ell_{\mathrm{ML}}(\alpha)$ on $(0, \infty)$. □

5.3. *Asymptotic confidence intervals*

It is a well-established result in statistical inference that when the standard regularity conditions are satisfied, the ML estimator $\widehat{\alpha}_{\mathrm{ML}}$ has a limiting normal distribution centered around the true parameter value α. Formally, we can write $\sqrt{n}(\widehat{\alpha}_{\mathrm{ML}} - \alpha) \xrightarrow{d} \mathcal{N}\big(0, \mathcal{I}^{-1}(\alpha)\big)$, where $\mathcal{I}(\alpha)$ denotes the Fisher information (FI) matrix pertaining to α. Since the expected FI matrix is generally difficult to derive in closed form for non standard models, asymptotic inference is instead developed using the observed FI matrix, which is obtained from the second derivative of the log-likelihood function. Accordingly, differentiating Eq (5.2) with respect to α a second time gives

$$\frac{\partial^2 \ell_{\mathrm{ML}}(\alpha)}{\partial \alpha^2} = -\frac{2n}{\alpha^2} - \frac{2n(1-\alpha^2)}{(\alpha^2+1)^2} - \sum_{i=1}^{n} \frac{(1-x_i)^2}{\left[\alpha - (\alpha-1)x_i\right]^2}. \tag{5.14}$$

Substituting $\widehat{\alpha}_{\mathrm{ML}}$ into the negative of the second derivative yields the observed FI, namely

$$\widehat{\mathcal{I}}(\widehat{\alpha}_{\mathrm{ML}}) = -\left.\frac{\partial^2 \ell_{\mathrm{ML}}(\alpha)}{\partial \alpha^2}\right|_{\alpha = \widehat{\alpha}_{\mathrm{ML}}}. \tag{5.15}$$

Accordingly, the asymptotic variance of $\widehat{\alpha}_{\mathrm{ML}}$ is approximated by the inverse of the observed FI; that is, $\widehat{\mathrm{Var}}(\widehat{\alpha}_{\mathrm{ML}}) = \widehat{\mathcal{I}}^{-1}(\widehat{\alpha}_{\mathrm{ML}})$. It then follows that an approximate two-sided $100(1-\gamma)\%$ ACI for α is given by $\widehat{\alpha}_{\mathrm{ML}} \pm z_{\gamma/2}\sqrt{\widehat{\mathrm{Var}}(\widehat{\alpha}_{\mathrm{ML}})}$, where $z_{\gamma/2}$ denotes the upper $\gamma/2$ quantile of the standard normal distribution.

For any function of the parameter, such as the RF and the HF, approximate large-sample variances may be obtained through the delta method [37]. In the present case, the required first derivatives with respect to α are given by

$$R_{\alpha}(x;\alpha) = -\frac{\alpha x\left[\alpha(\alpha^2+3)(1-x)+(\alpha^2+1)x\right]}{(\alpha^2+1)^2(1-x)^2}\, e^{-\frac{\alpha x}{1-x}},$$

and

$$h_{\alpha}(x;\alpha) = \frac{\alpha\left[\alpha^3(1-x)^2+2\alpha^2 x(1-x)+\alpha(4x^2-6x+3)+2x(1-x)\right]}{(1-x)^2\left[(\alpha^2+1)(1-x)+\alpha x\right]^2}.$$

Accordingly, the delta method yields

$$\widehat{\mathrm{Var}}(R(x;\widehat{\alpha}_{\mathrm{ML}})) = R_{\alpha}^2(x;\alpha)\Big|_{\alpha=\widehat{\alpha}_{\mathrm{ML}}}\widehat{\mathrm{Var}}(\widehat{\alpha}_{\mathrm{ML}}) \quad \text{and} \quad \widehat{\mathrm{Var}}(h(x;\widehat{\alpha}_{\mathrm{ML}})) = h_{\alpha}^2(x;\alpha)\Big|_{\alpha=\widehat{\alpha}_{\mathrm{ML}}}\widehat{\mathrm{Var}}(\widehat{\alpha}_{\mathrm{ML}}).$$

Consequently, the corresponding approximate two-sided $100(1-\gamma)\%$ ACIs for $R(x;\alpha)$ and $h(x;\alpha)$ are given, respectively, by

$$R(x;\widehat{\alpha}_{\mathrm{ML}}) \pm z_{\gamma/2}\sqrt{\widehat{\mathrm{Var}}(R(x;\widehat{\alpha}_{\mathrm{ML}}))} \quad \text{and} \quad h(x;\widehat{\alpha}_{\mathrm{ML}}) \pm z_{\gamma/2}\sqrt{\widehat{\mathrm{Var}}(h(x;\widehat{\alpha}_{\mathrm{ML}}))}.$$

A parallel asymptotic development can be established for the MPS estimator $\widehat{\alpha}_{\mathrm{MPS}}$. In particular, the ACIs for α, $R(x;\alpha)$, and $h(x;\alpha)$ are obtained by replacing $\widehat{\alpha}_{\mathrm{ML}}$ with $\widehat{\alpha}_{\mathrm{MPS}}$ and using the observed FI matrix based on $\ell_{\mathrm{MPS}}(\alpha)$. Consequently, the resulting intervals provide a practical large-sample quantification of estimation uncertainty under both the ML and MPS approaches [35–37].

6. Bayesian estimation of the UShD

From a Bayesian perspective, uncertainty regarding the UShD parameter α is quantified using a probability distribution. Eliciting a prior that accurately reflects the available information, or the absence thereof, presents a well-documented methodological challenge; indeed, no single rule has gained universal acceptance across different inferential contexts [38]. Since α is strictly positive, a natural and computationally convenient choice is the gamma distribution, which is sufficiently flexible to accommodate a wide range of empirical or subjective beliefs [39]. Consequently, we adopt a gamma prior distribution for α, with a PDF expressed by the following formula:

$$\mathcal{G}(\alpha) \propto \alpha^{\zeta-1}e^{-\xi\alpha}, \qquad \zeta>0,\ \xi>0,\ \alpha>0, \tag{6.1}$$

where ζ and ξ are hyperparameters governing, respectively, the prior mean ζ/ξ and the variance ζ/ξ^2.

When genuine prior information is at hand, the pair (ζ,ξ) can be determined by moment matching [40]: One equates the prior mean and variance to the corresponding sample moments of an initial frequentist estimate, such as $\widehat{\alpha}_{\mathrm{ML}}$ or $\widehat{\alpha}_{\mathrm{MPS}}$. Conversely, when the analyst wishes to let the data speak for themselves, an objective specification is preferable. In the present setting, Jeffreys' prior $\mathcal{G}(\alpha)\propto\alpha^{-1}$ serves this role; it can be viewed as the limiting form of Eq (6.1) obtained by letting $\zeta\to 0$ and $\xi\to 0$.

6.1. Posterior distribution based on the likelihood

Suppose that $x_1, x_2, \ldots, x_n$ constitute a random sample of size n from the UShD with the parameter $\alpha > 0$, where the corresponding PDF is given in Eq (4.1). Combining $\mathcal{L}(\alpha)$ in Eq (5.1) with $\mathcal{G}(\alpha)$ in Eq (6.1), the posterior density of α conditional on the observed data $\mathbf{x} = (x_1, \ldots, x_n)$ is obtained from Bayes' theorem as follows:

$$\mathcal{G}^*_{\mathrm{ML}}(\alpha \mid \mathbf{x}) = \mathcal{A}_1^{-1} \alpha^{\zeta-1} e^{-\xi\alpha} \prod_{i=1}^{n} \left[\frac{\alpha^2(\alpha - (\alpha-1)x_i)}{(\alpha^2+1)(1-x_i)^3} \, e^{-\frac{\alpha x_i}{1-x_i}} \right], \tag{6.2}$$

where the normalizing constant $\mathcal{A}_1$ is given by

$$\mathcal{A}_1 = \int_0^\infty \alpha^{\zeta-1} e^{-\xi\alpha} \prod_{i=1}^{n} \left[\frac{\alpha^2(\alpha - (\alpha-1)x_i)}{(\alpha^2+1)(1-x_i)^3} \, e^{-\frac{\alpha x_i}{1-x_i}} \right] d\alpha.$$

Owing to the non conjugate structure of this kernel, the posterior does not belong to any standard parametric family, and its moments must be approximated numerically.

6.2. Posterior distribution based on the product of spacings

Suppose that $x_{1:n}, x_{2:n}, \ldots, x_{n:n}$ constitute an ordered sample of size n from the UShD with parameter $\alpha > 0$, where $x_{1:n} < x_{2:n} < \cdots < x_{n:n}$. Combining $\mathcal{P}(\alpha)$ in Eq (5.5) with $\mathcal{G}(\alpha)$ in Eq (6.1), the posterior density of α conditional on the observed data $\mathbf{x} = (x_{1:n}, \ldots, x_{n:n})$ is obtained from Bayes' theorem as

$$\begin{aligned}\mathcal{G}^*_{\mathrm{MPS}}(\alpha \mid \mathbf{x}) = \mathcal{A}_2^{-1} \alpha^{\zeta-1} e^{-\xi\alpha} & \left[1 - \frac{(\alpha^2+1)(1-x_{1:n}) + \alpha x_{1:n}}{(\alpha^2+1)(1-x_{1:n})} \, e^{-\frac{\alpha x_{1:n}}{1-x_{1:n}}} \right] \left[\frac{(\alpha^2+1)(1-x_{n:n}) + \alpha x_{n:n}}{(\alpha^2+1)(1-x_{n:n})} \, e^{-\frac{\alpha x_{n:n}}{1-x_{n:n}}} \right] \\ \times \prod_{i=2}^{n} & \left[\frac{(\alpha^2+1)(1-x_{(i-1):n}) + \alpha x_{(i-1):n}}{(\alpha^2+1)(1-x_{(i-1):n})} \, e^{-\frac{\alpha x_{(i-1):n}}{1-x_{(i-1):n}}} - \frac{(\alpha^2+1)(1-x_{i:n}) + \alpha x_{i:n}}{(\alpha^2+1)(1-x_{i:n})} \, e^{-\frac{\alpha x_{i:n}}{1-x_{i:n}}} \right].\end{aligned} \tag{6.3}$$

where the normalizing constant $\mathcal{A}_2$ is given by

$$\begin{aligned}\mathcal{A}_2 = \int_0^\infty \alpha^{\zeta-1} e^{-\xi\alpha} & \left[1 - \frac{(\alpha^2+1)(1-x_{1:n}) + \alpha x_{1:n}}{(\alpha^2+1)(1-x_{1:n})} \, e^{-\frac{\alpha x_{1:n}}{1-x_{1:n}}} \right] \left[\frac{(\alpha^2+1)(1-x_{n:n}) + \alpha x_{n:n}}{(\alpha^2+1)(1-x_{n:n})} \, e^{-\frac{\alpha x_{n:n}}{1-x_{n:n}}} \right] \\ \times \prod_{i=2}^{n} & \left[\frac{(\alpha^2+1)(1-x_{(i-1):n}) + \alpha x_{(i-1):n}}{(\alpha^2+1)(1-x_{(i-1):n})} \, e^{-\frac{\alpha x_{(i-1):n}}{1-x_{(i-1):n}}} - \frac{(\alpha^2+1)(1-x_{i:n}) + \alpha x_{i:n}}{(\alpha^2+1)(1-x_{i:n})} \, e^{-\frac{\alpha x_{i:n}}{1-x_{i:n}}} \right] d\alpha.\end{aligned}$$

All Bayesian point and interval estimates are derived under the squared-error loss (SEL) function, $L(\alpha, \widehat{\alpha}) = (\widehat{\alpha} - \alpha)^2$. For any function $g(\alpha)$, the Bayes estimator is the posterior mean

$$\widehat{g}_{\mathrm{SEL}}(\alpha) = \mathbb{E}[g(\alpha) \mid \mathbf{x}] = \int_0^\infty g(\alpha) \, \mathcal{G}^*(\alpha \mid \mathbf{x}) \, d\alpha, \tag{6.4}$$

where $\mathcal{G}^*(\alpha \mid \mathbf{x})$ stands for either $\mathcal{G}^*_{\mathrm{ML}}(\alpha \mid \mathbf{x})$ or $\mathcal{G}^*_{\mathrm{MPS}}(\alpha \mid \mathbf{x})$.

Since the integrals in Eqs (6.2)–(6.4) lack closed-form solutions, we use Markov chain Monte Carlo (MCMC) for posterior inference. Specifically, we use a Gibbs sampler with embedded random-walk Metropolis–Hastings (M–H) updates to draw samples from the posterior. Because the posterior densities are approximately normal, as illustrated in Figure 3, Gaussian proposal distributions provide efficient exploration.

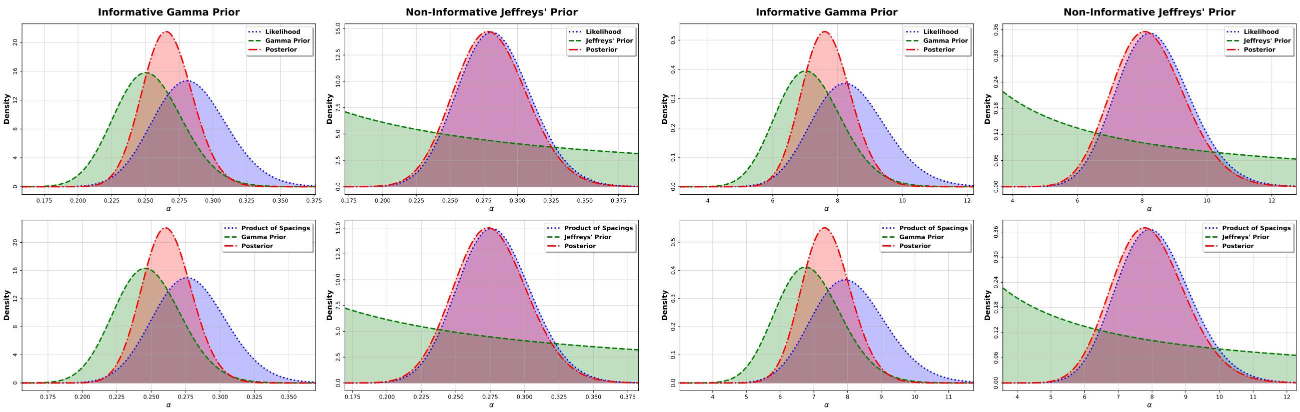

(a) α = 0.25 **(b)** α = 7.0

Figure 3. Prior and posterior distributions at α under two likelihood specifications: Standard likelihood (top) and product of spacings (bottom).

The M–H acceptance probability guarantees convergence to the target posterior [41, 42]; see Algorithm 1 for implementation details. We compute Bayesian point estimates and highest posterior density (HPD) credible intervals (CRIs) from these samples.

7. Monte Carlo simulation study

In this section, a Monte Carlo simulation (MCS) study is carried out to evaluate the finite-sample behavior of the proposed estimation procedures for the UShD. The investigation is conducted under several sample sizes n and selected values of the parameter α. For each configuration, $\mathcal{M}_g = 1000$ independent samples are generated from the UShD using the inverse transform method based on its QF. For every generated sample, the ML and MPS estimates are computed numerically. The corresponding 90% and 95% ACIs are then constructed using the observed FI matrix, while the delta method is used to obtain the ACIs of $R(x;\alpha)$ and $h(x;\alpha)$ at $x = 0.35$.

Bayesian estimation is implemented under the SEL function using two prior specifications: An informative gamma prior with the hyperparameters (ζ, ξ) assigned according to each (n, α) scenario, and Jeffreys' non informative prior to assess prior sensitivity. Posterior point estimates and HPD CRIs at the 90% and 95% levels are obtained through the M–H algorithm described in Algorithm 1. For each replication, the MCMC sampler is run for $\mathcal{M}^\bullet = 12{,}000$ iterations, with the first $\mathcal{M}_0 = 2000$ draws discarded as burn-in. The simulation settings, together with the gamma prior hyperparameters (ζ, ξ), are reported in Table 4.

Point estimation performance is summarized using the average estimate (AE), root mean squared error (RMSE), and mean relative absolute bias (MRAB), whereas interval estimation performance is evaluated through the empirical coverage probability (CP) and average length (AL). All numerical optimization is performed using the L-BFGS-B algorithm from the SciPy library under Python 3.10 on the Google Colab platform. The main computational procedure is summarized in Algorithm 2.

Table 4. Simulation settings for the UShD with the corresponding gamma prior hyperparameters (ζ, ξ).

n	α				
	0.15	0.45	1.35	4.05	13.00
25	(47.9, 313.9)	(53.8, 117.9)	(46.0, 33.4)	(26.6, 6.3)	(22.6, 1.7)
50	(99.8, 660.1)	(111.8, 246.8)	(99.0, 72.6)	(57.6, 14.0)	(48.6, 3.7)
100	(207.1, 1374.3)	(231.1, 511.6)	(208.1, 153.4)	(121.8, 29.8)	(102.3, 7.8)
200	(407.7, 2713.0)	(454.9, 1009.3)	(411.9, 304.4)	(241.3, 59.3)	(202.3, 15.5)
400	(801.4, 5338.2)	(892.7, 1982.5)	(813.1, 601.7)	(477.1, 117.6)	(399.7, 30.7)
800	(1614.4, 10759.3)	(1801.1, 4001.5)	(1638.2, 1213.0)	(958.0, 236.4)	(802.1, 61.6)

Algorithm 1 Random-walk M–H algorithm for α

Step 1. Specify the initial value $\alpha^{(0)} = \widehat{\alpha}$, the proposal variance $\widehat{\mathrm{Var}}(\widehat{\alpha})$, the total number of iterations $\mathcal{M}^{\bullet}$, the burn-in size $\mathcal{M}_0$, the confidence level $(1-\gamma)$, and the posterior density $\mathcal{G}^*(\alpha \mid \mathbf{x})$.

Step 2. Iterate for $\kappa = 1, 2, \ldots, \mathcal{M}^{\bullet}$:

- (a) Generate a candidate value $\alpha^* \sim \mathcal{N}\Big(\alpha^{(\kappa-1)},\ \widehat{\mathrm{Var}}(\widehat{\alpha})\Big)$, $\alpha^* > 0$.
- (b) Compute the acceptance probability $\eta = \min\Big\{1,\ \frac{\mathcal{G}^*(\alpha^*|\mathbf{x})}{\mathcal{G}^*(\alpha^{(\kappa-1)}|\mathbf{x})}\Big\}$.
- (c) Generate $u \sim \mathcal{U}(0,1)$.
- (d) Update the chain according to $\alpha^{(\kappa)} = \begin{cases} \alpha^*, & \text{if } u \le \eta, \\ \alpha^{(\kappa-1)}, & \text{otherwise.} \end{cases}$
- (e) Compute $R(x;\alpha)$ and $h(x;\alpha)$ at $\alpha = \alpha^{(\kappa)}$.

Step 3. Discard the first $\mathcal{M}_0$ burn-in values and retain $\{\alpha^{(\mathcal{M}_0+1)}, \alpha^{(\mathcal{M}_0+2)}, \ldots, \alpha^{(\mathcal{M}^{\bullet})}\}$.

Step 4. Compute the SEL Bayes estimator as $\widetilde{\alpha}_{\mathrm{SEL}} = \frac{1}{\mathcal{M}^*} \sum_{\kappa=\mathcal{M}_0+1}^{\mathcal{M}^{\bullet}} \alpha^{(\kappa)},\ \mathcal{M}^* = \mathcal{M}^{\bullet} - \mathcal{M}_0$.

Step 5. Construct the $(1-\gamma)100\%$ HPD CRI as follows:

- (a) Sort the retained draws as $\alpha_{(1)} \le \alpha_{(2)} \le \cdots \le \alpha_{(\mathcal{M}^*)}$.
- (b) For $\kappa = 1, 2, \ldots, \lfloor \gamma \mathcal{M}^* \rfloor$, compute $\delta(\kappa) = \alpha_{(\kappa + \lfloor (1-\gamma)\mathcal{M}^* \rfloor)} - \alpha_{(\kappa)}$.
- (c) Determine $\kappa^* = \arg\min_{\kappa} \delta(\kappa)$.
- (d) The HPD CRI is $\Big(\alpha_{(\kappa^*)}, \alpha_{(\kappa^* + \lfloor (1-\gamma)\mathcal{M}^* \rfloor)}\Big)$.

Step 6. Repeat Steps 4 and 5 for $R(x;\alpha)$ and $h(x;\alpha)$.

Algorithm 2 MCS procedure for the UShD

Step 1. Specify the simulation settings α, n, and (ζ, ξ) from Table 4, with $x = 0.35$, $\mathcal{M}_g = 1000$, $\gamma \in \{0.05, 0.10\}$, $\mathcal{M}^\bullet = 12{,}000$, and $\mathcal{M}_0 = 2000$.

Step 2. For each replication, generate a random sample of size n from the UShD as follows.

(a) Generate $U_1, \ldots, U_n \overset{\text{i.i.d.}}{\sim} \text{Uniform}(0,1)$;

(b) For each $i = 1, \ldots, n$, compute

$$X_i = \frac{-W_{-1}\Big[-(\alpha^2+1)(1-U_i)e^{-(\alpha^2+1)}\Big] - (\alpha^2+1)}{\alpha - W_{-1}\Big[-(\alpha^2+1)(1-U_i)e^{-(\alpha^2+1)}\Big] - (\alpha^2+1)}.$$

Step 3. Compute $\widehat{\alpha}_{\text{ML}}$ and $\widehat{\alpha}_{\text{MPS}}$ by maximizing the corresponding objective functions.

Step 4. Obtain the plug-in estimates of $R(x;\alpha)$ and $h(x;\alpha)$ under ML and MPS.

Step 5. Construct the 90% and 95% ACIs for α, $R(x;\alpha)$, and $h(x;\alpha)$.

Step 6. Apply the M–H sampler as described in Algorithm 1 using the informative gamma and Jeffreys' priors.

Step 7. Compute the Bayesian SEL estimates along with their 90% and 95% HPD CRIs for α, $R(x;\alpha)$, and $h(x;\alpha)$.

Step 8. Repeat Steps 2–7 for $i = 1, 2, \ldots, \mathcal{M}_g$.

Step 9. Compute the point estimation measures. For a generic estimand ρ and its estimate $\widehat{\rho}_{(i)}$ from the ith replication, calculate

$$\mathsf{AE}(\widehat{\rho}) = \frac{1}{\mathcal{M}_g}\sum_{i=1}^{\mathcal{M}_g}\widehat{\rho}_{(i)}, \quad \mathsf{RMSE}(\widehat{\rho}) = \sqrt{\frac{1}{\mathcal{M}_g}\sum_{i=1}^{\mathcal{M}_g}\left(\widehat{\rho}_{(i)} - \rho\right)^2},$$

and

$$\mathsf{MRAB}(\widehat{\rho}) = \frac{1}{\mathcal{M}_g}\sum_{i=1}^{\mathcal{M}_g}\frac{\left|\widehat{\rho}_{(i)} - \rho\right|}{\rho}.$$

Step 10. Construct the corresponding ACIs and HPD CRIs. We then compute

$$\mathsf{AL}_{100(1-\gamma)\%}(\widehat{\rho}) = \frac{1}{\mathcal{M}_g}\sum_{i=1}^{\mathcal{M}_g}\left(\mathsf{U}_{\widehat{\rho}_{(i)}} - \mathsf{L}_{\widehat{\rho}_{(i)}}\right) \quad \text{and} \quad \mathsf{CP}_{100(1-\gamma)\%}(\widehat{\rho}) = \frac{1}{\mathcal{M}_g}\sum_{i=1}^{\mathcal{M}_g}\mathbb{I}\left[\mathsf{L}_{\widehat{\rho}_{(i)}} \le \rho \le \mathsf{U}_{\widehat{\rho}_{(i)}}\right],$$

where $\mathbb{I}[\cdot]$ denotes the indicator function, and $\mathsf{L}_{\widehat{\rho}_{(i)}}$ and $\mathsf{U}_{\widehat{\rho}_{(i)}}$ represent the lower and upper bounds, respectively.

7.1. Simulation results

This subsection offers a brief discussion of the outcomes from the MCS study conducted for the UShD within the simulation framework outlined in Algorithm 2. The study examines the finite-sample behavior of the proposed inferential methods for estimating the parameter α, along with the associated reliability quantities $R(x;\alpha)$ and $h(x;\alpha)$, specifically evaluated at $x = 0.35$. The compared procedures comprise the classical ML and MPS approaches and their Bayesian versions under the SEL function, namely S-ML-I, S-ML-N, S-MPS-I, and S-MPS-N, where the suffixes I and N indicate the use of the informative gamma prior and Jeffreys' non-informative prior, respectively.

The numerical results are presented graphically by means of the heatmaps in Figures 4–8, with the corresponding numerical values displayed within each heatmap. This format provides a compact summary of the simulation results across the considered sample sizes, parameter scenarios, and competing estimation methods. Figures 4–8 are complementary, presenting the AE, RMSE, MRAB, AL, and CP measures, respectively, and thereby enabling both point and interval estimation performance to be assessed without requiring an extensive sequence of separate numerical tables.

The key conclusions derived from the investigation of the MCS study are presented below.

(1) The AE, RMSE, and MRAB results show that all estimators approach the true values of α, $R(x;\alpha)$, and $h(x;\alpha)$ as n increases. Hence, the proposed ML, MPS, and Bayesian estimators exhibit clear consistency.

(2) The RMSE values decrease steadily with increasing n, confirming improved estimation accuracy in larger samples. The informative-prior Bayesian methods, especially S-ML-I and S-MPS-I, generally provide the smallest errors.

(3) The MRAB values also decline as n increases, indicating reduced relative bias. Informative Bayesian estimators usually have the lowest bias, while MPS-based methods may show larger variability in small samples.

(4) The AL results demonstrate that interval lengths become shorter as n increases. The informative-prior HPD CRIs are typically the narrowest, whereas the MPS intervals are often wider.

(5) The CP values are generally close to the nominal levels. MPS intervals appear to be conservative, while informative HPD CRIs strike a favorable balance between coverage and interval width.

(6) Overall, the informative Bayesian procedures, particularly S-ML-I, show the best finite-sample performance. Their advantage is most visible for small and moderate samples, while all methods become more comparable for large values of n.

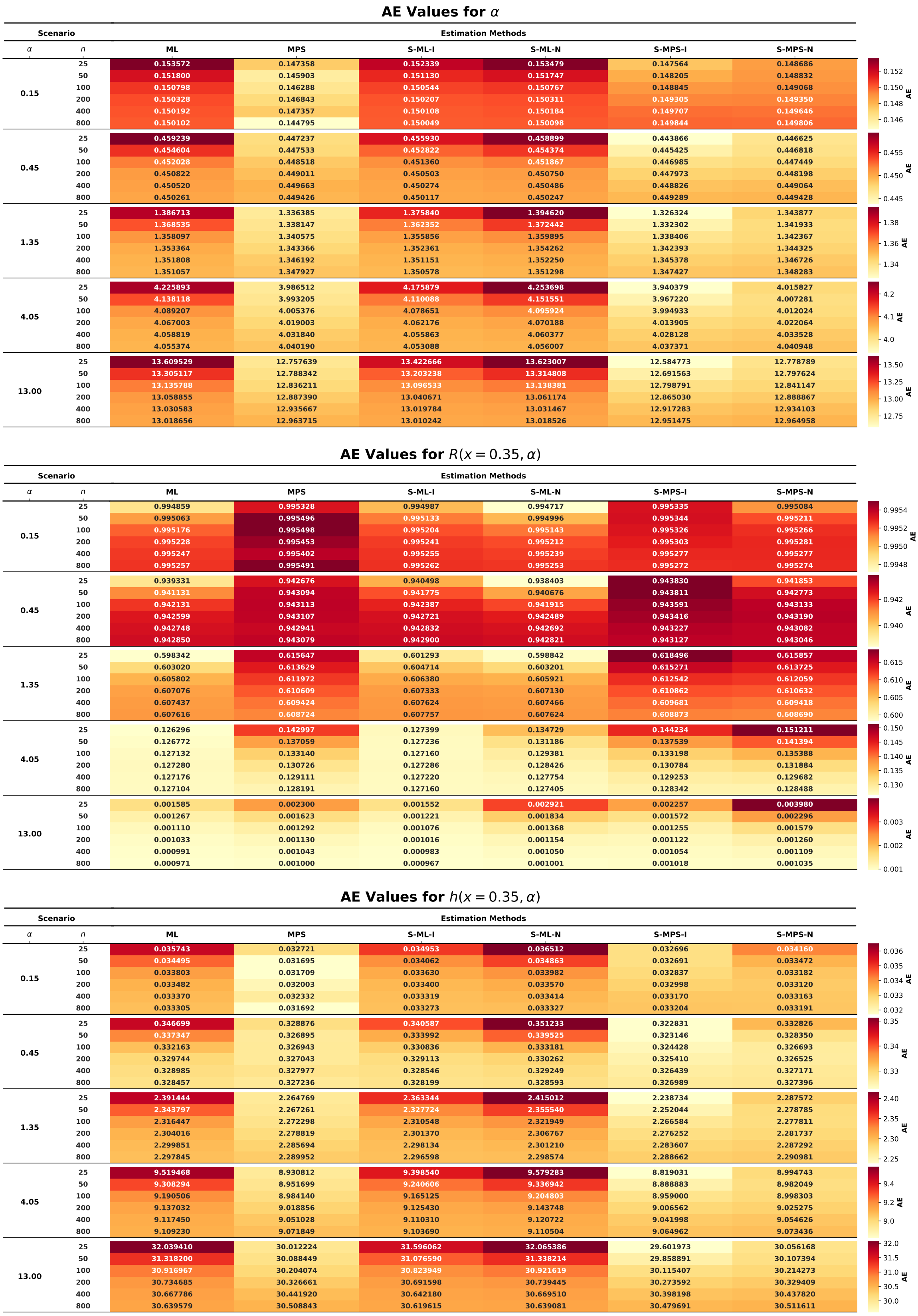

AE Values for α

Scenario α	n	ML	MPS	S-ML-I	S-ML-N	S-MPS-I	S-MPS-N
0.15	25	0.153572	0.147358	0.152339	0.153479	0.147564	0.148686
	50	0.151800	0.145903	0.151130	0.151747	0.148205	0.148832
	100	0.150798	0.146288	0.150544	0.150767	0.148845	0.149068
	200	0.150328	0.146843	0.150207	0.150311	0.149305	0.149350
	400	0.150192	0.147357	0.150108	0.150184	0.149707	0.149646
	800	0.150102	0.144795	0.150049	0.150098	0.149844	0.149806
0.45	25	0.459239	0.447237	0.455930	0.458899	0.443866	0.446625
	50	0.454604	0.447533	0.452822	0.454374	0.445425	0.446818
	100	0.452028	0.448518	0.451360	0.451867	0.446985	0.447449
	200	0.450822	0.449011	0.450503	0.450750	0.447973	0.448198
	400	0.450520	0.449663	0.450274	0.450486	0.448826	0.449064
	800	0.450261	0.449426	0.450117	0.450247	0.449289	0.449428
1.35	25	1.386713	1.336385	1.375840	1.394620	1.326324	1.343877
	50	1.368535	1.338147	1.362352	1.372442	1.332302	1.341933
	100	1.358097	1.340575	1.355856	1.359895	1.338406	1.342367
	200	1.353364	1.343366	1.352361	1.354262	1.342393	1.344325
	400	1.351808	1.346192	1.351151	1.352250	1.345378	1.346726
	800	1.351057	1.347927	1.350578	1.351298	1.347427	1.348283
4.05	25	4.225893	3.986512	4.175879	4.253698	3.940379	4.015827
	50	4.138118	3.993205	4.110088	4.151551	3.967220	4.007281
	100	4.089207	4.005376	4.078651	4.095924	3.994933	4.012024
	200	4.067003	4.019003	4.062176	4.070188	4.013905	4.022064
	400	4.058819	4.031840	4.055863	4.060377	4.028128	4.033528
	800	4.055374	4.040190	4.053088	4.056007	4.037371	4.040948
13.00	25	13.609529	12.757639	13.422666	13.623007	12.584773	12.778789
	50	13.305117	12.788342	13.203238	13.314808	12.691563	12.797624
	100	13.135788	12.836211	13.096533	13.138381	12.798791	12.841147
	200	13.058855	12.887390	13.040671	13.061174	12.865030	12.888867
	400	13.030583	12.935667	13.019784	13.031467	12.917283	12.934103
	800	13.018656	12.963715	13.010242	13.018526	12.951475	12.964958

AE Values for $R(x = 0.35, \alpha)$

Scenario α	n	ML	MPS	S-ML-I	S-ML-N	S-MPS-I	S-MPS-N
0.15	25	0.994859	0.995328	0.994987	0.994717	0.995335	0.995084
	50	0.995063	0.995496	0.995133	0.994996	0.995344	0.995211
	100	0.995176	0.995498	0.995204	0.995143	0.995326	0.995266
	200	0.995228	0.995453	0.995241	0.995212	0.995303	0.995281
	400	0.995247	0.995402	0.995255	0.995239	0.995277	0.995277
	800	0.995257	0.995491	0.995262	0.995253	0.995272	0.995274
0.45	25	0.939331	0.942676	0.940498	0.938403	0.943830	0.941853
	50	0.941131	0.943094	0.941775	0.940676	0.943811	0.942773
	100	0.942131	0.943113	0.942387	0.941915	0.943591	0.943133
	200	0.942599	0.943107	0.942721	0.942489	0.943416	0.943190
	400	0.942748	0.942941	0.942832	0.942692	0.943227	0.943082
	800	0.942850	0.943079	0.942900	0.942821	0.943127	0.943046
1.35	25	0.598342	0.615647	0.601293	0.598842	0.618496	0.615857
	50	0.603020	0.613629	0.604714	0.603201	0.615271	0.613725
	100	0.605802	0.611972	0.606380	0.605921	0.612542	0.612059
	200	0.607076	0.610609	0.607333	0.607130	0.610862	0.610632
	400	0.607437	0.609424	0.607624	0.607466	0.609681	0.609418
	800	0.607616	0.608724	0.607757	0.607624	0.608873	0.608690
4.05	25	0.126296	0.142997	0.127399	0.134729	0.144234	0.151211
	50	0.126772	0.137059	0.127236	0.131186	0.137539	0.141394
	100	0.127132	0.133140	0.127160	0.129381	0.133198	0.135388
	200	0.127280	0.130726	0.127286	0.128426	0.130784	0.131884
	400	0.127176	0.129111	0.127220	0.127754	0.129253	0.129682
	800	0.127104	0.128191	0.127160	0.127405	0.128342	0.128488
13.00	25	0.001585	0.002300	0.001552	0.002921	0.002257	0.003980
	50	0.001267	0.001623	0.001221	0.001834	0.001572	0.002296
	100	0.001110	0.001292	0.001076	0.001368	0.001255	0.001579
	200	0.001033	0.001130	0.001016	0.001154	0.001122	0.001260
	400	0.000991	0.001043	0.000983	0.001050	0.001054	0.001109
	800	0.000971	0.001000	0.000967	0.001001	0.001018	0.001035

AE Values for $h(x = 0.35, \alpha)$

Scenario α	n	ML	MPS	S-ML-I	S-ML-N	S-MPS-I	S-MPS-N
0.15	25	0.035743	0.032721	0.034953	0.036512	0.032696	0.034160
	50	0.034495	0.031695	0.034062	0.034863	0.032691	0.033472
	100	0.033803	0.031709	0.033630	0.033982	0.032837	0.033182
	200	0.033482	0.032003	0.033400	0.033570	0.032998	0.033120
	400	0.033370	0.032332	0.033319	0.033414	0.033170	0.033163
	800	0.033305	0.031692	0.033273	0.033327	0.033204	0.033191
0.45	25	0.346699	0.328876	0.340587	0.351233	0.322831	0.332826
	50	0.337347	0.326895	0.333992	0.339525	0.323146	0.328350
	100	0.332163	0.326943	0.330836	0.333181	0.324428	0.326693
	200	0.329744	0.327043	0.329113	0.330262	0.325410	0.326525
	400	0.328985	0.327977	0.328546	0.329249	0.326439	0.327171
	800	0.328457	0.327236	0.328199	0.328593	0.326989	0.327396
1.35	25	2.391444	2.264769	2.363344	2.415012	2.238734	2.287572
	50	2.343797	2.267261	2.327724	2.355540	2.252044	2.278785
	100	2.316447	2.272298	2.310548	2.321949	2.266584	2.277811
	200	2.304016	2.278819	2.301370	2.306767	2.276252	2.281737
	400	2.299851	2.285694	2.298134	2.301210	2.283607	2.287292
	800	2.297845	2.289952	2.296598	2.298574	2.288662	2.290981
4.05	25	9.519468	8.930812	9.398540	9.579283	8.819031	8.994743
	50	9.308294	8.951699	9.240606	9.336942	8.888883	8.982049
	100	9.190506	8.984140	9.165125	9.204803	8.959000	8.998303
	200	9.137032	9.018856	9.125430	9.143748	9.006562	9.025275
	400	9.117450	9.051028	9.110310	9.120722	9.041998	9.054626
	800	9.109230	9.071849	9.103690	9.110504	9.064962	9.073436
13.00	25	32.039410	30.012224	31.596062	32.065386	29.601973	30.056168
	50	31.318200	30.088449	31.076590	31.338214	29.858891	30.107394
	100	30.916967	30.204074	30.823949	30.921619	30.115407	30.214273
	200	30.734685	30.326661	30.691598	30.739445	30.273592	30.329409
	400	30.667786	30.441920	30.642180	30.669510	30.398198	30.437820
	800	30.639579	30.508843	30.619615	30.639081	30.479691	30.511611

Figure 4. Heatmap representations of the AE values for the UShD parameter α (top), the RF $R(x;\alpha)$ (center), and the HF $h(x;\alpha)$ (bottom).

RMSE Values for α

Scenario		Estimation Methods					
α	n	ML	MPS	S-ML-I	S-ML-N	S-MPS-I	S-MPS-N
0.15	25	0.022043	0.020383	0.011290	0.022023	0.011133	0.021224
	50	0.015613	0.014723	0.007833	0.015594	0.007855	0.015306
	100	0.010708	0.011016	0.005304	0.010699	0.005367	0.010613
	200	0.007480	0.011995	0.003729	0.007471	0.004438	0.007463
	400	0.005288	0.014060	0.002666	0.005284	0.004466	0.005303
	800	0.003868	0.022985	0.001942	0.003868	0.003634	0.003871
0.45	25	0.062138	0.059924	0.031762	0.062185	0.031323	0.060084
	50	0.044197	0.043024	0.022145	0.044237	0.022138	0.043465
	100	0.030391	0.029285	0.015041	0.030381	0.015077	0.030145
	200	0.021284	0.020393	0.010610	0.021244	0.010675	0.021223
	400	0.015071	0.021575	0.007595	0.015059	0.007917	0.015114
	800	0.010992	0.010981	0.005515	0.010989	0.005587	0.011003
1.35	25	0.203071	0.189452	0.105233	0.207304	0.099089	0.191683
	50	0.141731	0.136247	0.071319	0.143137	0.069899	0.137015
	100	0.096179	0.094403	0.047780	0.096644	0.047836	0.094701
	200	0.066940	0.066399	0.033389	0.066995	0.033954	0.066467
	400	0.047129	0.046964	0.023783	0.047180	0.025906	0.046985
	800	0.034556	0.034466	0.017385	0.034612	0.017644	0.034519
4.05	25	0.818020	0.749425	0.425326	0.823987	0.394252	0.749334
	50	0.561939	0.534426	0.283099	0.564281	0.277328	0.534104
	100	0.377835	0.369048	0.187804	0.378586	0.189210	0.368808
	200	0.261926	0.259226	0.130637	0.262010	0.135387	0.259584
	400	0.184410	0.183647	0.093071	0.184357	0.099167	0.183591
	800	0.135608	0.135064	0.068313	0.135611	0.077801	0.135259
13.00	25	2.856777	2.631095	1.481651	2.854490	1.394023	2.628608
	50	1.965853	1.876563	0.990131	1.967429	0.984297	1.876829
	100	1.323471	1.295888	0.657192	1.323361	0.666440	1.295037
	200	0.917959	0.909717	0.458064	0.917465	0.491671	0.909965
	400	0.646718	0.647584	0.326364	0.646891	0.387774	0.646009
	800	0.475676	0.473750	0.239794	0.475600	0.331403	0.474713

RMSE Values for $R(x = 0.35, \alpha)$

Scenario		Estimation Methods					
α	n	ML	MPS	S-ML-I	S-ML-N	S-MPS-I	S-MPS-N
0.15	25	0.001750	0.001514	0.000871	0.001833	0.000781	0.001646
	50	0.001184	0.000980	0.000584	0.001212	0.000551	0.001136
	100	0.000789	0.000658	0.000388	0.000798	0.000378	0.000769
	200	0.000544	0.000605	0.000270	0.000546	0.000315	0.000537
	400	0.000381	0.000649	0.000192	0.000382	0.000319	0.000380
	800	0.000278	0.001004	0.000139	0.000278	0.000260	0.000277
0.45	25	0.017930	0.016694	0.009059	0.018248	0.008416	0.016846
	50	0.012503	0.011902	0.006212	0.012625	0.005981	0.012049
	100	0.008475	0.008079	0.004177	0.008510	0.004092	0.008292
	200	0.005893	0.005621	0.002929	0.005895	0.002907	0.005825
	400	0.004154	0.007000	0.002091	0.004156	0.002163	0.004146
	800	0.003024	0.003013	0.001516	0.003025	0.001529	0.003018
1.35	25	0.067961	0.065788	0.035876	0.067195	0.035658	0.065208
	50	0.048679	0.047849	0.024749	0.048386	0.025082	0.047663
	100	0.033565	0.033365	0.016754	0.033466	0.017109	0.033343
	200	0.023520	0.023500	0.011769	0.023451	0.012105	0.023490
	400	0.016636	0.016644	0.008407	0.016621	0.009215	0.016641
	800	0.012219	0.012215	0.006153	0.012226	0.006266	0.012229
4.05	25	0.050646	0.056214	0.027901	0.050843	0.034185	0.058458
	50	0.036745	0.039485	0.019221	0.036846	0.022511	0.040634
	100	0.025888	0.027164	0.013099	0.025926	0.014718	0.027706
	200	0.018287	0.018867	0.009234	0.018306	0.010203	0.019141
	400	0.013064	0.013316	0.006631	0.013059	0.007336	0.013413
	800	0.009661	0.009750	0.004881	0.009663	0.005676	0.009809
13.00	25	0.002256	0.003214	0.001250	0.003717	0.001977	0.005047
	50	0.001231	0.001614	0.000653	0.001762	0.000965	0.002282
	100	0.000769	0.000925	0.000388	0.000963	0.000519	0.001168
	200	0.000503	0.000564	0.000254	0.000573	0.000329	0.000654
	400	0.000346	0.000371	0.000176	0.000371	0.000242	0.000407
	800	0.000252	0.000262	0.000127	0.000261	0.000197	0.000280

RMSE Values for $h(x = 0.35, \alpha)$

Scenario		Estimation Methods					
α	n	ML	MPS	S-ML-I	S-ML-N	S-MPS-I	S-MPS-N
0.15	25	0.011178	0.009761	0.005596	0.011594	0.005087	0.010507
	50	0.007630	0.006415	0.003776	0.007770	0.003596	0.007333
	100	0.005110	0.004362	0.002515	0.005158	0.002469	0.004991
	200	0.003532	0.004089	0.001753	0.003544	0.002056	0.003490
	400	0.002479	0.004445	0.001247	0.002483	0.002081	0.002472
	800	0.001808	0.006936	0.000907	0.001810	0.001693	0.001803
0.45	25	0.095225	0.088913	0.048113	0.096998	0.044950	0.089832
	50	0.066435	0.063372	0.033024	0.067088	0.031912	0.064189
	100	0.045073	0.043013	0.022223	0.045258	0.021820	0.044174
	200	0.031361	0.029926	0.015590	0.031368	0.015495	0.031029
	400	0.022113	0.037738	0.011130	0.022123	0.011525	0.022083
	800	0.016101	0.016046	0.008073	0.016106	0.008147	0.016074
1.35	25	0.513457	0.476276	0.265865	0.523776	0.247795	0.480760
	50	0.358158	0.343013	0.180074	0.361588	0.175378	0.344472
	100	0.242778	0.237753	0.120558	0.243910	0.120250	0.238299
	200	0.168893	0.167304	0.084213	0.169013	0.085454	0.167390
	400	0.118859	0.118353	0.059973	0.118984	0.065243	0.118372
	800	0.087135	0.086872	0.043835	0.087276	0.044459	0.086991
4.05	25	2.003419	1.843280	1.043268	2.014665	0.973981	1.841618
	50	1.379267	1.315424	0.695529	1.383716	0.684432	1.314337
	100	0.928792	0.908723	0.461881	0.930170	0.466610	0.908138
	200	0.644300	0.638289	0.321455	0.644354	0.333666	0.639213
	400	0.453840	0.452211	0.229085	0.453649	0.244308	0.452099
	800	0.333799	0.332563	0.168167	0.333785	0.191620	0.333057
13.00	25	6.792441	6.261308	3.523679	6.786469	3.320230	6.256635
	50	4.675602	4.465760	2.355297	4.679134	2.343577	4.466998
	100	3.148517	3.083949	1.563566	3.148200	1.586443	3.082222
	200	2.184039	2.164859	1.089902	2.182850	1.170241	2.165577
	400	1.538814	1.541035	0.776576	1.539218	0.922866	1.537352
	800	1.131869	1.127358	0.570597	1.131685	0.788660	1.129671

Figure 5. Heatmap representations of the RMSE values for the UShD parameter α (top), the RF $R(x; \alpha)$ (center), and the HF $h(x; \alpha)$ (bottom).

MRAB Values for α

Scenario α	n	ML	MPS	S-ML-I	S-ML-N	S-MPS-I	S-MPS-N
0.15	25	0.115303	0.103827	0.060065	0.115191	0.059753	0.113131
	50	0.082630	0.066841	0.042007	0.082552	0.042293	0.081917
	100	0.056593	0.043160	0.028167	0.056511	0.028878	0.056675
	200	0.039299	0.035658	0.019648	0.039216	0.023589	0.039533
	400	0.028497	0.032744	0.014393	0.028489	0.024090	0.028541
	800	0.020650	0.047912	0.010379	0.020641	0.019395	0.020694
0.45	25	0.108798	0.106203	0.056337	0.108755	0.056079	0.106878
	50	0.078235	0.076264	0.039570	0.078297	0.039793	0.077683
	100	0.053633	0.051549	0.026659	0.053603	0.027076	0.053710
	200	0.037297	0.035716	0.018646	0.037238	0.018928	0.037479
	400	0.027032	0.027861	0.013646	0.027021	0.014200	0.027142
	800	0.019594	0.019570	0.009839	0.019579	0.009929	0.019605
1.35	25	0.116412	0.111564	0.062258	0.118326	0.059113	0.112364
	50	0.082521	0.080744	0.042437	0.083196	0.041798	0.080973
	100	0.056260	0.055980	0.028167	0.056414	0.028609	0.056032
	200	0.038975	0.039082	0.019530	0.038974	0.020106	0.039111
	400	0.028223	0.028144	0.014282	0.028250	0.015545	0.028120
	800	0.020445	0.020390	0.010298	0.020476	0.010416	0.020436
4.05	25	0.153716	0.146635	0.083489	0.154298	0.078855	0.145882
	50	0.108267	0.105539	0.056030	0.108568	0.055373	0.105295
	100	0.073128	0.072887	0.036738	0.073131	0.037626	0.072693
	200	0.050783	0.050971	0.025509	0.050710	0.026895	0.050975
	400	0.036696	0.036648	0.018602	0.036689	0.019773	0.036667
	800	0.026659	0.026561	0.013454	0.026635	0.015356	0.026638
13.00	25	0.167571	0.160719	0.090470	0.167216	0.087105	0.160307
	50	0.118182	0.115584	0.061030	0.118271	0.061335	0.115555
	100	0.079839	0.079753	0.040028	0.079837	0.041257	0.079644
	200	0.055471	0.055751	0.027856	0.055448	0.030420	0.055802
	400	0.040084	0.040170	0.020311	0.040099	0.024196	0.040160
	800	0.029132	0.028967	0.014710	0.029129	0.020349	0.029057

MRAB Values for $R(x = 0.35, \alpha)$

Scenario α	n	ML	MPS	S-ML-I	S-ML-N	S-MPS-I	S-MPS-N
0.15	25	0.001305	0.001116	0.000685	0.001352	0.000631	0.001251
	50	0.000915	0.000692	0.000466	0.000932	0.000447	0.000892
	100	0.000618	0.000438	0.000308	0.000622	0.000307	0.000611
	200	0.000426	0.000346	0.000213	0.000427	0.000252	0.000425
	400	0.000308	0.000299	0.000156	0.000309	0.000259	0.000307
	800	0.000223	0.000368	0.000112	0.000223	0.000209	0.000223
0.45	25	0.014579	0.013880	0.007589	0.014734	0.007200	0.013970
	50	0.010388	0.009973	0.005258	0.010455	0.005135	0.010144
	100	0.007075	0.006750	0.003517	0.007084	0.003507	0.006998
	200	0.004904	0.004680	0.002450	0.004899	0.002462	0.004891
	400	0.003548	0.003694	0.001791	0.003549	0.001853	0.003549
	800	0.002570	0.002562	0.001290	0.002569	0.001298	0.002567
1.35	25	0.088845	0.087255	0.047435	0.087850	0.047035	0.086478
	50	0.063856	0.063408	0.032844	0.063467	0.033224	0.063123
	100	0.043914	0.044065	0.022001	0.043774	0.022697	0.044014
	200	0.030539	0.030770	0.015313	0.030454	0.015914	0.030782
	400	0.022164	0.022161	0.011217	0.022149	0.012266	0.022127
	800	0.016068	0.016049	0.008094	0.016078	0.008208	0.016079
4.05	25	0.320516	0.349208	0.174550	0.317216	0.209018	0.361844
	50	0.234568	0.248345	0.122135	0.233503	0.139869	0.254496
	100	0.162763	0.170234	0.082176	0.162936	0.091844	0.173493
	200	0.114359	0.118012	0.057710	0.114459	0.064052	0.119806
	400	0.083241	0.084436	0.042226	0.083129	0.046213	0.084986
	800	0.060620	0.060929	0.030596	0.060517	0.035493	0.061301
13.00	25	1.331128	1.893125	0.858903	2.350132	1.452395	3.357110
	50	0.872829	1.104849	0.496312	1.223989	0.748404	1.616738
	100	0.579965	0.676331	0.307150	0.707552	0.408774	0.856140
	200	0.396809	0.436485	0.206476	0.442982	0.266041	0.502800
	400	0.285389	0.300674	0.146393	0.300358	0.196727	0.324628
	800	0.206640	0.211623	0.104817	0.211680	0.159379	0.223531

MRAB Values for $h(x = 0.35, \alpha)$

Scenario α	n	ML	MPS	S-ML-I	S-ML-N	S-MPS-I	S-MPS-N
0.15	25	0.252297	0.217488	0.132212	0.259240	0.123210	0.242084
	50	0.177703	0.135700	0.090451	0.180128	0.087428	0.173320
	100	0.120333	0.086064	0.059909	0.120847	0.059971	0.119052
	200	0.083113	0.068296	0.041529	0.083128	0.049263	0.082915
	400	0.060090	0.059399	0.030345	0.060185	0.050598	0.059959
	800	0.043493	0.074507	0.021862	0.043515	0.040775	0.043492
0.45	25	0.223063	0.212848	0.116025	0.225660	0.110588	0.214618
	50	0.158965	0.152843	0.080440	0.160052	0.078792	0.155601
	100	0.108293	0.103400	0.053830	0.108454	0.053775	0.107290
	200	0.075077	0.071676	0.037513	0.075017	0.037728	0.074947
	400	0.054327	0.056628	0.027423	0.054346	0.028390	0.054372
	800	0.039353	0.039241	0.019760	0.039336	0.019885	0.039309
1.35	25	0.172748	0.164861	0.092438	0.175295	0.087058	0.165439
	50	0.122458	0.119506	0.062984	0.123366	0.061723	0.119603
	100	0.083462	0.082917	0.041784	0.083641	0.042314	0.082886
	200	0.057812	0.057920	0.028967	0.057792	0.029769	0.057916
	400	0.041859	0.041722	0.021183	0.041894	0.023035	0.041673
	800	0.030322	0.030233	0.015274	0.030367	0.015440	0.030296
4.05	25	0.168086	0.160842	0.091264	0.168504	0.086694	0.160018
	50	0.118513	0.115753	0.061325	0.118769	0.060827	0.115500
	100	0.080107	0.079934	0.040243	0.080092	0.041304	0.079741
	200	0.055647	0.055890	0.027953	0.055561	0.029508	0.055906
	400	0.040218	0.040180	0.020387	0.040207	0.021685	0.040205
	800	0.029220	0.029119	0.014746	0.029192	0.016838	0.029204
13.00	25	0.169372	0.162550	0.091437	0.169019	0.088140	0.162190
	50	0.119468	0.116887	0.061692	0.119561	0.062046	0.116883
	100	0.080716	0.080648	0.040468	0.080717	0.041728	0.080548
	200	0.056083	0.056373	0.028164	0.056061	0.030763	0.056430
	400	0.040528	0.040617	0.020536	0.040543	0.024467	0.040608
	800	0.029455	0.029289	0.014873	0.029451	0.020576	0.029380

Figure 6. Heatmap representations of the MRAB values for the UShD parameter α (top), the RF $R(x;\alpha)$ (center), and the HF $h(x;\alpha)$ (bottom).

AL Values for α

Scenario		90% C.L. Estimation Methods						95% C.L. Estimation Methods					
α	n	ML	MPS	S-ML-I	S-ML-N	S-MPS-I	S-MPS-N	ML	MPS	S-ML-I	S-ML-N	S-MPS-I	S-MPS-N
0.15	25	0.07060	0.35076	0.04995	0.06973	0.04814	0.06709	0.08413	0.41796	0.05947	0.08307	0.05733	0.07992
	50	0.04937	0.34162	0.03473	0.04890	0.03377	0.04758	0.05883	0.40707	0.04137	0.05825	0.04026	0.05671
	100	0.03469	0.33960	0.02427	0.03446	0.02367	0.03373	0.04134	0.40466	0.02890	0.04105	0.02817	0.04014
	200	0.02446	0.33940	0.01720	0.02429	0.01824	0.02381	0.02914	0.40442	0.02048	0.02893	0.02171	0.02838
	400	0.01728	0.33983	0.01221	0.01717	0.01540	0.01684	0.02059	0.40493	0.01453	0.02045	0.01833	0.02005
	800	0.01221	0.33358	0.00862	0.01214	0.01144	0.01186	0.01455	0.39749	0.01026	0.01446	0.01362	0.01412
0.45	25	0.20012	1.00611	0.14148	0.19807	0.13655	0.19080	0.23845	1.19885	0.16846	0.23588	0.16256	0.22738
	50	0.14017	0.99150	0.09854	0.13904	0.09568	0.13547	0.16702	1.18145	0.11731	0.16559	0.11401	0.16146
	100	0.09858	0.98590	0.06894	0.09792	0.06712	0.09600	0.11747	1.17478	0.08210	0.11659	0.07991	0.11434
	200	0.06953	0.98322	0.04886	0.06911	0.04750	0.06775	0.08285	1.17158	0.05816	0.08229	0.05653	0.08071
	400	0.04913	0.98282	0.03470	0.04888	0.03423	0.04788	0.05855	1.17110	0.04130	0.05818	0.04069	0.05701
	800	0.03473	0.98138	0.02448	0.03455	0.02368	0.03369	0.04138	1.16939	0.02916	0.04113	0.02819	0.04017
1.35	25	0.64031	3.15709	0.45400	0.63458	0.42764	0.60120	0.76298	3.76191	0.54083	0.75677	0.50947	0.71755
	50	0.44420	3.10348	0.31264	0.44123	0.29990	0.42534	0.52929	3.69803	0.37244	0.52594	0.35716	0.50731
	100	0.31066	3.08090	0.21737	0.30873	0.21050	0.30051	0.37017	3.67112	0.25896	0.36778	0.25105	0.35810
	200	0.21857	3.07447	0.15373	0.21733	0.14966	0.21269	0.26044	3.66345	0.18302	0.25884	0.17823	0.25324
	400	0.15427	3.07528	0.10898	0.15349	0.10941	0.15001	0.18382	3.66442	0.12974	0.18280	0.13030	0.17860
	800	0.10900	3.07691	0.07693	0.10852	0.07440	0.10572	0.12988	3.66636	0.09156	0.12921	0.08860	0.12586
4.05	25	2.53104	12.31660	1.79453	2.47914	1.66826	2.31455	3.01592	14.67614	2.13754	2.95630	1.98830	2.76058
	50	1.74699	12.09804	1.23010	1.72438	1.17071	1.64452	2.08166	14.41571	1.46493	2.05464	1.39412	1.96128
	100	1.21847	12.01744	0.85249	1.20745	0.82136	1.16861	1.45190	14.31966	1.01538	1.43800	0.97853	1.39269
	200	0.85617	12.00316	0.60228	0.84950	0.58650	0.82596	1.02020	14.30265	0.71699	1.01149	0.69835	0.98443
	400	0.60400	12.01698	0.42680	0.60032	0.42345	0.58400	0.71971	14.31911	0.50803	0.71482	0.50324	0.69598
	800	0.42667	12.03065	0.30138	0.42445	0.30842	0.41224	0.50841	14.33540	0.35877	0.50548	0.36730	0.49036
13.00	25	8.85655	43.23737	6.28127	8.68376	5.86508	8.11317	10.55323	51.52051	7.48367	10.35277	6.99305	9.68258
	50	6.12058	42.47048	4.31130	6.04691	4.11024	5.77613	7.29312	50.60669	5.13617	7.20132	4.89459	6.88911
	100	4.27206	42.18263	2.99040	4.23013	2.88340	4.09920	5.09047	50.26371	3.56269	5.03918	3.43879	4.88219
	200	3.00286	42.12716	2.11266	2.98145	2.09730	2.89830	3.57813	50.19761	2.51524	3.55110	2.49352	3.45399
	400	2.11869	42.17408	1.49691	2.10588	1.56444	2.04739	2.52458	50.25351	1.78170	2.50727	1.86042	2.43962
	800	1.49676	42.21033	1.05699	1.48741	1.19936	1.44683	1.78350	50.29671	1.25863	1.77066	1.42921	1.72532

AL Values for $R(x = 0.35, \alpha)$

Scenario		90% C.L. Estimation Methods						95% C.L. Estimation Methods					
α	n	ML	MPS	S-ML-I	S-ML-N	S-MPS-I	S-MPS-N	ML	MPS	S-ML-I	S-ML-N	S-MPS-I	S-MPS-N
0.15	25	0.00537	0.02521	0.00365	0.00522	0.00337	0.00482	0.00640	0.03004	0.00437	0.00629	0.00404	0.00581
	50	0.00364	0.02390	0.00251	0.00358	0.00238	0.00340	0.00434	0.02848	0.00300	0.00429	0.00284	0.00407
	100	0.00252	0.02368	0.00174	0.00249	0.00168	0.00240	0.00300	0.02822	0.00208	0.00298	0.00200	0.00287
	200	0.00176	0.02382	0.00123	0.00175	0.00130	0.00170	0.00210	0.02839	0.00147	0.00208	0.00155	0.00203
	400	0.00124	0.02405	0.00087	0.00123	0.00110	0.00120	0.00148	0.02865	0.00104	0.00147	0.00131	0.00143
	800	0.00088	0.02355	0.00062	0.00087	0.00082	0.00085	0.00104	0.02807	0.00073	0.00104	0.00097	0.00101
0.45	25	0.05642	0.27675	0.03910	0.05487	0.03678	0.05155	0.06722	0.32977	0.04662	0.06552	0.04387	0.06163
	50	0.03902	0.27196	0.02715	0.03836	0.02595	0.03681	0.04650	0.32406	0.03234	0.04576	0.03095	0.04393
	100	0.02725	0.27044	0.01896	0.02694	0.01829	0.02617	0.03247	0.32224	0.02259	0.03210	0.02178	0.03120
	200	0.01915	0.26973	0.01342	0.01899	0.01298	0.01852	0.02282	0.32141	0.01598	0.02262	0.01545	0.02207
	400	0.01352	0.26987	0.00953	0.01343	0.00937	0.01312	0.01611	0.32157	0.01135	0.01599	0.01115	0.01563
	800	0.00955	0.26930	0.00673	0.00949	0.00649	0.00924	0.01138	0.32089	0.00801	0.01130	0.00773	0.01102
1.35	25	0.21817	1.10275	0.15741	0.21399	0.15179	0.20770	0.25997	1.31401	0.18680	0.25316	0.18016	0.24622
	50	0.15426	1.09377	0.10962	0.15243	0.10668	0.14907	0.18381	1.30330	0.13032	0.18097	0.12679	0.17716
	100	0.10905	1.09056	0.07662	0.10808	0.07482	0.10610	0.12994	1.29948	0.09120	0.12851	0.08913	0.12614
	200	0.07710	1.08965	0.05433	0.07656	0.05314	0.07528	0.09187	1.29840	0.06466	0.09109	0.06326	0.08954
	400	0.05453	1.08985	0.03856	0.05422	0.03882	0.05312	0.06497	1.29864	0.04590	0.06454	0.04622	0.06321
	800	0.03856	1.09017	0.02723	0.03838	0.02638	0.03744	0.04595	1.29901	0.03241	0.04569	0.03141	0.04456
4.05	25	0.16524	0.91791	0.12016	0.16011	0.12780	0.17053	0.19690	1.09376	0.14354	0.19146	0.15265	0.20349
	50	0.11927	0.89647	0.08527	0.11710	0.08808	0.12125	0.14212	1.06821	0.10164	0.13967	0.10505	0.14458
	100	0.08535	0.88320	0.06006	0.08434	0.06076	0.08569	0.10170	1.05240	0.07156	0.10048	0.07239	0.10215
	200	0.06069	0.87475	0.04281	0.06015	0.04284	0.06015	0.07232	1.04232	0.05098	0.07163	0.05104	0.07165
	400	0.04300	0.86901	0.03044	0.04271	0.03068	0.04221	0.05124	1.03549	0.03623	0.05086	0.03647	0.05029
	800	0.03043	0.86569	0.02153	0.03026	0.02223	0.02964	0.03626	1.03153	0.02563	0.03605	0.02648	0.03528
13.00	25	0.00605	0.04337	0.00335	0.00676	0.00474	0.00904	0.00721	0.05168	0.00457	0.00968	0.00637	0.01270
	50	0.00371	0.03315	0.00221	0.00381	0.00276	0.00467	0.00442	0.03950	0.00282	0.00509	0.00350	0.00619
	100	0.00241	0.02773	0.00152	0.00240	0.00173	0.00271	0.00287	0.03304	0.00188	0.00305	0.00212	0.00343
	200	0.00162	0.02495	0.00108	0.00161	0.00119	0.00172	0.00194	0.02973	0.00131	0.00198	0.00144	0.00211
	400	0.00112	0.02342	0.00077	0.00111	0.00085	0.00114	0.00133	0.02791	0.00092	0.00134	0.00103	0.00138
	800	0.00078	0.02265	0.00054	0.00077	0.00064	0.00077	0.00093	0.02699	0.00065	0.00093	0.00077	0.00093

AL Values for $h(x = 0.35, \alpha)$

Scenario		90% C.L. Estimation Methods						95% C.L. Estimation Methods					
α	n	ML	MPS	S-ML-I	S-ML-N	S-MPS-I	S-MPS-N	ML	MPS	S-ML-I	S-ML-N	S-MPS-I	S-MPS-N
0.15	25	0.03456	0.16373	0.02368	0.03368	0.02203	0.03128	0.04118	0.19510	0.02831	0.04047	0.02635	0.03762
	50	0.02360	0.15605	0.01632	0.02322	0.01553	0.02212	0.02812	0.18594	0.01949	0.02776	0.01855	0.02647
	100	0.01636	0.15481	0.01136	0.01619	0.01094	0.01565	0.01949	0.18447	0.01354	0.01933	0.01303	0.01867
	200	0.01146	0.15558	0.00803	0.01136	0.00846	0.01106	0.01366	0.18539	0.00956	0.01355	0.01007	0.01320
	400	0.00808	0.15684	0.00569	0.00802	0.00716	0.00784	0.00962	0.18689	0.00678	0.00955	0.00853	0.00933
	800	0.00570	0.15357	0.00402	0.00567	0.00533	0.00552	0.00679	0.18299	0.00478	0.00675	0.00635	0.00658
0.45	25	0.30028	1.47612	0.20841	0.29320	0.19654	0.27605	0.35780	1.75890	0.24855	0.35033	0.23445	0.33010
	50	0.20773	1.44964	0.14463	0.20461	0.13844	0.19659	0.24752	1.72735	0.17228	0.24412	0.16515	0.23467
	100	0.14506	1.44081	0.10100	0.14357	0.09749	0.13958	0.17285	1.71683	0.12032	0.17110	0.11613	0.16642
	200	0.10197	1.43675	0.07149	0.10117	0.06917	0.09871	0.12150	1.71200	0.08512	0.12052	0.08233	0.11763
	400	0.07198	1.43777	0.05076	0.07153	0.04993	0.06989	0.08576	1.71320	0.06043	0.08517	0.05937	0.08325
	800	0.05083	1.43422	0.03581	0.05055	0.03458	0.04922	0.06057	1.70898	0.04265	0.06018	0.04117	0.05868
1.35	25	1.61393	7.92452	1.14258	1.59142	1.07142	1.50126	1.92312	9.44264	1.36018	1.89582	1.27575	1.78968
	50	1.11981	7.80324	0.78755	1.10949	0.75340	1.06673	1.33433	9.29813	0.93790	1.32177	0.89699	1.27154
	100	0.78318	7.75507	0.54783	0.77732	0.52968	0.75543	0.93322	9.24073	0.65254	0.92571	0.63165	0.90001
	200	0.55103	7.74409	0.38750	0.54754	0.37690	0.53540	0.65659	9.22766	0.46131	0.65205	0.44882	0.63738
	400	0.38896	7.74972	0.27473	0.38685	0.27567	0.37792	0.46347	9.23437	0.32708	0.46069	0.32830	0.44991
	800	0.27482	7.75577	0.19395	0.27356	0.18751	0.26644	0.32747	9.24157	0.23085	0.32573	0.22330	0.31719
4.05	25	6.21470	30.33503	4.41406	6.09460	4.11657	5.70664	7.40527	36.14642	5.25756	7.26600	4.90578	6.80447
	50	4.29503	29.80102	3.02714	4.24213	2.88661	4.05330	5.11784	35.51011	3.60488	5.05404	3.43730	4.83319
	100	2.99788	29.60108	2.09835	2.97171	2.02408	2.87939	3.57220	35.27186	2.49925	3.53894	2.41130	3.43142
	200	2.10724	29.56199	1.48267	2.09116	1.44474	2.03455	2.51093	35.22528	1.76506	2.48985	1.72027	2.42478
	400	1.48678	29.59151	1.05071	1.47785	1.04286	1.43819	1.77160	35.26046	1.25067	1.75971	1.23934	1.71392
	800	1.05034	29.62212	0.74197	1.04492	0.75947	1.01506	1.25155	35.29693	0.88324	1.24439	0.90445	1.20742
13.00	25	21.06837	102.92182	14.94670	20.66806	13.96591	19.32353	25.10452	122.63891	17.80859	24.64190	16.65240	23.06241
	50	14.56205	101.08598	10.25900	14.39042	9.78459	13.75187	17.35175	120.45137	12.22201	17.13826	11.65192	16.40184
	100	10.16493	100.39276	7.11584	10.06649	6.86284	9.75722	12.11226	119.62536	8.47770	11.99194	8.18482	11.62109
	200	7.14529	100.25468	5.02721	7.09480	4.99139	6.89787	8.51413	119.46082	5.98523	8.45042	5.93437	8.22039
	400	5.04148	100.36157	3.56199	5.01114	3.72299	4.87234	6.00729	119.58819	4.23969	5.96632	4.42738	5.80577
	800	3.56159	100.44519	2.51517	3.53941	2.85410	3.44298	4.24389	119.68783	2.99498	4.21343	3.40106	4.10568

Figure 7. Heatmap representations of the AL values for the UShD parameter α (top), the RF $R(x; \alpha)$ (center), and the HF $h(x; \alpha)$ (bottom).

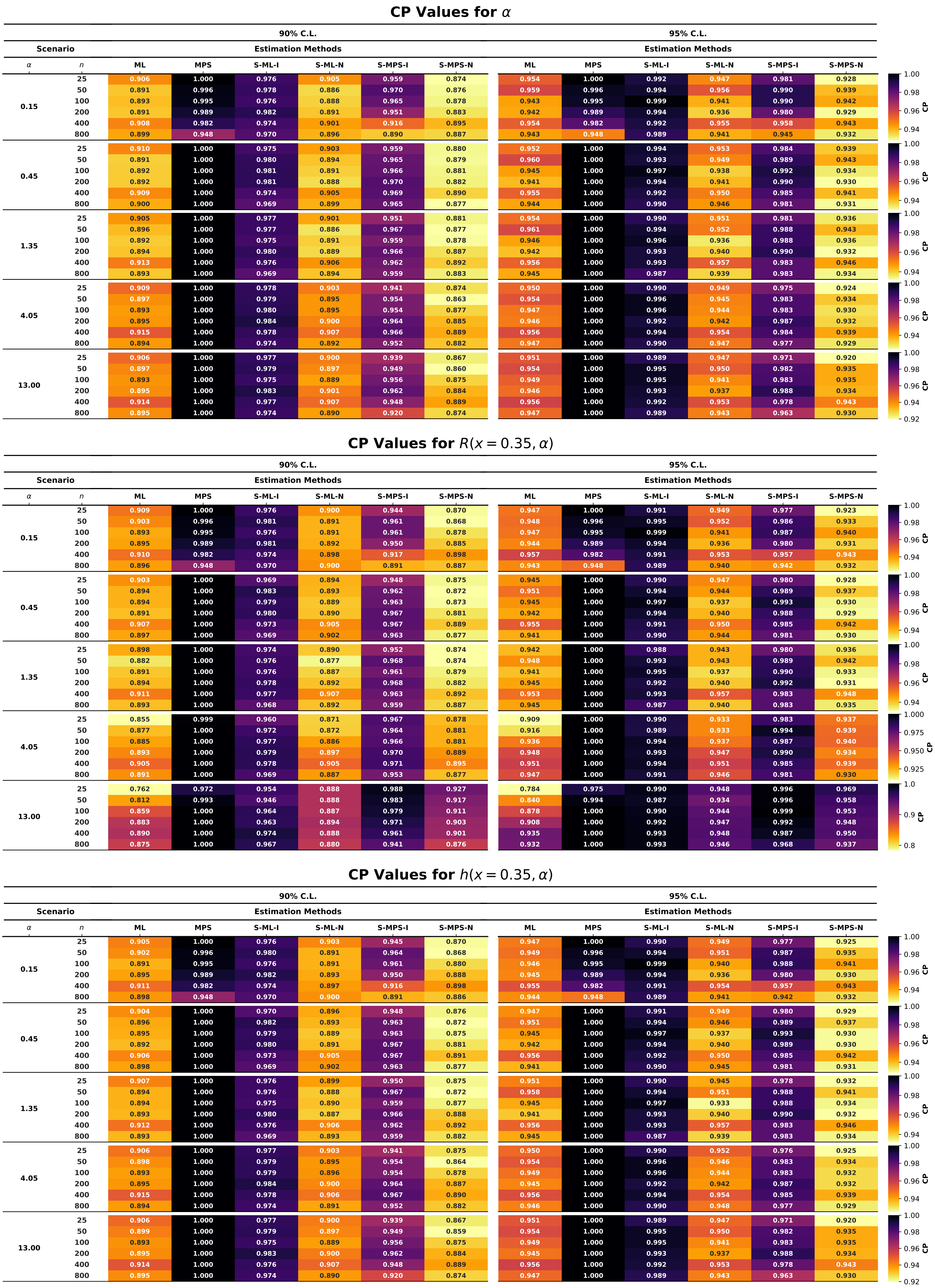

Figure 8. Heatmap representations of the CP values for the UShD parameter α (top), the RF $R(x;\alpha)$ (center), and the HF $h(x;\alpha)$ (bottom).

8. Applications and data analysis

In this section, we explore the practical behavior, operational flexibility, and inferential performance of the proposed UShD using two real datasets from distinct engineering disciplines. The first dataset comprises the waiting times between successive failures of repairable mechanical equipment (RME) units, as documented in [43, 44]. The second dataset includes the observed breakdown times of 20 electric bulbs (EB), also cited in [44]. Since the UShD is defined on the unit interval, we adjust the raw measurements to fit within the range of (0, 1) by applying the transformation $X = T/(1 + T)$. The resulting transformed observations, rounded to five decimal places, are presented below.

- Dataset I: RME

  0.52381, 0.75000, 0.80000, 0.81818, 0.85507, 0.86301, 0.87500, 0.87654, 0.88095, 0.88506, 0.90385, 0.91379, 0.92126, 0.92481, 0.92481, 0.92537, 0.93464, 0.93590, 0.93711, 0.94565, 0.94792, 0.94898, 0.95169, 0.95708, 0.95951, 0.96094, 0.96337, 0.97191, 0.97758, 0.97930.

- Dataset II: EB

  0.28058, 0.56897, 0.57082, 0.77925, 0.78261, 0.83471, 0.84277, 0.86772, 0.87835, 0.88519, 0.89919, 0.91349, 0.92051, 0.92521, 0.92548, 0.92658, 0.95148, 0.95526, 0.95618, 0.97343.

Before conducting any formal parametric inference, we explore the underlying distributional shapes of both datasets using nonparametric graphical methods. The resulting visual summaries are presented in Figures 9 and 10.

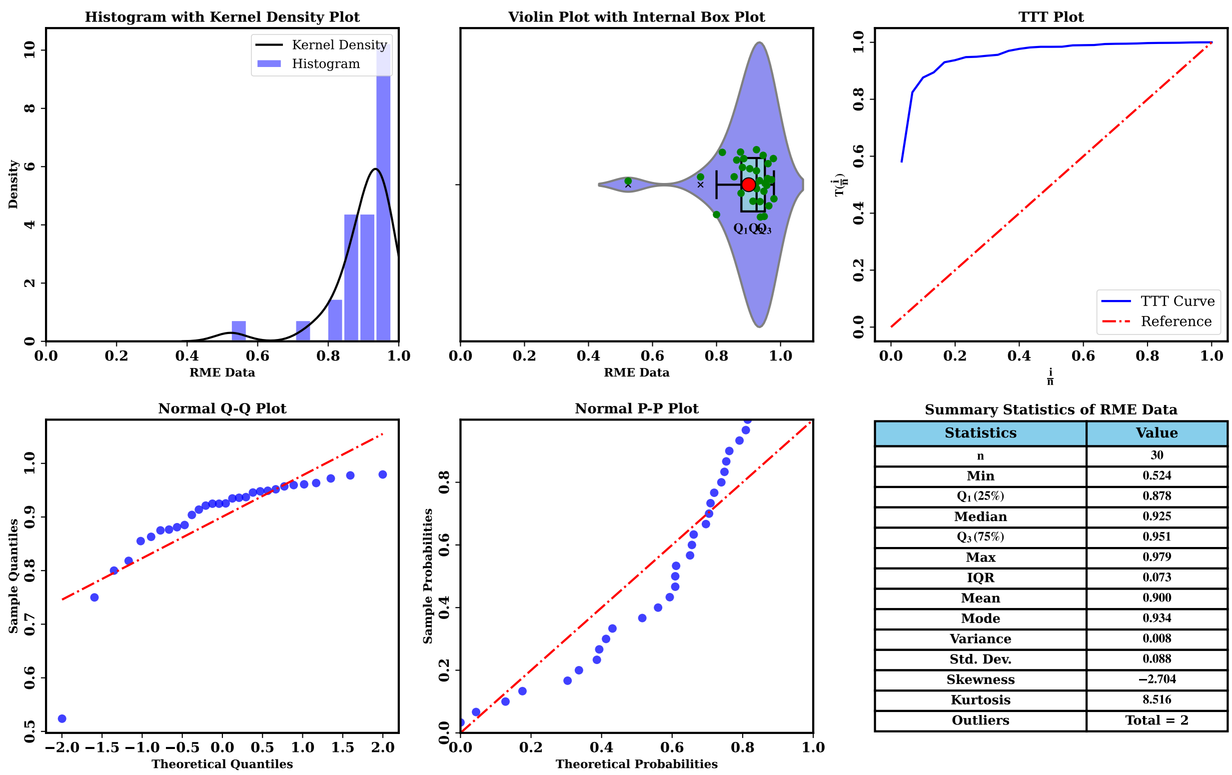

Statistics	Value
n	30
Min	0.524
Q_1 (25%)	0.878
Median	0.925
Q_3 (75%)	0.951
Max	0.979
IQR	0.073
Mean	0.900
Mode	0.934
Variance	0.008
Std. Dev.	0.088
Skewness	−2.704
Kurtosis	8.516
Outliers	Total = 2

Figure 9. Nonparametric visual assessment and sample descriptive statistics for the RME data.

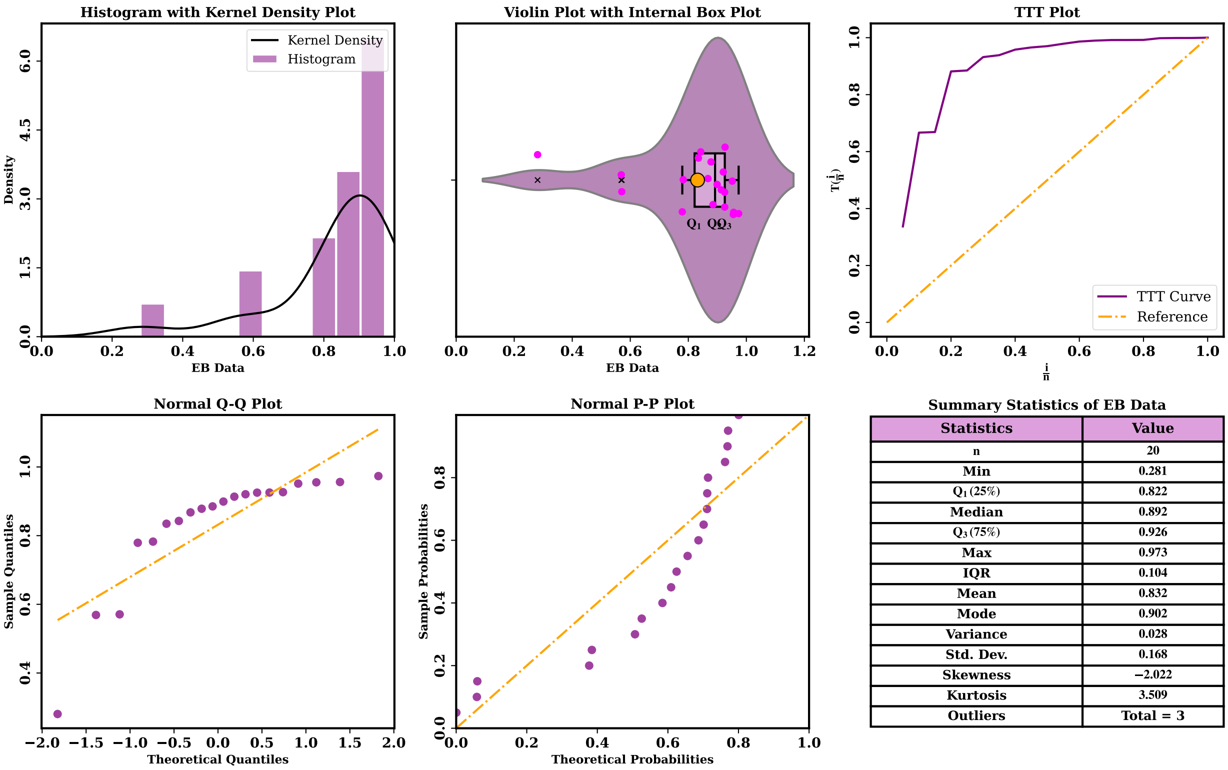

Figure 10. Nonparametric visual assessment and sample descriptive statistics for the EB data.

A joint inspection of the descriptive measures and visual displays for both the RME and EB datasets reveals broadly similar empirical patterns. Both the density histogram (with a superimposed kernel estimate) and the violin diagram reveal a marked accumulation of transformed observations near the upper boundary of the unit interval, with the bulk of measurements falling roughly between 0.80 and 0.98. Such clustering implies an asymmetric, bounded configuration for both datasets, punctuated by a handful of comparatively small realizations in the lower tail. These visual impressions are reinforced by the numerical summaries: In both cases, the arithmetic mean falls below the median, while the estimated skewness coefficients take negative values, signaling a strong leftward asymmetry. Furthermore, the kurtosis estimates point to sharply peaked forms with pronounced tail heaviness, an effect especially visible in the RME series.

In addition, the total time on test (TTT) curves consistently lie above the 45° diagonal, offering visual confirmation of a monotone increasing hazard rate and, by extension, a wear-out or aging regime. Likewise, the normal quantile–quantile (Q–Q) and probability–probability (P–P) plots exhibit clear, structured deviations from their respective theoretical benchmarks, ruling out the Gaussian model for the transformed measurements. From a reliability perspective, the observed IFR behavior indicates that the instantaneous failure risk increases with transformed operating time, which is consistent with progressive aging and wear-out in both the RME and EB applications. Taken together, these features indicate that traditional symmetric distributions are unlikely to fit adequately, and support the use of the UShD for both datasets.

For comparative benchmarking, the proposed UShD is evaluated alongside seven established unit-interval distributions. Its parameter is estimated using the ML approach, and this same inferential framework is applied to each of the competing distributions: unit Xgamma distribution (UXGD) [45], unit improved second-degree Lindley distribution (UISDLD) [46], unit Zeghdoudi distribution (UZD) [47], sine power unit inverse Lindley distribution (SPUILD) [48], unit Gumbel Type II distribution (UGTIID) [49], unit inverse exponentiated Pareto distribution (UIEPD) [50], and unit gamma-Lindley distribution (UGLD) [51]. All numerical maximizations are carried out using common algorithmic settings and shared convergence thresholds, which helps maintain methodological consistency throughout the comparison. The outputs of the optimization process include the parameter estimates, their estimated standard errors (SEs), the value of −2 times the maximized log-likelihood (-2ℓ), and a set of penalized information criteria. The relative performance of the models is assessed using the Akaike information criterion (AIC), the consistent Akaike information criterion (CAIC), the Bayesian information criterion (BIC), and the Hannan–Quinn information criterion (HQIC). Moreover, the agreement between each fitted distribution and the empirical data is measured via empirical distribution function statistics, specifically the Kolmogorov–Smirnov (K-S), Cramér–von Mises (C-VM), and Anderson–Darling (A-D) test statistics supplemented by the associated K-S p-values. The comprehensive estimation and diagnostic results for both datasets are assembled in Tables 5 and 6.

Table 5. ML estimates, SEs, model selection criteria, and goodness-of-fit diagnostics for the RME data.

Criterion	Model							
	UShD	UXGD	UISDLD	UZD	SPUILD	UGTIID	UIEPD	UGLD
$\hat{\alpha}$	0.129	0.176	0.183	0.189	0.019	1.073	15.700	10.195
SE($\hat{\alpha}$)	0.016	0.019	0.019	0.020	0.086	0.131	6.078	11.933
$\hat{\beta}$	− − −	− − −	− − −	− − −	674.072	8.894	1.276	1.288
SE($\hat{\beta}$)	− − −	− − −	− − −	− − −	3124.310	2.416	0.179	1.401
-2ℓ	−91.334	−90.028	−89.983	−89.090	−85.131	−77.880	−81.104	−79.592
AIC	−89.334	−88.028	−87.983	−87.090	−81.131	−73.880	−77.104	−75.592
CAIC	−89.191	−87.885	−87.841	−86.947	−80.687	−73.435	−76.660	−75.147
BIC	−87.933	−86.627	−86.582	−85.688	−78.329	−71.077	−74.302	−72.789
HQIC	−88.886	−87.580	−87.535	−86.641	−80.235	−72.983	−76.208	−74.695
A-D	0.139	0.256	0.399	0.557	0.572	1.229	0.921	1.156
C-VM	0.018	0.034	0.051	0.067	0.090	0.183	0.138	0.166
K-S	0.067	0.091	0.120	0.132	0.133	0.134	0.135	0.158
p-value	0.998	0.946	0.737	0.623	0.617	0.608	0.600	0.401

Table 6. ML estimates, SEs, model selection criteria, and goodness-of-fit diagnostics for the EB data .

Criterion	Model							
	UShD	UISDLD	UXGD	UZD	UGLD	UIEPD	UGTIID	SPUILD
$\hat{\alpha}$	0.189	0.262	0.245	0.274	2.168	4.752	0.797	0.010
SE($\hat{\alpha}$)	0.029	0.034	0.034	0.035	1.221	1.766	0.122	0.036
$\hat{\beta}$	− − −	− − −	− − −	− − −	3.502	1.017	2.941	657.558
SE($\hat{\beta}$)	− − −	− − −	− − −	− − −	2.297	0.201	0.701	2315.457
-2ℓ	−37.188	−34.839	−38.039	−31.792	−31.441	−29.992	−27.019	−29.150
AIC	−35.188	−32.839	−36.039	−29.792	−27.441	−25.992	−23.019	−25.150
CAIC	−34.966	−32.616	−35.816	−29.570	−26.735	−25.286	−22.313	−24.444
BIC	−34.192	−31.843	−35.043	−28.796	−25.449	−24.001	−21.028	−23.159
HQIC	−34.994	−32.644	−35.844	−29.598	−27.052	−25.604	−22.631	−24.761
A-D	0.452	0.887	0.386	1.341	0.841	1.017	1.256	1.716
C-VM	0.038	0.081	0.053	0.105	0.130	0.176	0.214	0.297
K-S	0.117	0.131	0.134	0.150	0.178	0.186	0.195	0.217
p-value	0.919	0.839	0.822	0.704	0.498	0.443	0.381	0.262

The empirical results reported in Tables 5 and 6 demonstrate favorable and competitive fitting performance of the proposed UShD relative to the considered unit distributions. For the RME data, the UShD achieves the most favorable values of -2ℓ, all four information criteria, and all the reported goodness-of-fit statistics. For the EB data, however, the comparison is criterion-dependent. In particular, the UXGD attains more favorable values of the -2ℓ, AIC, CAIC, BIC, and HQIC, as well as the smaller A-D statistic, whereas the UShD provides the smallest C-VM and K-S statistics and the largest K-S p-value. Thus, no single model uniformly dominates the EB data across all the considered model selection and goodness-of-fit measures. In particular, the K-S p-values for the UShD are 0.998 and 0.919 for the RME and EB data, respectively, providing no statistical evidence against the fitted UShD in either application. Hence, the RME data provide the stronger empirical fit for the UShD, while the EB data constitute a more challenging application in which its performance remains competitive.

The graphical results in Figures 11 and 12 further clarify the numerical comparison. For the RME data, the fitted UShD follows the empirical CDF and RF closely over most of the support, while the P–P and Q–Q plots remain near the reference line apart from limited lower-tail deviations. The corresponding PDF and HF reproduce the overall left-skewed and increasing hazard behavior, although the empirical hazard exhibits local fluctuations. For the EB data, the graphical agreement is visibly weaker. In particular, the sample contains several separated lower observations together with a pronounced concentration near the upper boundary, producing an irregular empirical structure that is not fully reproduced by the smooth fitted PDFs.

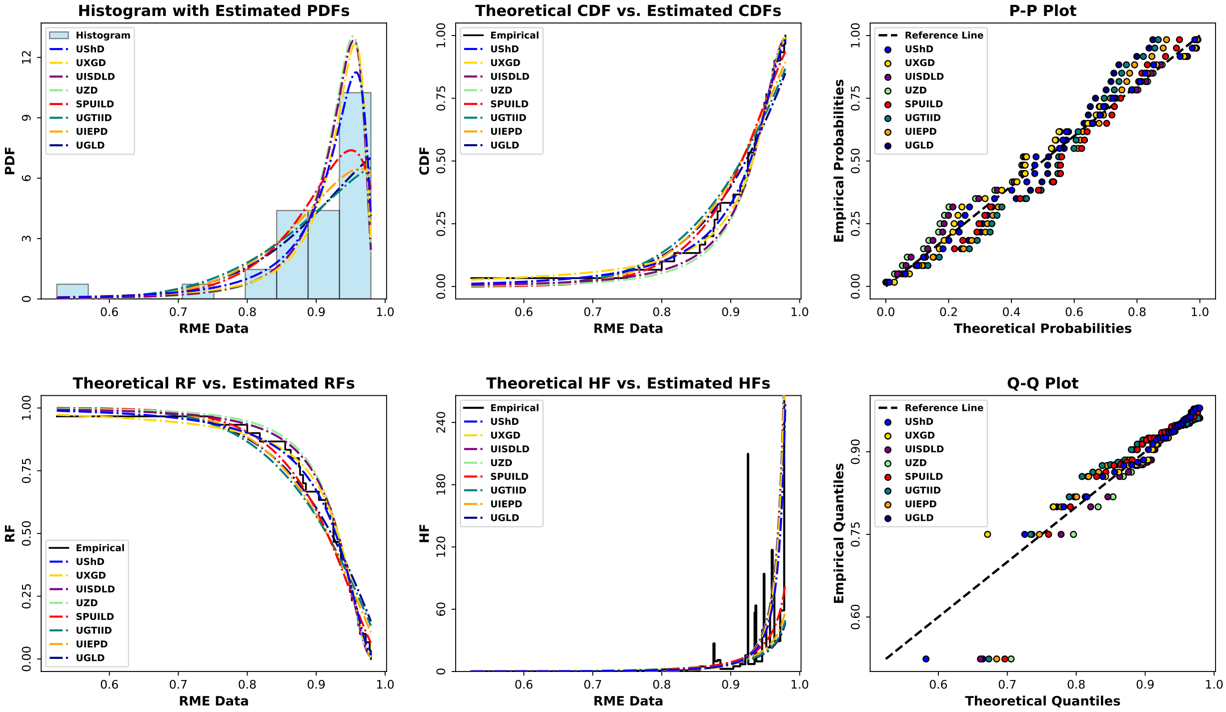

Figure 11. Visual diagnostics of empirical adequacy and fitted model performance for the RME data.

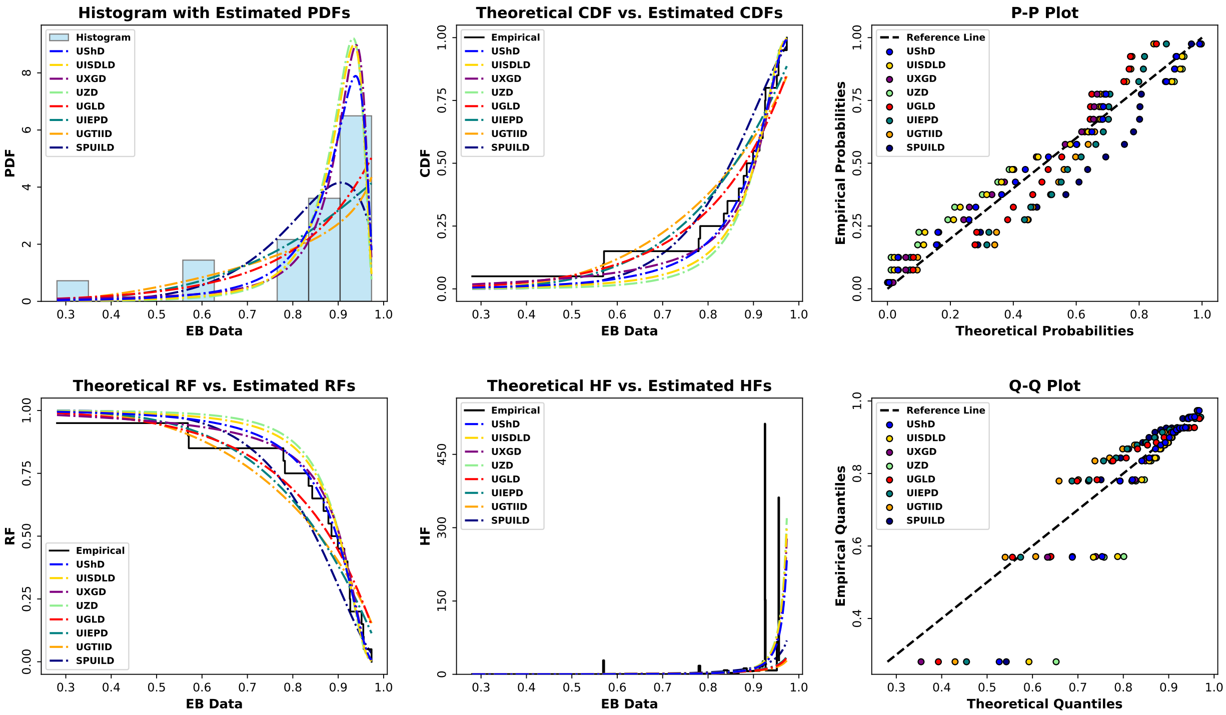

Figure 12. Visual diagnostics of empirical adequacy and fitted model performance for the EB data.

The P–P and Q–Q plots exhibit larger deviations, and the empirical HF shows pronounced local variation that none of the fitted smooth parametric hazard functions reproduces exactly. Nevertheless, the UShD captures the overall decreasing reliability and increasing hazard behavior and remains competitive according to the C-VM, K-S, and K-S p-value results in Table 6. Hence, the EB data represent a more demanding application for the proposed one-parameter UShD than the RME data.

To further assess the inferential performance and robustness of the proposed UShD, we performed Bayesian estimation of the parameter α, along with the RF and HF, $R(x;\alpha)$ and $h(x;\alpha)$, evaluated at the fixed point $x = 0.35$ for the two real datasets. Two prior structures were examined: An informative gamma prior and Jeffreys' non informative prior. This analysis assessed the sensitivity of the posterior results to the prior specification. Posterior summaries were obtained by MCMC using the M–H sampler, as outlined in Algorithm 1, within both the ML-based and MPS-based estimation frameworks. The sampler generated 60,000 iterations, with the first 10,000 discarded as burn-in.

The results presented in Tables 7 and 8 show strong agreement between the classical and Bayesian estimates, confirming the numerical stability and consistency of the proposed inferential procedures. Specifically, the Bayesian SEL estimates closely match the corresponding ML and MPS estimates, confirming the stability of the Bayesian implementation. Furthermore, the use of an informative gamma prior typically results in smaller SEs and shorter HPD CRIs, highlighting the precision gained through the incorporation of prior information. Although Jeffreys' prior produces wider CRIs, as expected from its non informative nature, the resulting point estimates remain highly comparable with those obtained from the informative prior. This similarity demonstrates that the main posterior conclusions are not substantially affected by the prior specification.

Table 7. ML, MPS, and Bayesian posterior estimates under the informative gamma and Jeffreys' priors of α, $R(x;\alpha)$, and $h(x;\alpha)$ at $x = 0.35$ for the RME data.

Par.	Methods	Est.	SE	90% C.L.			95% C.L.		
				Low.	Upp.	Wid.	Low.	Upp.	Wid.
α	ML	0.1285	0.0165	0.1015	0.1556	0.0542	0.0963	0.1608	0.0645
	MPS	0.1237	0.0161	0.0973	0.1501	0.0528	0.0922	0.1552	0.0629
	S-ML-I	0.1294	0.0119	0.1098	0.1486	0.0387	0.1063	0.1526	0.0464
	S-ML-N	0.1285	0.0169	0.1013	0.1562	0.0549	0.0959	0.1611	0.0653
	S-MPS-I	0.1239	0.0109	0.1061	0.1419	0.0357	0.1025	0.1454	0.0429
	S-MPS-N	0.1241	0.0162	0.0971	0.1499	0.0527	0.0934	0.1565	0.0631
$R(x;\alpha)$	ML	0.9967	0.0010	0.9951	0.9982	0.0032	0.9948	0.9985	0.0038
	MPS	0.9969	0.0009	0.9955	0.9984	0.0029	0.9952	0.9987	0.0035
	S-ML-I	0.9966	0.0007	0.9955	0.9977	0.0023	0.9952	0.9979	0.0027
	S-ML-N	0.9966	0.0010	0.9950	0.9982	0.0032	0.9945	0.9983	0.0038
	S-MPS-I	0.9969	0.0006	0.9959	0.9979	0.0020	0.9957	0.9981	0.0024
	S-MPS-N	0.9968	0.0009	0.9955	0.9984	0.0029	0.9950	0.9985	0.0035
$h(x;\alpha)$	ML	0.0240	0.0065	0.0134	0.0346	0.0212	0.0114	0.0367	0.0253
	MPS	0.0222	0.0060	0.0122	0.0321	0.0198	0.0103	0.0340	0.0236
	S-ML-I	0.0246	0.0048	0.0168	0.0320	0.0152	0.0157	0.0340	0.0183
	S-ML-N	0.0245	0.0068	0.0137	0.0350	0.0213	0.0126	0.0380	0.0255
	S-MPS-I	0.0224	0.0042	0.0158	0.0292	0.0134	0.0143	0.0304	0.0160
	S-MPS-N	0.0228	0.0063	0.0130	0.0326	0.0197	0.0118	0.0355	0.0237

Table 8. ML, MPS, and Bayesian posterior estimates under the informative gamma and Jeffreys' priors of α, $R(x;\alpha)$, and $h(x;\alpha)$ at $x = 0.35$ for the EB data.

Par.	Methods	Est.	SE	90% C.L.			95% C.L.		
				Low.	Upp.	Wid.	Low.	Upp.	Wid.
α	ML	0.1885	0.0293	0.1403	0.2367	0.0964	0.1311	0.2459	0.1148
	MPS	0.1807	0.0280	0.1346	0.2268	0.0921	0.1258	0.2356	0.1098
	S-ML-I	0.1906	0.0212	0.1561	0.2252	0.0692	0.1489	0.2318	0.0829
	S-ML-N	0.1884	0.0300	0.1396	0.2368	0.0972	0.1311	0.2469	0.1158
	S-MPS-I	0.1830	0.0205	0.1501	0.2167	0.0666	0.1444	0.2245	0.0800
	S-MPS-N	0.1813	0.0284	0.1334	0.2252	0.0919	0.1267	0.2367	0.1100
$R(x;\alpha)$	ML	0.9920	0.0028	0.9874	0.9967	0.0093	0.9865	0.9976	0.0111
	MPS	0.9928	0.0026	0.9886	0.9970	0.0084	0.9878	0.9978	0.0100
	S-ML-I	0.9917	0.0021	0.9885	0.9952	0.0067	0.9873	0.9954	0.0081
	S-ML-N	0.9917	0.0030	0.9872	0.9964	0.0092	0.9858	0.9969	0.0111
	S-MPS-I	0.9924	0.0020	0.9894	0.9956	0.0061	0.9887	0.9961	0.0074
	S-MPS-N	0.9924	0.0027	0.9885	0.9967	0.0083	0.9872	0.9972	0.0101
$h(x;\alpha)$	ML	0.0538	0.0176	0.0248	0.0828	0.0579	0.0193	0.0883	0.0690
	MPS	0.0492	0.0161	0.0228	0.0756	0.0529	0.0177	0.0807	0.0630
	S-ML-I	0.0559	0.0132	0.0345	0.0762	0.0417	0.0325	0.0829	0.0504
	S-ML-N	0.0553	0.0187	0.0262	0.0835	0.0573	0.0235	0.0925	0.0690
	S-MPS-I	0.0513	0.0121	0.0315	0.0699	0.0385	0.0292	0.0755	0.0463
	S-MPS-N	0.0510	0.0170	0.0244	0.0763	0.0519	0.0222	0.0854	0.0632

At $x = 0.35$ on the transformed unit-time scale, the ML estimates for the RME data are $R(0.35;\widehat{\alpha}_{\mathrm{ML}}) = 0.9967$ and $h(0.35;\widehat{\alpha}_{\mathrm{ML}}) = 0.0240$, indicating a 99.67% survival probability and, for small $\Delta x > 0$, a conditional failure probability of approximately $0.0240\,\Delta x$. For the EB data, the corresponding estimates are 0.9920 and 0.0538, indicating 99.20% survival and a conditional failure probability of approximately $0.0538\,\Delta x$.

Moreover, the parameter has a direct reliability interpretation because

$$\frac{\partial R(x;\alpha)}{\partial\alpha} < 0, \qquad \frac{\partial h(x;\alpha)}{\partial\alpha} > 0, \qquad 0 < x < 1, \quad \alpha > 0.$$

Hence, at any fixed transformed operating time, increasing α decreases the reliability and increases the hazard rate. Since $\widehat{\alpha}_{\mathrm{ML}} = 0.1285$ for the RME data and $\widehat{\alpha}_{\mathrm{ML}} = 0.1885$ for the EB data, the larger estimated parameter for the EB data is consistent with its lower estimated reliability and higher local failure intensity at $x = 0.35$. Together with the IFR and DMRL properties, these findings provide a direct reliability interpretation of the fitted parameter and indicate progressive aging toward the upper boundary.

The MCMC diagnostic plots displayed in Figures 13 and 14 further indicate satisfactory convergence, stable chain behavior, and efficient posterior sampling. Overall, these findings provide additional empirical evidence that the proposed UShD offers a precise, stable, and robust framework for reliability analysis on the unit interval.

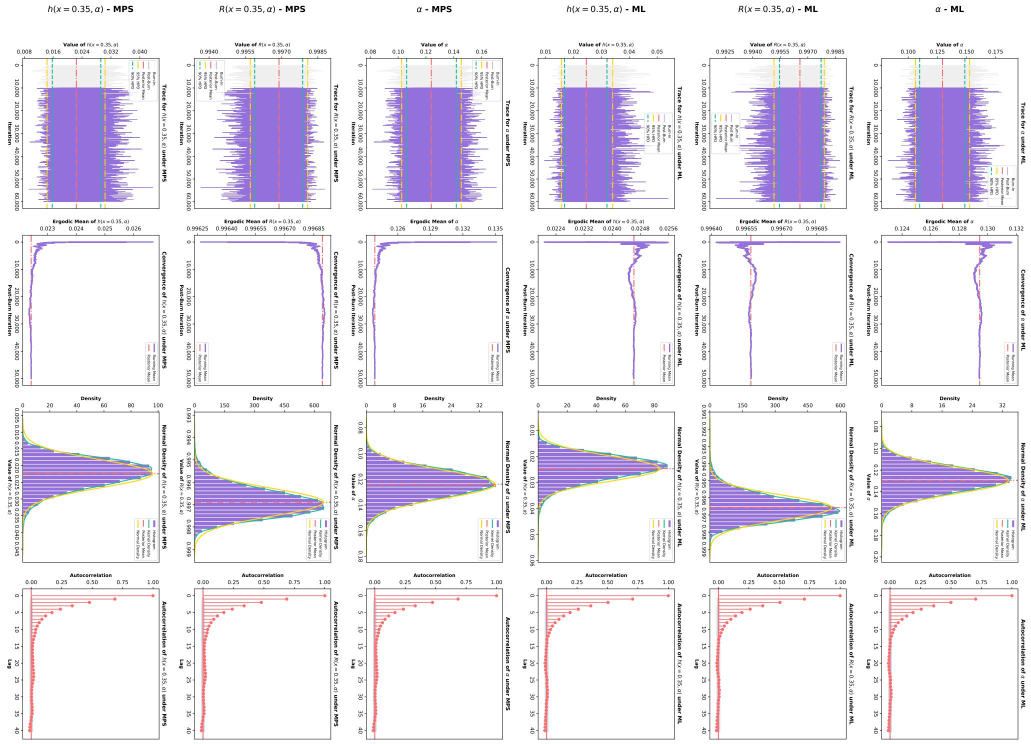

(a) Gamma prior

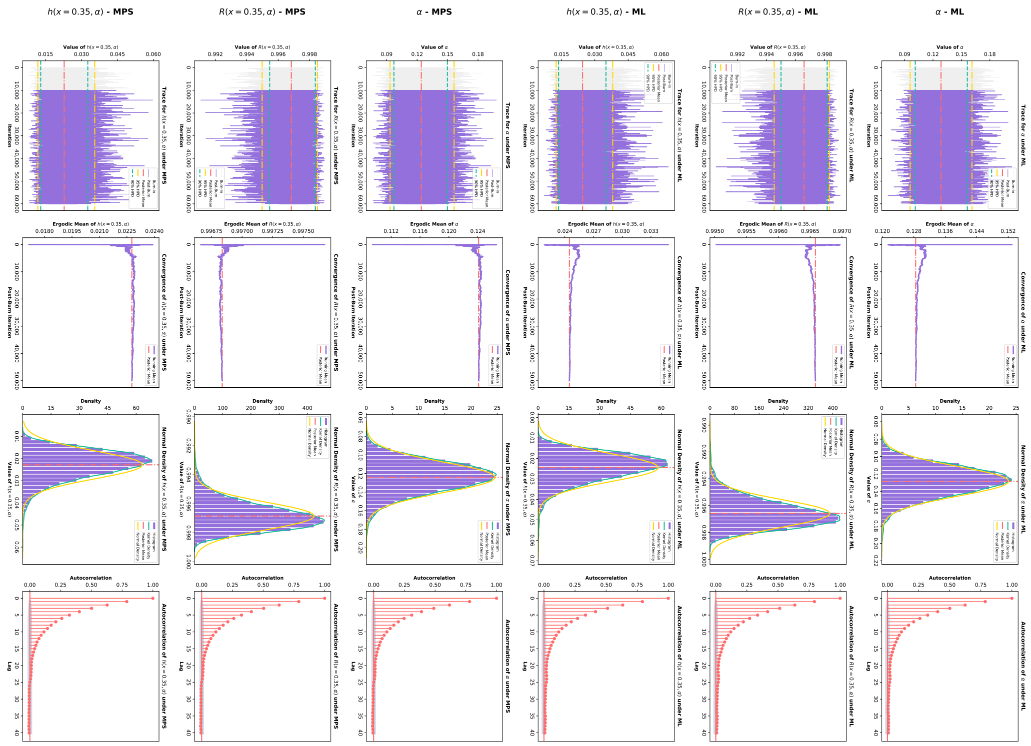

(b) Jeffreys' prior

Figure 13. MCMC diagnostic plots, including trace, convergence, posterior density, and autocorrelation plots, for the posterior sampling behavior of α, $R(x;\alpha)$, and $h(x;\alpha)$ evaluated at $x = 0.35$ under the informative gamma and Jeffreys' prior specifications for the RME data.

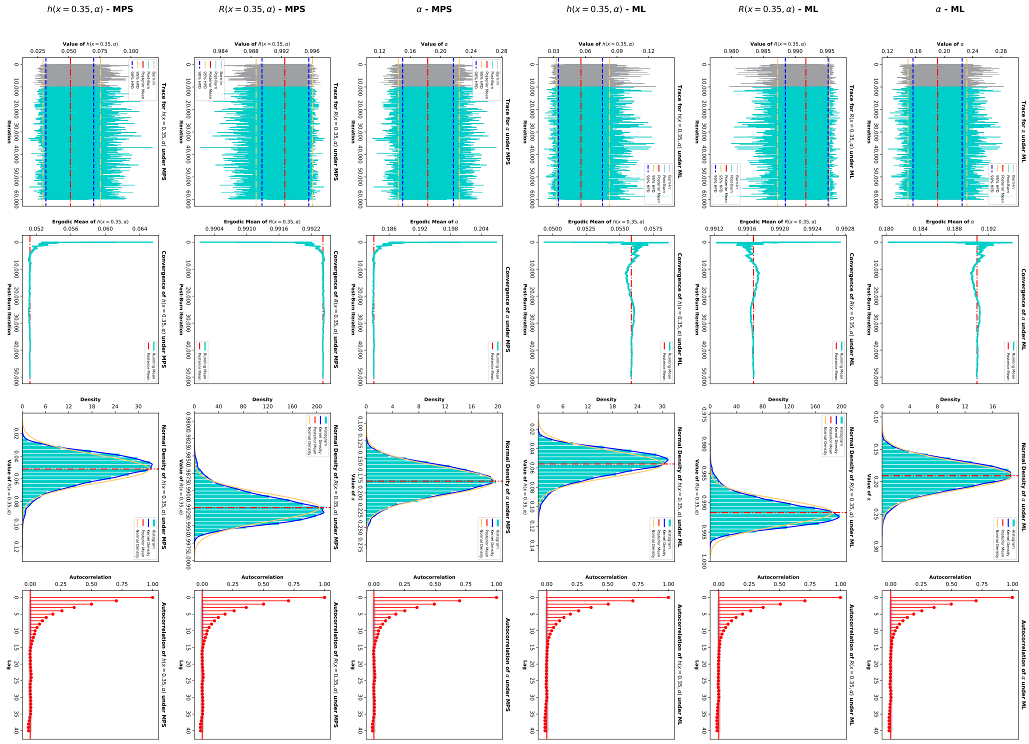

(a) Gamma prior

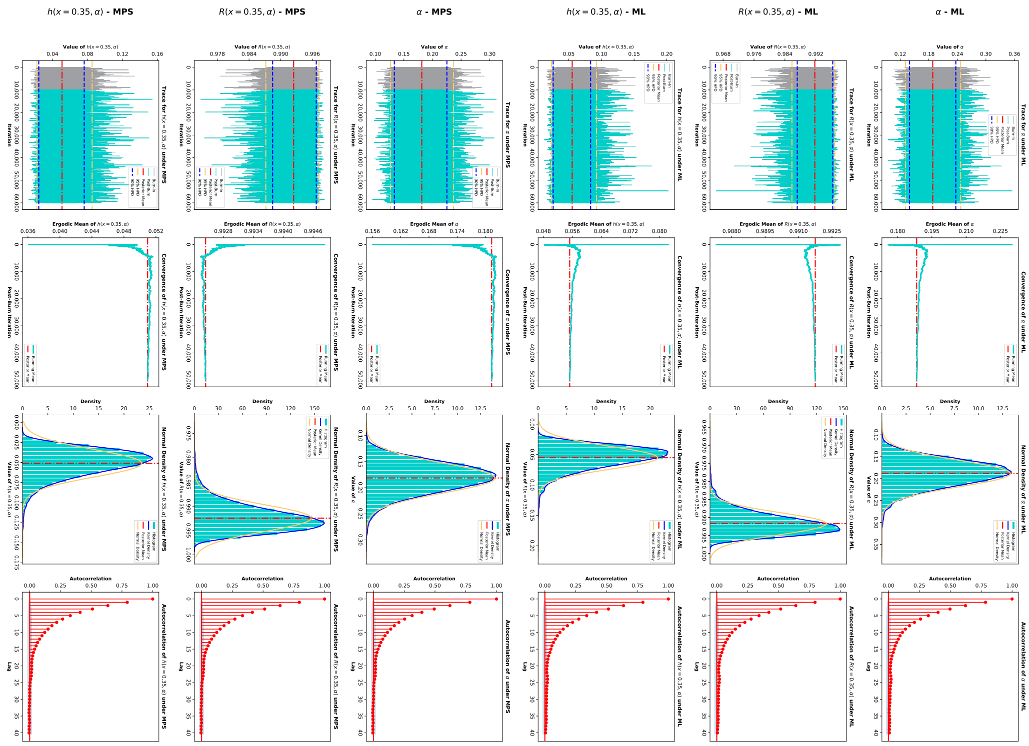

(b) Jeffreys' prior

Figure 14. MCMC diagnostic plots, including trace, convergence, posterior density, and autocorrelation plots, for the posterior sampling behavior of α, $R(x;\alpha)$, and $h(x;\alpha)$ evaluated at $x = 0.35$ under the informative gamma and Jeffreys' prior specifications for the EB data.

9. Conclusions

This paper developed a unit-interval formulation derived from the positive-support two-parameter family through the standard transformation $X = T/(1+T)$. The main contribution lies in the systematic development of the resulting framework for bounded data, which unifies several Lindley-type unit distributions and provides general results for their distributional, reliability, actuarial, order statistic, entropy, and extropy properties. The theoretical findings establish the tractability of the framework and indicate its suitability for skewed and boundary-concentrated data arising from bounded aging and wear-out phenomena.

The UShD was examined as an important one-parameter special case of the TPFUD. Its simple structure permits ML, MPS, and Bayesian estimation of the unknown parameter and selected reliability functions. The simulation results showed that estimation accuracy generally improved as the sample size increased, while the informative Bayesian procedure often provided the best finite-sample performance. In the real-data applications, the UShD fitted the RME data particularly well and remained competitive for the EB data. It also produced favorable likelihood, information criterion, and goodness-of-fit results relative to the considered competing unit models.

Two limitations should be acknowledged. First, the inferential and empirical analyses were restricted to the one-parameter UShD and complete samples. Second, the TPFUD belongs to the IFR class and is therefore intended primarily for bounded aging and wear-out data rather than for mechanisms exhibiting decreasing or nonmonotone hazard patterns.

Overall, the TPFUD provides a tractable framework for bounded data and reliability analysis, while the UShD offers a parsimonious special case with closed-form distributional and reliability functions and promising empirical performance.

Future research may extend the framework to covariate-dependent parameterizations, mean- or median-based regression structures, Type I, Type II, interval, and progressive censoring schemes, accelerated lifetime models, and distributions with more flexible hazard shapes. Additional directions include truncated samples, multivariate and mixture extensions, alternative Bayesian priors and loss functions, Bayesian hierarchical modeling, and broader applications in biomedical, environmental, financial, engineering, and quality control studies.

Author contributions

Hebatalla H. Mohammad: Methodology, validation, resources, eriting—review and editing, funding acquisition; Moustafa N. Mousa: Conceptualization, methodology, software, data curation, writing—original draft, visualization; Khalaf S. Sultan: Conceptualization, methodology, formal analysis, investigation, supervision; Mahmoud M. M. Mansour: Conceptualization, methodology, software, validation, investigation, resources. All authors have read and approved the final version of the manuscript for publication

Use of generative AI tools declaration

The authors declare that they have not used Artificial Intelligence (AI) tools in the creation of this article.

Acknowledgments

The authors acknowledge that this research project was funded by Princess Nourah bint Abdulrahman University Researchers Supporting Project number (PNURSP2026R745), Princess Nourah bint Abdulrahman University, Riyadh, Saudi Arabia.

Funding

This research project was funded by Princess Nourah bint Abdulrahman University Researchers Supporting Project number (PNURSP2026R745), Princess Nourah bint Abdulrahman University, Riyadh, Saudi Arabia.

Conflict of interest

All authors declare no conflicts of interest in this paper.

References

1. A. S. Al-Moisheer, K. S. Sultan, M. N. Mousa, M. M. M. Mansour, The unit arcsine–exponential distribution and its statistical properties with inference and application to reliability data, *Axioms*, **15** (2026), 218. http://dx.doi.org/10.3390/axioms15030218
2. A. S. Al-Moisheer, K. S. Sultan, M. N. Mousa, M. M. M. Mansour, A novel version of the arcsine–rayleigh distribution with entropy measures, statistical inference, and applications, *Entropy*, **28** (2026), 464. http://dx.doi.org/10.3390/e28040464
3. M. R. Irshad, S. Aswathy, R. Maya, A. I. Al-Omari, G. Alomani, A flexible model for bounded data with bathtub shaped hazard rate function and applications, *AIMS Math.*, **9** (2024), 24810–24831. http://dx.doi.org/10.3934/math.20241208
4. A. M. Gemeay, M. I. A. Araibi, E. M. Almetwally, I. Elbatal, C. Tanış, L. P. Sapkota, et al. , Modeling with the inverse unit new xlindley distribution: properties and real-world applications, *Eng. Rep.*, **7** (2025), e70354. http://dx.doi.org/10.1002/eng2.70354
5. J. Mazucheli, A. F. B. Menezes, S. Chakraborty, On the one parameter unit-Lindley distribution and its associated regression model for proportion data, *J. Appl. Stat.*, **46** (2019), 700–714. http://dx.doi.org/10.1080/02664763.2018.1511774
6. M. C. Belili, A. M. Alshangiti, A. M. Gemeay, H. Zeghdoudi, K. Karakaya, M. E. Bakr, et al., Two-parameter family of distributions: properties, estimation, and applications, *AIP Adv.*, **13** (2023), 105008. http://dx.doi.org/10.1063/5.0173532
7. D. V. Lindley, Fiducial distributions and Bayes' theorem, *J. R. Stat. Soc. B*, **20** (1958), 102–107. http://dx.doi.org/10.1111/j.2517-6161.1958.tb00278.x
8. R. Shanker, Shanker distribution and its applications, *International Journal of Statistics and Applications*, **5** (2015), 338–348.
9. R. Shanker, Komal distribution with properties and application in survival analysis, *Biom. Biostat. Int. J.*, **12** (2023), 40–44. http://dx.doi.org/10.15406/bbij.2023.12.00381

10. R. Shanker, Garima distribution and its application to model behavioral science data, *Biom. Biostat. Int. J.*, **4** (2016), 275–281. http://dx.doi.org/10.15406/bbij.2016.04.00116

11. B. K. Sah, One-parameter linear-exponential distribution, *International Journal of Statistics and Applied Mathematics*, **6** (2021), 06–15. http://dx.doi.org/10.22271/maths.2021.v6.i6a.744

12. R. Shanker, A. Mishra, A two-parameter lindley distribution, *Statistics in Transition New Series*, **14** (2013), 45–56. http://dx.doi.org/10.59170/stattrans-2013-003

13. S. Nedjar, H. Zeghdoudi, On Gamma lindley distribution: properties and simulations, *J. Comput. Appl. Math.*, **298** (2016), 167–174. http://dx.doi.org/10.1016/j.cam.2015.11.047

14. C. Benatmane, H. Zeghdoudi, A. Ezzebsa, L. Bouchahed, Note on quasi lindley distribution: some remarks and corrections, *Asian Journal of Probability and Statistics*, **15** (2021), 324–329. http://dx.doi.org/10.9734/ajpas/2021/v15i430383

15. R. Shanker, A. H. Ghebretsadik, A new quasi lindley distribution, *Int. J. Stat. Syst.*, **8** (2013), 143–156.

16. R. Shanker, S. Sharma, R. Shanker, A two-parameter lindley distribution for modeling waiting and survival times data, *Appl. Math.*, **4** (2013), 363–368. http://dx.doi.org/10.4236/am.2013.42056

17. S. Nedjar, H. Zeghdoudi, On pseudo Lindley distribution: Properties and applications, *New Trends in Mathematical Sciences*, **5**(1) (2017), 59–65.

18. S. Chouia, H. Zeghdoudi, The XLindley distribution: properties and application, *J. Stat. Theory Appl.*, **20** (2021), 318–327. http://dx.doi.org/10.2991/jsta.d.210607.001

19. B. C. Arnold, N. Balakrishnan, H. N. Nagaraja, *A first course in order statistics*, New York: Wiley, 1992.

20. M. Shaked, J. G. Shanthikumar, *Stochastic orders and their applications*, Boston: Academic Press, 1994.

21. A. Rényi, On measures of entropy and information, In: *Proceedings of the Fourth Berkeley Symposium on Mathematical Statistics and Probability, Volume 1: Contributions to the Theory of Statistics*, BerkeleyL: University of California Press, 1961, 547–561.

22. S. Arimoto, Information-theoretical considerations on estimation problems, *Information and Control*, **19** (1971), 181–194. http://dx.doi.org/10.1016/S0019-9958(71)90065-9

23. C. Tsallis, Possible generalization of Boltzmann–Gibbs statistics, *J. Stat. Phys.*, **52** (1988), 479–487. http://dx.doi.org/10.1007/BF01016429

24. J. Havrda, F. Charvát, Quantification method of classification processes. concept of structural a-entropy, *Kybernetika*, **3** (1967), 30–35.

25. A. M. Mathai, H. G. Haubold, On generalized distributions and pathways, *Phys. Lett. A*, **372** (2008), 2109–2113. http://dx.doi.org/10.1016/j.physleta.2007.10.084

26. C. E. Shannon, A mathematical theory of communication, *The Bell System Technical Journal*, **27** (1948), 379–423. http://dx.doi.org/10.1002/j.1538-7305.1948.tb01338.x

27. F. Lad, G. Sanfilippo, G. Agrò, Extropy: complementary dual of entropy, *Stat. Sci.*, **30** (2015), 40–58. http://dx.doi.org/10.1214/14-STS430

28. M. Rao, Y. Chen, B. C. Vemuri, F. Wang, Cumulative residual entropy: A new measure of information, *IEEE T. Inform. Theory*, **50** (2004), 1220–1228. http://dx.doi.org/10.1109/TIT.2004.828057

29. S. M. A. Jahanshahi, H. Zarei, A. H. Khammar, On cumulative residual extropy, *Probab. Eng. Inform. Sci.*, **264** (2019), 605–625. http://dx.doi.org/10.1017/S0269964819000196

30. S. Tahmasebi, A. Toomaj, On negative cumulative extropy with applications, *Commun. Stat.-Theor. M.*, **51** (2022), 5025–5047. http://dx.doi.org/10.1080/03610926.2020.1831541

31. N. Balakrishnan, F. Buono, M. Longobardi, On weighted extropies, *Commun. Stat.-Theor. M.*, **51** (2022), 6250–6267. http://dx.doi.org/10.1080/03610926.2020.1860222

32. M. Hashempour, M. R. Kazemi, S. Tahmasebi, On weighted cumulative residual extropy: characterization, estimation and testing, *Statistics*, **56** (2022), 681–698. http://dx.doi.org/10.1080/02331888.2022.2072505

33. R. C. H. Cheng, N. A. K. Amin, Estimating parameters in continuous univariate distributions with a shifted origin, *J. R. Stat. Soc. B*, **45** (1983), 394–403. http://dx.doi.org/10.1111/j.2517-6161.1983.tb01268.x

34. P. Virtanen, R. Gommers, T. E. Oliphant, M. Haberland, T. Reddy, D. Cournapeau, et al., SciPy 1.0: Fundamental algorithms for scientific computing in Python, *Nat. Methods*, **17** (2020), 261–272. http://dx.doi.org/10.1038/s41592-019-0686-2

35. L. Held, D. S. Bové, *Applied statistical inference: likelihood and Bayes*, Berlin/Heidelberg: Springer, 2014. http://dx.doi.org/10.1007/978-3-642-37887-4

36. B. Ranneby, The maximum spacing method: An estimation method related to the maximum likelihood method, *Scand. J. Stat.*, **11** (1984), 93–112.

37. K. Webel, Greene, W. H., Econometric analysis, *Stat. Papers*, **52** (2011), 983–984. http://dx.doi.org/10.1007/s00362-010-0315-8

38. B. C. Arnold, S. J. Press, Bayesian inference for pareto populations, *J. Econometrics*, **21** (1983), 287–306. http://dx.doi.org/10.1016/0304-4076(83)90047-7

39. D. Kundu, Bayesian inference and life testing plan for the weibull distribution in presence of progressive censoring, *Technometrics*, **50** (2008), 144–154. http://dx.doi.org/10.1198/004017008000000217

40. S. Dey, T. Dey, D. J. Luckett, Statistical inference for the generalized inverted exponential distribution based on upper record values, *Math. Comput. Simulat.*, **120** (2016), 64–78. http://dx.doi.org/10.1016/j.matcom.2015.06.012

41. L. Tierney, Markov chains for exploring posterior distributions, *Ann. Statist.*, **22** (1994), 1701–1728. http://dx.doi.org/10.1214/aos/1176325750

42. W. R. Gilks, S. Richardson, D. J. Spiegelhalter *Markov chain Monte Carlo in practice*, New York: Chapman and Hall, 1995. http://dx.doi.org/10.1201/b14835

43. A. Elshahhat, H. M. Aljohani, A. Z. Afify, Bayesian and classical inference under type-ii censored samples of the extended inverse gompertz distribution with engineering applications, *Entropy*, **23** (2021), 1578. http://dx.doi.org/10.3390/e23121578

44. D. N. P. Murthy, M. Xie, R. Y. Jiang, *Weibull models*, Hoboken: Wiley, 2003. http://dx.doi.org/10.1002/047147326X

45. S. Hashmi, M. Ahsan-ul-Haq, J. Zafar, M. A. Khaleel, Unit Xgamma distribution: Its properties, estimation and application, *Proceedings of the Pakistan Academy of Sciences A: Physical and Computational Sciences*, **59** (2022), 15–28. http://dx.doi.org/10.53560/PPASA(59-1)636

46. E. Altun, G. M. Cordeiro, The unit-improved second-degree Lindley distribution: inference and regression modeling, *Comput. Stat.*, **35** (2020), 259–279. http://dx.doi.org/10.1007/s00180-019-00921-y

47. S. Bashiru, M. Kayid, R. Mahmoud, O. Balogun, M. Abd El-Raouf, A. Gemeay, Introducing the unit zeghdoudi distribution as a novel statistical model for analyzing proportional data, *J. Radiat. Res. Appl. Sc.*, **18** (2025), 101204. http://dx.doi.org/10.1016/j.jrras.2024.101204

48. A. S. Hassan, D. S. Metwally, M. Elgarhy, H. E. Semary, A. Faal, R. E. Mohamed, Sine power unit inverse lindley model: Bayesian analysis and practical application, *Engineering Reports*, **7** (2025), e70242. http://dx.doi.org/10.1002/eng2.70242

49. A. Shafiq, T. N. Sindhu, Z. Hussain, J. Mazucheli, B. Alves, A flexible probability model for proportion data: unit gumbel type-ii distribution, development, properties, different method of estimations and applications, *Aust. J. Stat.*, **52** (2023), 116–140. http://dx.doi.org/10.17713/ajs.v52i2.1407

50. A. S. Hassan, G. S. S. Abdalla, A. Faal, O. A. Saudi, Novel unit distribution for enhanced modeling capabilities: healthcare and geological applications, *Engineering Reports*, **7** (2025), e70277. http://dx.doi.org/10.1002/eng2.70277

51. K. Karakaya, Ş. Sağlam, Unit Gamma-Lindley distribution: properties, estimation, regression analysis, and practical applications, *Gazi U. J. Sci.*, **38** (2025), 1021–1040. http://dx.doi.org/10.35378/gujs.1549073